1997

The initiation of coarse bed load transport in gravel bed streams

Andrew C. Whitaker
The University of Montana

INFORMATION TO USERS

This manuscript has been reproduced from the microfilm master. UMI films the text directly from the original or copy submitted. Thus, some thesis and dissertation copies are in typewriter face, while others may be from any type of computer printer.

The quality of this reproduction is dependent upon the quality of the copy submitted. Broken or indistinct print, colored or poor quality illustrations and photographs, print bleedthrough, substandard margins, and improper alignment can adversely affect reproduction.
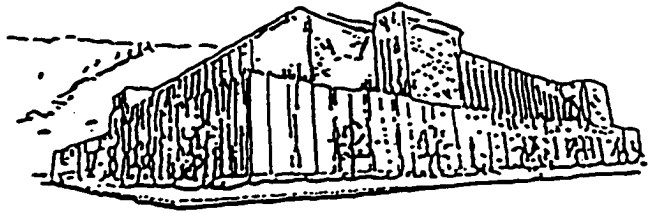
In the unlikely event that the author did not send UMI a complete manuscript and there are missing pages, these will be noted. Also, if unauthorized copyright material had to be removed, a note will indicate the deletion.

Oversize materials (e.g., maps, drawings, charts) are reproduced by sectioning the original, beginning at the upper left-hand corner and continuing from left to right in equal sections with small overlaps. Each original is also photographed in one exposure and is included in reduced form at the back of the book.

Photographs included in the original manuscript have been reproduced xerographically in this copy. Higher quality 6" x 9" black and white photographic prints are available for any photographs or illustrations appearing in this copy for an additional charge. Contact UMI directly to order.

UMI

Maureen and Mike
MANSFIELD LIBRARY

The University of **MONTANA**

Permission is granted by the author to reproduce this material in its entirety, provided that this material is used for scholarly purposes and is properly cited in published works and reports.

*** Please check "Yes" or "No" and provide signature ***

Yes, I grant permission _____✓_____

No, I do not grant permission _____

Author's Signature _____

Date ___5/21/97_____

Any copying for commercial purposes or financial gain may be undertaken only with the author's explicit consent.

THE INITIATION OF COARSE BED LOAD TRANSPORT
IN GRAVEL BED STREAMS

by

Andrew C. Whitaker

B.S. The University of Bristol, UK, 1991

M.S. The University of Newcastle-Upon-Tyne, UK, 1992

presented in partial fulfillment of the requirements

for the degree of

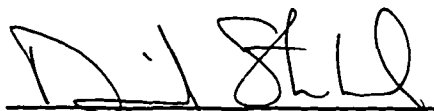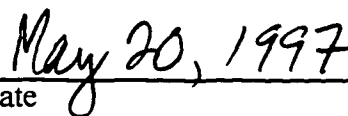Doctor of Philosophy

The University of Montana

1997

Approved by:

_____
Chairperson

_____
Dean, Graduate School

_____
Date

UMI Number: 9801856

Copyright 1998 by
Whitaker, Andrew Charles

UMI
300 North Zeeb Road
Ann Arbor, MI 48103

The Initiation of Coarse Bed Load Transport in Gravel Bed Streams

Director: Donald F. Potts

Determination of threshold flow conditions required to entrain bed material is important for the management of gravel bed streams and their watersheds. Current critical shear stress and critical unit discharge models used to estimate threshold conditions need to be tested in natural gravel bed rivers. The relationship between bed load size distribution and discharge also needs clarification. Gravel and cobble transport dynamics in Dupuyer Creek, a headwaters tributary of the Missouri River on Montana's Rocky Mountain Front, shed light on these issues. Bed load samples were obtained with a large aperture sampler (1 m by 0.45 m) which captures the largest particles in motion and the size distribution for particles >38 mm in diameter. Distance of travel for tracer particles was also monitored.

Measured hydraulic variables (depth, velocity, discharge and water surface slope) paired with sampled maximum bed load sizes show bed material is more mobile, and transport more size selective in Dupuyer Creek than existing models predict. The critical shear stress approach directly yields reasonable threshold predictions, while the critical unit discharge approach requires model adjustment. Maximum particle sizes sampled, and D_{50} to D_{95} percentiles in the bed load size distribution, are well correlated with both shear stress and unit discharge. This is due to a coarsening of the bed load size distribution with increasing flows.

Flow competence relationships based on maximum particle sizes are sensitive to the influence of outliers and sample size effects. More consistent relationships may therefore be obtained by modeling the change in the mean of the three largest particles with discharge. Entrainment is size selective for bed material sizes D_{70} and larger (88-175 mm), while particles in the range D_{25} to D_{70} (35-88 mm) may all be entrained at essentially the same flow. However, transport is always size selective because rates of transport for the different size fractions are not in proportion to the relative abundance of particles in the substrate. Coarse fractions remain under-represented in the bed load, while fine fractions are over-represented.

To David

ACKNOWLEDGMENTS

TABLE OF CONTENTS

10. APPENDICES 135

vi

LIST OF TABLES

6. RESULTS AND DISCUSSION

7. FLOW COMPETENCE ANALYSIS

LIST OF FIGURES

2. LITERATURE REVIEW

4. STUDY AREA

5. METHODS

6. RESULTS AND DISCUSSION

ix

x

7. FLOW COMPETENCE ANALYSIS

1. INTRODUCTION

Critical flow condition for the entrainment of bed material is an important consideration for the assessment of stability in gravel bed streams. The classic concept of flow competence is commonly used to estimate the magnitude of flows necessary to entrain the particle sizes present on the stream bed. A common characteristic of gravel bed streams is that bed particles are transported only about 5-10 percent of the time during the highest flows (Andrews and Nankervis, 1995). Only when these particles are mobilized is it possible for the channel morphology to change. More significant changes occur when the coarsest particle sizes are entrained. Therefore, data concerning the transport of coarse sediments is important because channel change can occur only when threshold conditions are exceeded for these boundary sediments (Grant, 1987; Carling, 1988; Leopold, 1992). When all particle sizes are in motion, scour and fill processes are most active, rates of bed load movement are high, and the channel boundary is unstable. An unstable boundary may cause rapid bank erosion and channel migration, and change in the pool and riffle locations from year to year. These changes are often of concern to managers.

The broad range of particle sizes present in gravel bed streams makes prediction of bed load initiation extremely complex. Sampling bed load to validate model predictions has been limited by the dangerous conditions during floods, the high rates of bed load transport, the need for large orifice samplers, and unmanageable sample sizes (Gomez and Emmett, 1991; Custer, 1992). Empirical predictive models of bed load transport have

1

therefore been largely developed in laboratory flume experiments, and there is a need to further evaluate their performance in rivers with coarse substrates. Two main criteria are recognized in the literature for predicting the competence of streamflow to entrain the channel substrate; the critical shear stress criterion (Andrews, 1983; Petit, 1994), and the critical unit discharge approach (Bathurst, 1987a; Ferguson, 1994). The validity of these criteria, however, in high energy gravel bed streams remains unclear. Field data are needed to assess the critical flow conditions for the entrainment of different size fractions, the size distribution of bed load, and rates of bed load movement for the various size fractions.

Difficulties in the observation and sampling of bed load in gravel bed streams continue to limit our understanding of the sediment transport process. Conceptualization of the bed load process is difficult due to continual variation with the passage of different flood hydrographs (Gomez, 1983; Reid et al., 1985; Bunte, 1992). Two schools of thought are deeply entrenched in the scientific community. The first considers bed load transport to be size selective, whereby progressively larger particle sizes are entrained over a significant range in flow (Milhous, 1973; Carling, 1983; Komar, 1987; Ashworth and Ferguson, 1989). The second considers that bed load particles experience essentially equal mobility, whereby almost all particle sizes are entrained over a very narrow range in flow (Parker et al., 1982a and 1982b; Andrews, 1983; Andrews and Parker. 1987; Wilcock and Southard, 1988).

Few authors would contend that bed load transport was either totally size selective or totally equally mobile. The main argument lies in determining the dominant form of

transport (Komar and Shih, 1992). Equal mobility of sand and fine gravels in pool regions can coexist with size selective transport over the coarser riffle sections in a channel with streamwise sorting (Lisle and Madej, 1992). Proponents of size selective transport maintain that as flows increase, progressively larger particles are entrained over a significant range in flow, until eventually all particle sizes are in transport. Bathurst (1987a) suggests that the wide size distribution present in boulder-bed rivers, such as the Roaring River in Colorado, produces size selective transport over the majority of the flow duration. Bunte (1992) also suggests that large rare floods are required to mobilize all size fractions, for the gravel bed Squaw Creek in Montana. On the other hand, proponents of equal mobility claim that the full range of particle sizes is mobilized over a very narrow range in discharge so that all particle sizes are in motion during even the frequent floods. This difference has important implications with regard to long-term patterns of bed load transport and the prediction of stream bed mobility.

If size selective transport is dominant, then the concept of flow competence is very useful. Relationships can be modeled between streamflow and the maximum size fraction entrained in transport, and used in applications where predictions of stream bed mobility are needed. In the design of channel maintenance flows, these models can be used to compute the quantity of bed material in each size fraction transported by increments of discharge (Andrews and Nankervis, 1995). If equal mobility is dominant, then predictive models need to focus on the identification of the narrow flow range in which all size fractions are mobilized.

Sampling of bed load size distributions at frequent intervals over complete flood hydrographs is required to determine whether size selective or equal mobility transport is dominant in gravel bed streams. A major limitation with most portable bed load samplers is that the instrument aperture size will not allow capture of the largest particles in motion, and sampler-stream bed contact is poor (Custer, 1992). Bed load traps set into the stream bed solve this particular problem (Milhous, 1973; Reid et al., 1985; Reid et al., 1995), but these provide integrated samples and bed load size distributions rather than series of samples at various flows. A primary objective of this research was to employ a portable bed load sampler, similar to that developed by Bunte (1990), which enabled capture of the largest particles and the coarse bed load size distributions at known flow conditions. A paired data set was obtained linking critical flow conditions to the mobility of different size fractions on the stream bed. The 'large frame-net' bed load sampler used here was inexpensive to construct and could easily be deployed on other streams.

2. LITERATURE REVIEW

Bed load transport in gravel bed rivers occurs only during periods of high flow, perhaps a few days each year or even every few years (Andrews and Nankervis, 1995). On the rising limb of floods, a point is reached when the tractive forces at the stream bed are sufficient to entrain particles. This critical flow at which bed load transport is initiated is the subject of much research and debate. Part of the debate concerns the particle size composition of the bed load, and how this varies with changing discharge over the flood hydrograph. We are still lacking a universally accepted conceptual model of how the bed load process operates, largely as a result of our inability to directly observe the transport process in turbid flood waters, and because of sampling difficulties.

Bed load transport behavior in gravel bed rivers is strongly influenced by the wide range in particle sizes commonly present. When particle sizes range from fine sand to large boulders, the size distribution of the bed material determines the bed load transport behavior of that channel, both in terms of the critical flow condition for entrainment, and the range in particle sizes in transport at a given flow. The two phase conceptual model proposed by Jackson and Beschta (1982) can be used to illustrate bed load behavior in these gravel bed streams. In phase 1 transport, the channel bed over the riffles remains predominantly immobile, and movement is limited to sands and fine gravels winnowed from storage areas such as pools and gravel bars. This phase 1 transport is by definition size selective. As flows increase, a threshold is reached when riffle sediments become

5

mobilized in phase 2 transport. What remains unclear is whether all particle sizes are entrained at this point, or whether the larger size fractions are still relatively immobile.

2.1 Flow Competence

Intuitively, the concept of flow competence (Gilbert and Murphy, 1914) suggests there is a maximum particle size a given discharge can transport which is limited by available stream power. Simply put, larger heavier particles require greater stream power before they are entrained, such that predictable relationships can be established between flow and the maximum particle size in motion. Figure 2.1 combines the concept of flow competence with the two phase conceptual model of bed load transport proposed by Jackson and Beschta (1982). Both of the relationships show that a threshold flow or shear stress must be exceeded before bed material is mobilized in phase 1 transport. Where the size selective and equal mobility hypotheses differ is in the nature of the flow competence relationships during phase 2 transport. Proponents of size selective transport would support the relationship in Figure 2.1a to predict the transport of different bed material percentiles and size fractions. Mobilization of riffle sediments in phase 2 transport may simply be represented by a change in slope of the flow competence curve. A steady increase in the discharge or shear stress results in progressively larger bed material percentiles being entrained.
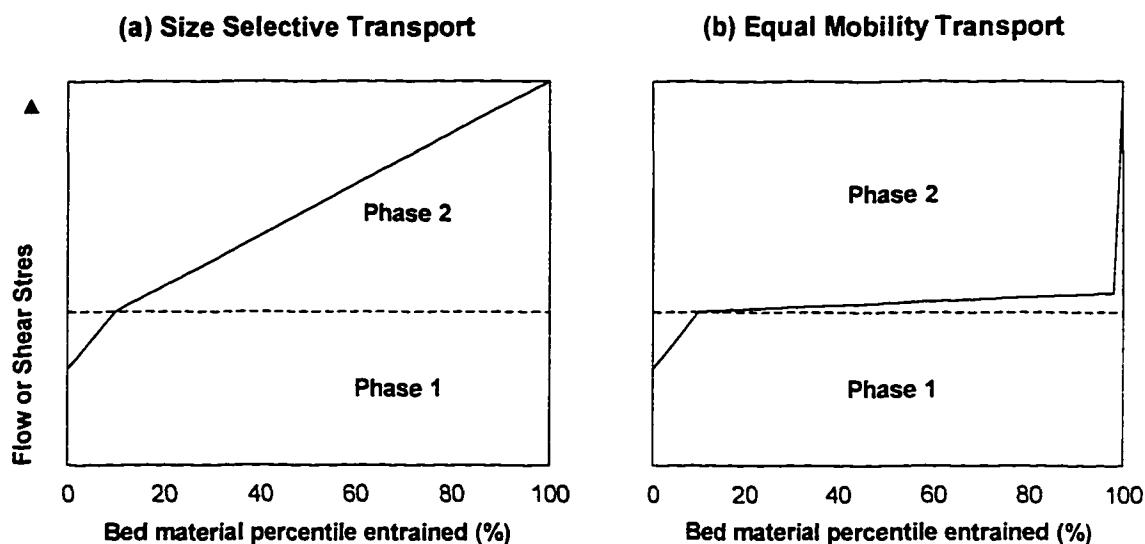
Figure 2.1 Illustration of the size selective hypothesis versus the equal mobility hypothesis for bed load transport in heterogeneous sediments. The transition from phase 1 to phase 2 transport occurs when the flow competence relationships cross the dashed line.

A more discontinuous relationship for flow competence is proposed in the equal mobility hypothesis in Figure 2.1b. Particle interactions during entrainment of the riffle sediments cause the majority of the bed material size distribution to be mobilized at a single threshold flow. In this situation, prediction of stream bed mobility is simplified to the identification of this threshold flow.

Entrainment criteria for gravel-sized particles on river beds are typically defined in terms of shear stress, although for steeper streams it is suggested that critical unit discharge relationships are more reliable and convenient (Bathurst et al., 1987). As both methods are based upon the Shields criterion, they have an equal theoretical footing and are subject to the same limitations (Bettess, 1984; Ferguson, 1994).

2.2 Shear Stress Criterion

The Shields criterion (Shields, 1936) is the most widely used method of predicting thresholds in bed load initiation:

$$\tau_{ci} = \theta_{ci}(\rho_s - \rho)gD_i \tag{1}$$

where τ_{ci} and θ_{ci} are, respectively, the critical shear stress and Shields dimensionless parameter to entrain a particle of diameter D_i, ρ_s and ρ are the densities of sediment and water respectively, and g is the acceleration due to gravity. Mean cross-sectional shear stress can be estimated as:

$$\tau = \rho gRS \tag{2}$$

where S is the water surface slope and R is the hydraulic radius (in wide and shallow channels R can be approximated by mean flow depth). Work in gravel bed rivers has shown that the critical shear stress varies as a function of both absolute particle size D_i and the relative size D_i/D_{50} (White and Day, 1982; Parker et al., 1982b; Andrews, 1983; Komar. 1987). The importance of relative particle size is attributed to the hiding and exposure effect. Larger-than-average particles are easier to move due to exposure, and smaller-than-average particles are more difficult to move due to hiding. Hiding and exposure effects can be explained quantitatively from the drag and lift forces acting on bed geometries with

different packing arrangements and pivot angles (Komar and Li, 1986; Naden, 1987; Wiberg and Smith, 1987).

Andrews (1983) modeled the hiding and exposure effects on critical shear stress via the Shields dimensionless parameter:

$$\theta_{ci} = \theta(D_i/D_{50})^x \tag{3}$$

where D_{50} is the median particle size of the bed material, θ represents the Shields dimensionless parameter in homogeneous sediment when $D_i/D_{50} = 1$, and the exponent x indicates the rate at which θ_{ci} diminishes as D_i increases. Taking values of θ and x from the literature (Komar, 1989; Petit, 1994), the critical dimensionless shear stress in (3) can be calculated and used in (1) to determine the critical shear stress for entrainment of a given particle size. Equation (2) can be rearranged to determine the critical depth for entrainment, which can then be translated into a critical discharge through a stage-discharge curve.

Values of x obtained by various workers range from 0.65 to 1.0 (Andrews, 1983; Ashworth and Ferguson, 1989; Komar, 1989; Parker et al., 1982b; Whitaker and Potts, 1996), suggesting that the critical stress to mobilize a particle depends more on particle size relative to the D_{50} than its own size. In the case of $x = 1.0$, all particle sizes present will move at the same critical stress or discharge demonstrating equal mobility in entrainment (Parker and Klingeman, 1982). There is consensus that equal mobility is reached at high excess stresses and transport rates, but there is disagreement concerning the range over which entrainment is size-selective (Bunte, 1992; Komar and Shih, 1992).

One reason for the wide range in values obtained for the exponent x is that the critical flow for the entrainment and transport of a given particle size is defined in two different ways. On the one hand, the maximum particle sizes sampled in transport at different flows is used to define the critical flow condition for mobilization of these sizes. If tracers are placed in the channel, the peak flow in a given flood is defined as critical for the largest particle entrained in that flood, provided larger immobile sizes are present in the channel (Carling, 1983; Komar, 1987). Alternatively, the relative transport rates of the different grain-size fractions are examined, and the threshold of motion for each size fraction defined as the flow which produces a small reference transport rate (Parker et al., 1982b; Wilcock and Southard, 1988). This often involves extrapolation of the relationship between measured transport rates and discharge, and hence can be in error if there are discontinuities in this relationship.

Petit (1987) demonstrated that shear stress calculated from equation (2) is a reliable criterion in explaining erosion and transport of bed load, which determines the shape of the stream bed. However, three related problems must be taken into consideration in the evaluation and application of this parameter. First, total shear stress has two components; one due to grain resistance over the stream bed surface, and one due to irregularities in the shape of the stream bed and banks. In theory, only the shear stress due to grain resistance should be considered in the transport of bed load, but in practice the division of total shear stress into these two components remains problematic. Therefore in most cases, authors have related total shear stress to particle entrainment in deriving flow competence relationships. This approximation is more reasonable in relatively wide and shallow

channels over riffles where bank effects are negligible and grain resistance is the dominant shear stress component (Hey, 1979). Carling (1983) demonstrated the significance of this variation in bed form resistance with channel width. In a narrow stream channel, he found that threshold values of total shear stress were considerably higher than those values obtained in a broad stream channel, because a greater proportion of shear stress is taken up in overcoming bed form resistance in narrower channels.

A better estimate of the grain resistance shear stress which determines bed load movement can be obtained by the method involving friction velocities. The problem with the friction velocity approach is that a roughness parameter for the stream bed must be defined. While bed roughness is dependent on the size distribution of stream bed sediments, complex interactions between unsteady flow, bed load transport, and bed roughness have been documented (De Jong and Ergenzinger, 1992; De Jong, 1993; Ergenzinger et al., 1994). Differences in the arrangement and mix of particles also play a significant role in determining the critical shear stress required to initiate movement of particles on the stream bed (Reid et al., 1985; Powell and Ashworth, 1995). For any given particle size, the critical shear stress can vary several fold, even after allowance for the hiding/exposure effect, due to factors which are not currently included in entrainment criteria. This unpredictable variation in the critical flow condition required to mobilize stream bed sediments may hinder the application of both the shear stress and the unit discharge criteria.

2.3 Unit Discharge Criterion

An alternative entrainment criterion follows the Schoklitsch approach (Schoklitsch. 1962, p.174) which is based on the water discharge per unit flow width rather than on the mean shear stress exerted by the flow. Bathurst et al. (1987) proposed the following equation to predict entrainment of individual size fractions, with adjustment necessary for the hiding and exposure effects:

$$q_c = 0.15g^{0.5}D^{1.5}S^{-1.12}$$ (4)

where q_c is the critical unit discharge to entrain a particle of diameter D. The above semi-empirical equation is based on flume data for uniform sediments ranging over 3-44 mm in b-axis and slopes of 0.25-20%. Bathurst (1987a) used this equation to predict entrainment of the reference particle size in heterogeneous stream bed gravels. The reference size is the particle diameter which is unaffected by any hiding or exposure, as in the case of a uniform size bed. The hiding and exposure effects are then modeled in the same form as equation (3):

$$q_{ci} = q_{cr}(D_i/D_r)^b$$ (5)

where q_{ci} is the critical unit discharge for entrainment of a given size fraction. q_{cr} is the critical unit discharge for the reference size calculated from (4), and b is an exponent.

Bathurst (1987a) proposed the following relationship to estimate the exponent b in equation (5):

$$b = 1.5(D_{84}/D_{16})^{-1} \qquad (6)$$

where the greater the difference between the D_{84} and D_{16}, the stronger is the hiding/exposure effect and the smaller b becomes. A small b produces a narrow range in discharge over which all particle sizes are brought into motion, and the bed load process tends toward more equal mobility.

The unit discharge criterion may be more suitable in small upland streams with boulder beds, where individual particles extend through a significant portion of the flow depth, or even extend above the water surface. Under these conditions the assumptions in the shear stress approach are far from being met, and it is easier to define flow discharges than mean stresses. In steep gravel bed streams of about one percent or more, a case may be made for the use of either entrainment criteria, but there has been no field research comparing their relative performance.

2.4 Armor and Pavement Layer Dynamics

The critical flow condition for the entrainment of bed material can be estimated with the empirical equations given above, using information regarding particle size and adjusting for the hiding/exposure effect. However, other features of gravel bed streams

which influence the entrainment process are not accounted for in these equations. Perhaps the most important feature is the frequent occurrence of a relatively coarse layer of sediments over the surface of the stream bed, referred to as armor or pavement (Andrews and Parker, 1987). Beneath this surface layer the size distribution of the sediments is significantly finer. The origin of this armor layer remains unclear, but may be due to size selective transport during smaller floods transporting finer fractions while coarser fractions are largely immobile (Gomez, 1983). Once formed, the coarse surface layer can inhibit entrainment and transport of the finer fractions below, which can not be mobilized until breakup of the surface occurs. Only during floods capable of disrupting the armor layer will equal mobility transport take place.

Parker and co-workers (Parker et al., 1982a and 1982b; Parker and Klingeman, 1982) believe that most armor features are frequently mobilized during bed load transport events, and therefore prefer the term 'pavement' rather than armor. Static armor is rare, but may be found downstream of dams where the supply of coarse sediment has been cut off. They suggest the pavement can coexist with the motion of all available grain sizes because motion is sporadic, so at any given time only a small percentage of surface grains are actually in motion. The pavement is seen as a fundamental feature of gravel bed streams, acting as a buffer between the flow and moving bed load, and the sub-pavement which constitutes the bulk of material temporarily stored in a reach. Parker and co-workers claim that this mobile pavement renders all grain sizes in temporary channel storage of near-equal mobility. Relatively small and large particles may be mobilized with similar frequency because the over representation of coarse sediments in the

pavement compensates for their greater mass and lower intrinsic mobility. However, the way in which equal mobility is defined causes much confusion in this respect.

When using the term equal mobility, one must clarify the subject is the process of particle entrainment alone, or the complete bed load transport process. For example, in the argument of Parker and co-workers, the gravel pavement equalizes the frequencies at which different particle sizes are entrained. But once entrained, the finer fractions are more likely to remain in transport for longer distances (Church and Hassan, 1992) and move at greater speeds producing greater transport rates than would be expected if only their relative abundance in the stream bed was considered. Bed load transport measurements from natural channels have shown selective transport over a range of stage (Milhous, 1973; Carling, 1983; Ashworth and Ferguson, 1989). Thus equal mobility may be expressed in terms of particle entrainment frequencies, without necessarily having equal mobility in terms of particle transport rates due to differences in travel distance and speed. These two definitions of equal mobility can be summarized as; (1) Entrainment equal mobility - frequency of entrainment across different size fractions remains constant; (2) Transport rate equal mobility - transport rates of different size fractions are proportional to the relative abundance of each size fraction in the substrate size distribution.

Therefore, it does not necessarily follow that all sediment sizes in the stream channel are transported at equal rates. Indeed, the fact that gravel bed stream sediments tend to become finer in the downstream direction is often cited as evidence for the dominance of size dependent transport rates in these systems. Also, large depositional features in the

channel composed of exclusively fine sediments is evidence for size selective transport over significant periods of time. Rates of transport for the finer particles must far exceed those for the coarser fractions for these deposits to develop.

Progressive armoring of the stream bed between floods may change the critical flow condition for the initiation of bed load transport, and rates of bed load transport at a given flow (Gomez, 1983; Reid et al., 1985). The characteristics of the bed surface are strongly affected by antecedent flow conditions, such as the magnitude of the most recent preceding event capable of transporting bed material. Reid et al. (1985) used a continuous sampling record to show that the threshold of bed load initiation varied according to the elapsed time between bed load moving floods. Long periods of inactivity allowed consolidation of the channel bed so that bed load was largely confined to the recession limb of the next flood wave. But when floods followed each other closely, the bed material remained comparatively loose and was entrained at lower shear stress values. Critical shear stress values for bed load initiation ranged up to five times the overall mean in the case of isolated floods or those which were the first of the season.

Additionally, Reid et al. (1985) demonstrated that the threshold of bed load initiation occurred at levels of shear stress three times those for which motion ceased. Higher threshold values for initial motion may be due to particle interlock and to the hiding of one grain by another, especially where clusters are a significant component of the microrelief (Brayshaw et al., 1983; Reid et al., 1984; Brayshaw, 1984, 1985; De Jong, 1991; Reid et al., 1992). More power may be required to initiate than to maintain bed

load motion due to the differences between static and dynamic friction (Francis, 1973; Reid and Frostick, 1984).

Laronne and Carson (1976) presented a good discussion of the importance of bed morphology and structure in determining the critical flow for entrainment of different grain sizes. They reasoned that where the particle size range is large, features of the channel bed such as imbrication and vertically-infilled tight structures can develop which increase the critical flow for entrainment. Mobilization of the particles was associated with the destruction of these interlocking structures, or at least movement of those particles immediately upstream. This imparts a degree of equal mobility in particle entrainment, which the authors claim restricts the utility of flow competence modeling in such channels. Laronne and Carson (1976) also considered the ease of transport of different sized material over an uneven channel bed surface. Particle mobility, as indicated by distance of travel of tracer material, decreased from small pebbles to large cobbles, but also decreased for the finest bed material.

2.5 Bed Load Sampling to Evaluate Flow Competence

Flow competence relationships have traditionally been based upon the largest particle sizes found in samples taken across a range in flows. However, characterization of the transported sediments by one or a few large particles may be unreliable or misleading. Komar and Carling (1991) explored the possibility that competence evaluations may be better based on median rather than maximum bed load grain sizes, using two bed load

data sets which contained information on the full range of particle sizes in transport. Their analysis indicates that the largest particles are an integral part of the overall bed load size distributions, responding to changing flow hydraulics along with the rest of the size distribution. This suggests that flow competence can be defined by either median bed load particle sizes, or coarser size fractions up to the largest particle sizes.

Wilcock (1992) disagreed, maintaining that estimates of flow competence based on an extreme value in the transport size distribution are subject to large errors, and are sensitive to the effect of sample size which tends to vary widely in gravel bed rivers with unsteady transport rates. Large errors and unknown bias render the largest sampled mobile grain an unreliable predictor of either critical shear stress or flow magnitude, so that only central values in bed load size distributions will be reliable (Wilcock, 1992).

Given the above contradictory claims, it seems preferable to sample as much of the bed load size distribution as possible, allowing examination of changes in the maximum particle size as well as changes in the overall bed load size distribution. To achieve this, bed load traps set into the stream bed have been widely used (Milhous, 1973; Reid et al., 1985; Reid et al., 1995). However, the problem with bed load traps is that sample durations often have to be extended over complete flood waves, making it more difficult to link critical flow conditions to the capture of certain particle sizes. A portable sampler that can be positioned in the flow at frequent regular intervals over the passage of a flood hydrograph can achieve higher sampling resolution. Portable samplers also allow a greater number of streams to be studied without the necessity for expensive installations.

Unfortunately, most portable bed load samplers used to date have been of the Helley-Smith design (Helley and Smith, 1971) which is very inefficient in the capture of coarse bed load fractions, has poor sampler-stream bed contact, and will not allow the largest particles to be sampled when they approach the size of the sampler mouth (Custer, 1992). Fluid drag forces exerted by high flows on the Helley-Smith type samplers also make them inoperable when the coarser size fractions are in motion, with the result that sampling is biased towards the finer bed load size fractions. This problem was overcome by Bunte (1990, 1992) who developed a 'large frame-net' bed load sampler. Coarse bed load together with the largest particles in motion were easily captured, although the smallest size fractions passed through the 10 mm net mesh. Further development of this type of sampler would be beneficial in obtaining more information on the dynamics of coarse bed load transport, and it would enable validation of flow competence criteria in current usage.

3. OBJECTIVES

1. Determine whether equal mobility or size selectivity is dominant in bed load transport in a gravel bed stream.

This was achieved by obtaining the size distribution of the bed load, and especially that of the coarse size fractions, over the passage of flood hydrographs. An innovative large frame-net sampler enabled capture of the largest particle size fractions. Distance of travel for different size tracer particles was also observed.

2. Determine whether flow competence relationships can be established for gravel bed streams, and if so, whether the critical shear stress or the critical discharge model is the better predictor.

This was achieved by obtaining the maximum particle size in transport for any given flow. Flow conditions were monitored, and over periods of relatively steady flow, sample groups were taken and the maximum particle sizes measured.

3. Determine which variables are the most reliable in flow competence modeling. The maximum particle size variable was examined together with alternatives such as the mean of the three largest particles and percentiles of the bed load size distribution.

This was achieved through regression analysis with the flow competence data set.

20

4. Determine whether particle mobility is best predicted by particle size, or by particle mass.

This was achieved by analysis of tracer particle movement, where distance of travel was measured for particles of known size and mass. Also, flow competence relationships were compared using either maximum particle size or maximum particle mass in transport at a given flow.

5. Examine changes in the channel morphology associated with coarse bed load transport.

This was achieved through surveys of channel cross sections and long profiles between flood events.

4. STUDY AREA

4.1 Identification of Suitable Sampling Site

The purpose of this study was to investigate the relative mobility of different size fractions in the channel bed for streams composed primarily of gravels and cobbles. To maximize the opportunity to sample this type of bed load, a stream was chosen which displays regular movement of these gravels and cobbles. Evidence for high channel bed mobility includes; absence of a coarse pavement layer, loose arrangement of particles, smooth and rounded particle shapes, and freshly deposited gravel bars containing the full range of particle sizes. Active channel migration, as evidenced by widespread bank erosion and fresh bar deposits, also indicates that bed load transport is unlikely to be limited by any shortage in the supply of coarse sediment. Dupuyer Creek has these characteristics of an active alluvial channel. The sampling site was located on the Theodore Roosevelt Memorial Ranch, situated in Teton County some 120 km northwest of Great Falls, Montana (Figure 4.1).

4.2 Watershed Geologic and Hydrologic Characteristics

Dupuyer Creek originates east of the Continental Divide in the Sawtooth Range of Montana's Rocky Mountain Front (Figure 4.2). North and South Forks emerge from the mountains in separate canyons, before joining and flowing across the plains towards the

22
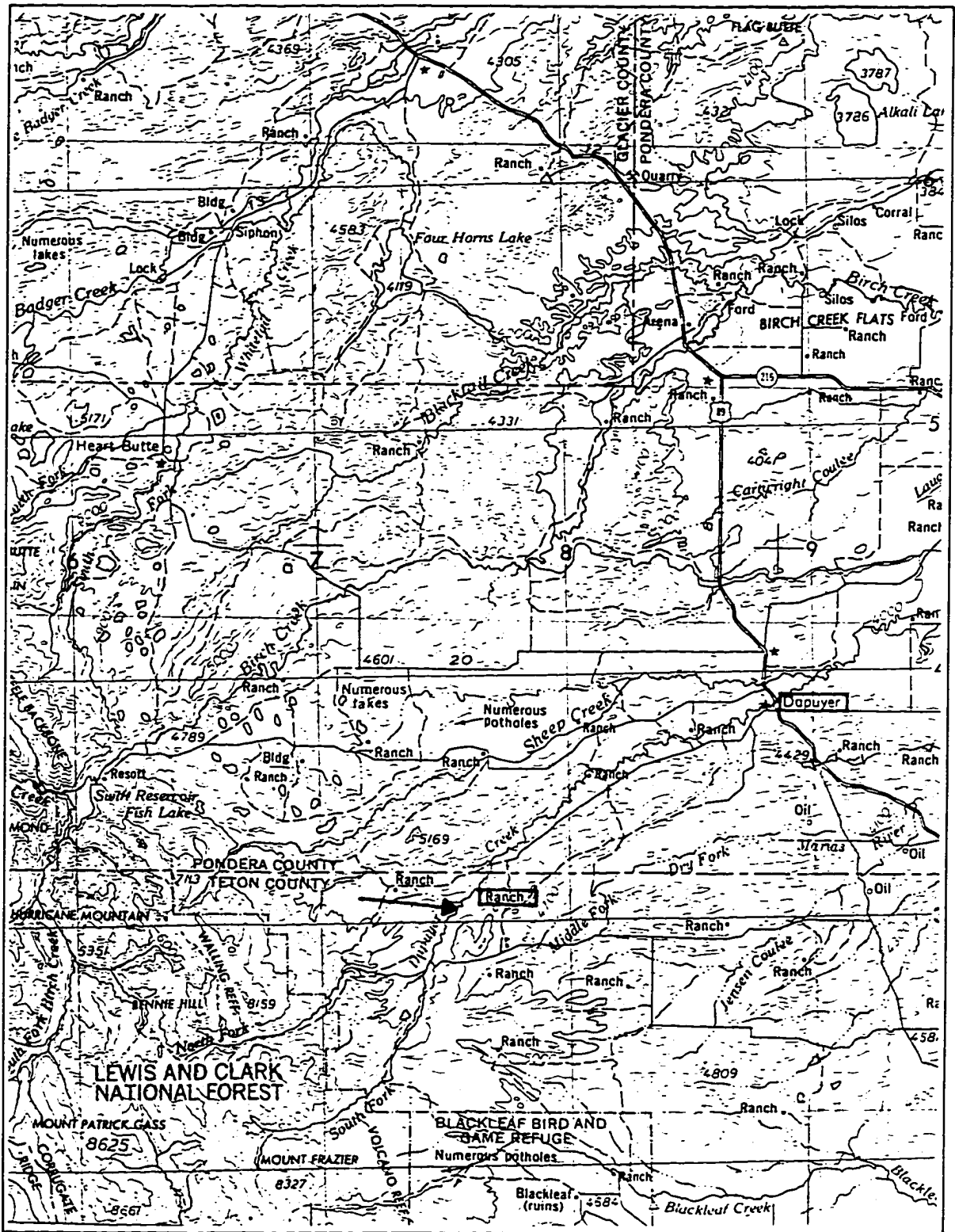
Figure 4.1 Location of Dupuyer Creek and the study reach in Teton County, Montana
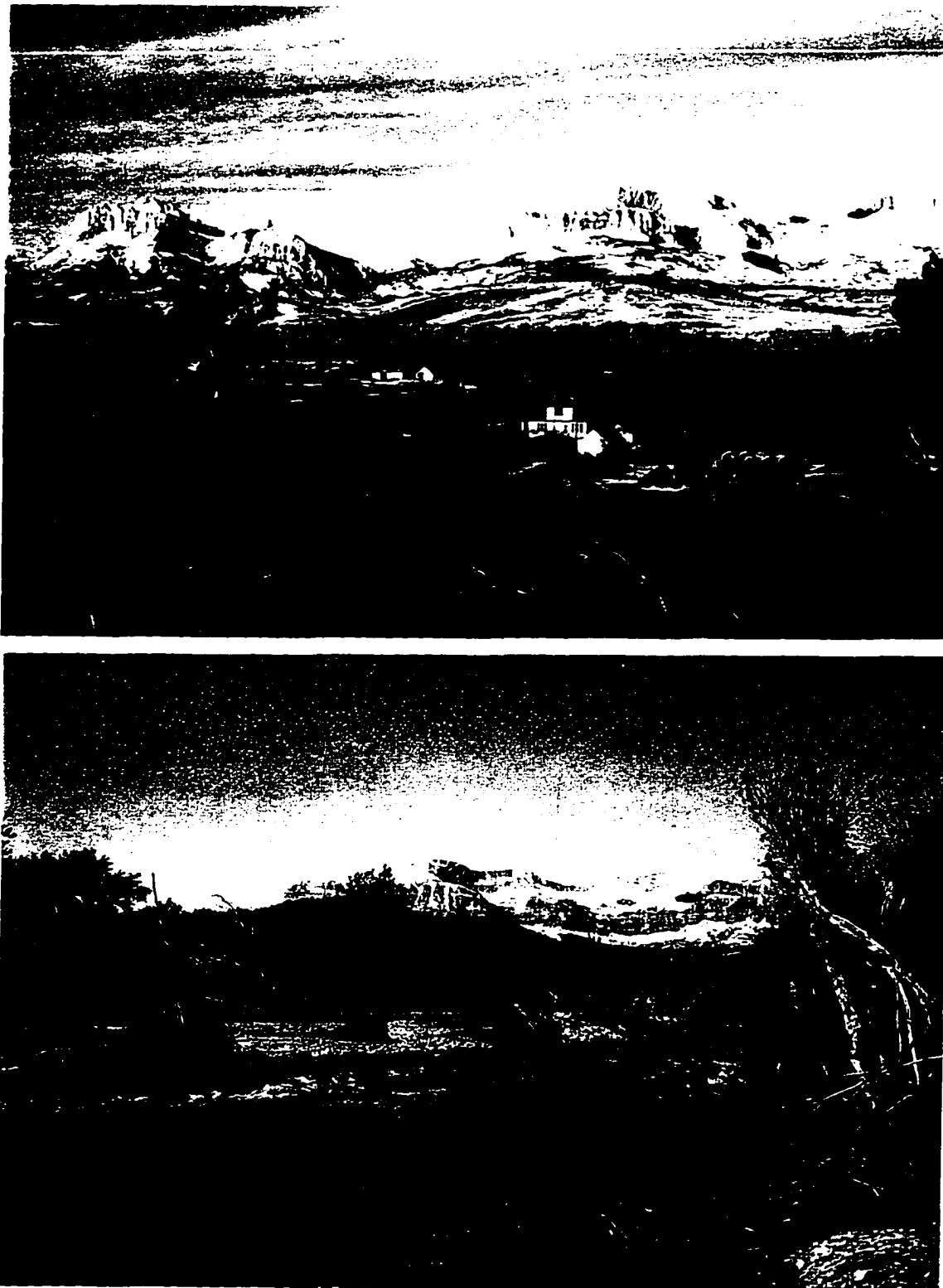
Figure 4.2 Dupuyer Creek watershed on Montana's Rocky Mt. Front, study reach in the center ground (top). Dupuyer Creek at high flow, June 1995, downstream from the point of bed load sampling (bottom).

Missouri River. The sampling site is located about 3 km downstream from the confluence, and 8 km from the mountain front, with a catchment area of 83 km^2. The geology in the upper part of the watershed is dominated by thrust belt folding and faulting in Paleozoic Madison Limestone and Mesozoic sandstones and shales (Ross, 1959). The result is a landscape of steep topography with parallel ridges of limestone separated by deep valleys and canyons. The eastern rampart of the Sawtooth Range is composed of 600 m high cliffs of Madison Limestone thrust over Mesozoic sandstones, clays, shales and mudstones of the foothills and plains. North and South Forks exit narrow limestone canyons at an elevation of 1700 m, and flow over Mesozoic rocks to an elevation of 1400 m at the study reach.

The hydrologic characteristics of Dupuyer Creek and its tributaries are strongly influenced by the geological structures and rock types. The creek produces rapid hydrologic response to rainfall and snowmelt. The first order tributaries are very steep ephemeral washes which transport large quantities of coarse sediment, scree and boulders. These feed into gentler intermittent channels which join to form the perennial North and South Forks. There is very little soil development in the upper drainages, with large slopes of bare rock limiting the extent of forest cover to the lower slopes and valley bottoms (Inceptisols & Alfisols: Cryochrepts-Cryoboralfs-Lithic Cryoborolls). The foothills and range land to the east of the mountains have soils which are often rich in clay, particularly at the surface, limiting infiltration and leading to widespread overland flow during prolonged spring rains (Mollisols & Inceptisols: Argiborolls-Calciborolls-

Cryobrolls-Cryochrepts-Ustochrepts). These factors combine to produce a relatively flashy hydrologic regime in Dupuyer Creek.

The seasonal flow regime is dominated by spring floods from rainfall and snowmelt. The channel-forming flows move large quantities of bed load in the months of May and June. Mountain snow pack accumulations are often insufficient to produce large floods by snowmelt alone, but prolonged frontal rainfall in combination with snowmelt causes extensive flooding. Rain-on-snow floods produce an abrupt rise in the hydrograph from the winter base flow, followed by extended high flows which can entrain bed load over a period of several days in larger events. Diurnal snowmelt peaks do occur, but the rainfall component often dominates the hydrograph behavior. Bed load transport is therefore restricted to one or two floods each year, producing perhaps five to ten days of activity.

4.3 Watershed Land Use

The primary land use in the watershed is livestock grazing. The upper mountainous section lies within the Bob Marshall Wilderness of the Lewis and Clark National Forest. While there has been no road construction, mining, or timber harvesting, there is significant cattle grazing during the summer months. Historical records indicate that livestock grazing may have been intense in the early part of this century, but current livestock numbers are relatively low and visible impacts are mainly associated with crossings. In these localized regions the grazing can be seen as having an effect, but at the larger reach scale it is difficult to determine the significance of grazing influences. Below

the wilderness, the stream channel is locally influenced by the maintenance of road bridge crossings and fords, and small irrigation diversions.

4.4 Characteristics of the Study Reach

The main fork of Dupuyer Creek above the sampling site consists of a meandering single thread channel, with alternate, transverse, and mid-channel bars, and sequences of riffles and pools. Pool spacing is notably uneven. The tendency is for longer riffles to alternate with clusters of pools. Bankfull width averages 10 m, mean slope is one percent, and channel bed materials are predominantly gravels and cobbles with a median particle size of about 50 mm. Several reaches of Dupuyer Creek are confined between steep banks of loose and uncohesive sand, gravel, and cobbles (Figure 4.3). Confinement prevents stream access to the flood plain during the frequent 1-2 year return period flood events. These confined reaches alternate with unconfined reaches which are able to flood gravel bars and the flood plain during the more frequent events (Figure 4.3). Flow depths are higher in the confined reaches, with correspondingly higher shear stresses and unit discharges, which produce efficient transport of bed load through these channel sections.

The study reach map (Figure 4.4) shows the location of the sampling bridge and stilling well on a particularly long and straight riffle section. This enables relatively uniform flow conditions to be reached across the channel width at the sampled cross section. Cross section 3 (Figure 4.4), positioned just upstream of the bed load sampling point, illustrates the flume-like nature of the channel which also promotes more uniform

Figure 4.3 Main riffle in confined part of the study reach, where bed load was sampled from the bridge (top). Upper riffle in the study reach was less confined (bottom).
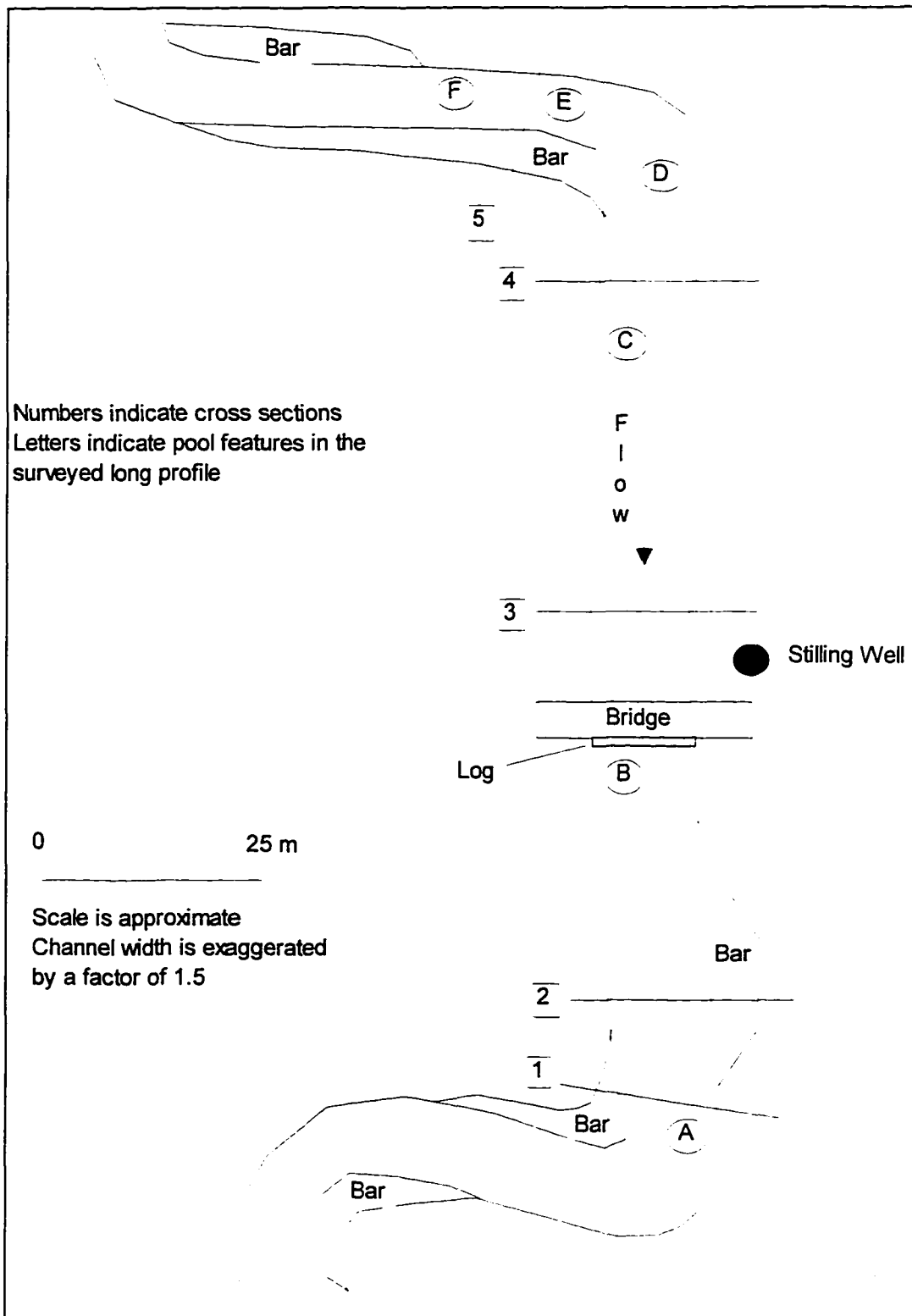
Figure 4.4 Study reach sketch map locating the bed load sampling bridge and the surveyed channel features.

flow. The wide and flat channel bed produces flow depths that are relatively constant across the channel width, with mean depth closely approximating the hydraulic radius.

The stream bed sediments appear clean of algae after a flood, and the surface layer is very loose and easily disrupted, indicating recent movement of the material. Limestone particles dominate the coarse sediments, and are rounded. Less abundant sandstone clasts tend to be platy. Orderly sedimentary structures such as imbrication and clustering are mainly absent, and excavation of the channel bed did not reveal the presence of any significant coarsening in the surface layer. These observations imply the absence of pavement. As is common in gravel bed rivers, the size distribution of the channel is highly variable depending on the location relative to pools and riffles, and other local
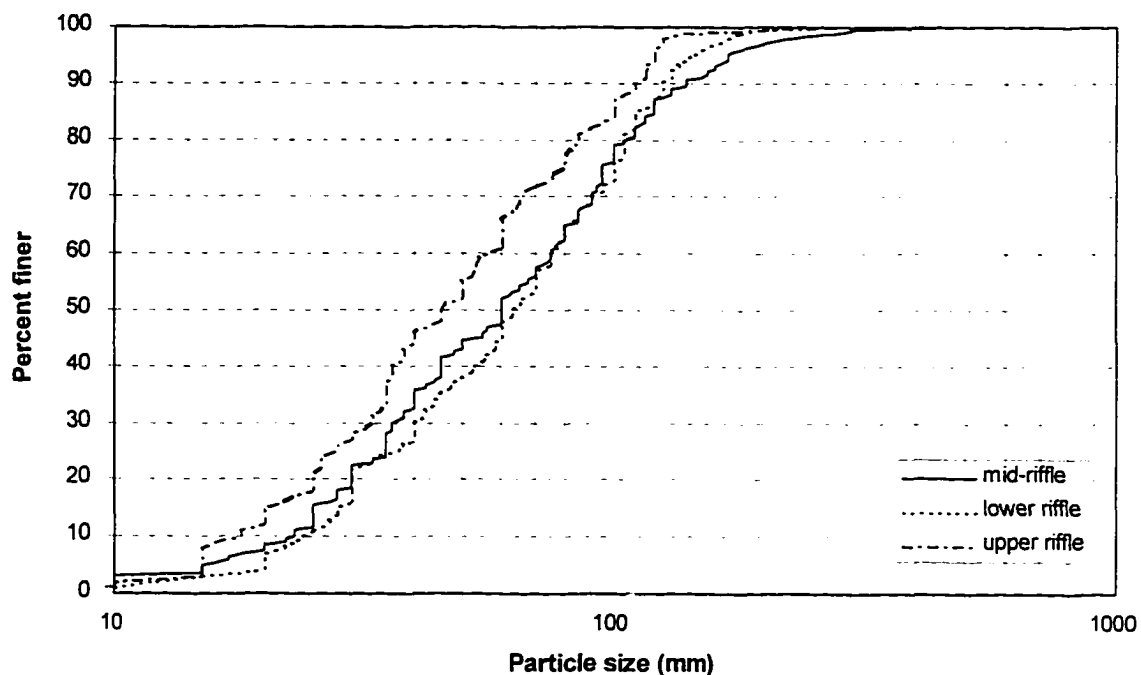
Figure 4.5 Particle size distribution over the riffle where bed load was sampled, pre-flood pebble counts.

flow phenomena. Size selective deposition of finer material occurs on gravel bars, and in other regions of reduced velocity such as pools during the tail end of flood hydrographs. Figure 4.5 shows the results of initial Wolman pebble counts (Wolman, 1954) over the long riffle where bed load was sampled. The D_{50} ranged from 45-63 mm, and the D_{84} ranged from 100-112 mm.

5. METHODS

5.1 Coarse Bed Load Sampling

Flow competence criteria relate streamflow parameters to a maximum particle size that can be entrained in transport. In validating flow competence criteria it is essential that the largest particles in motion on the stream bed can be efficiently sampled, and related to the flow conditions at the time of sampling. The problem is that most bed load samplers have been designed to capture the finer bed load fractions, and they are incapable of capturing the maximum particle sizes in motion (Custer, 1992). An important part of this study was therefore the design and construction of a bed load sampler which captures all particles gravel sized and larger.

Bunte (1990, 1992) developed the 'large frame-net' bed load sampler which used a 10 mm net mesh attached to a wooden frame opening measuring 1.6 m by 0.3 m. In this study a stronger and more stream-lined sampler was constructed by using a steel pipe frame opening 1.0 m wide by 0.4 m tall, to which a nylon net of mesh size 32 mm was attached (Figure 5.1). The significance of the sampler design will be discussed, and comparison made to the commonly used Helley-Smith samplers (Helley and Smith, 1971). The influence of temporal variations in bed load transport on sample duration and sample size is also addressed.

32
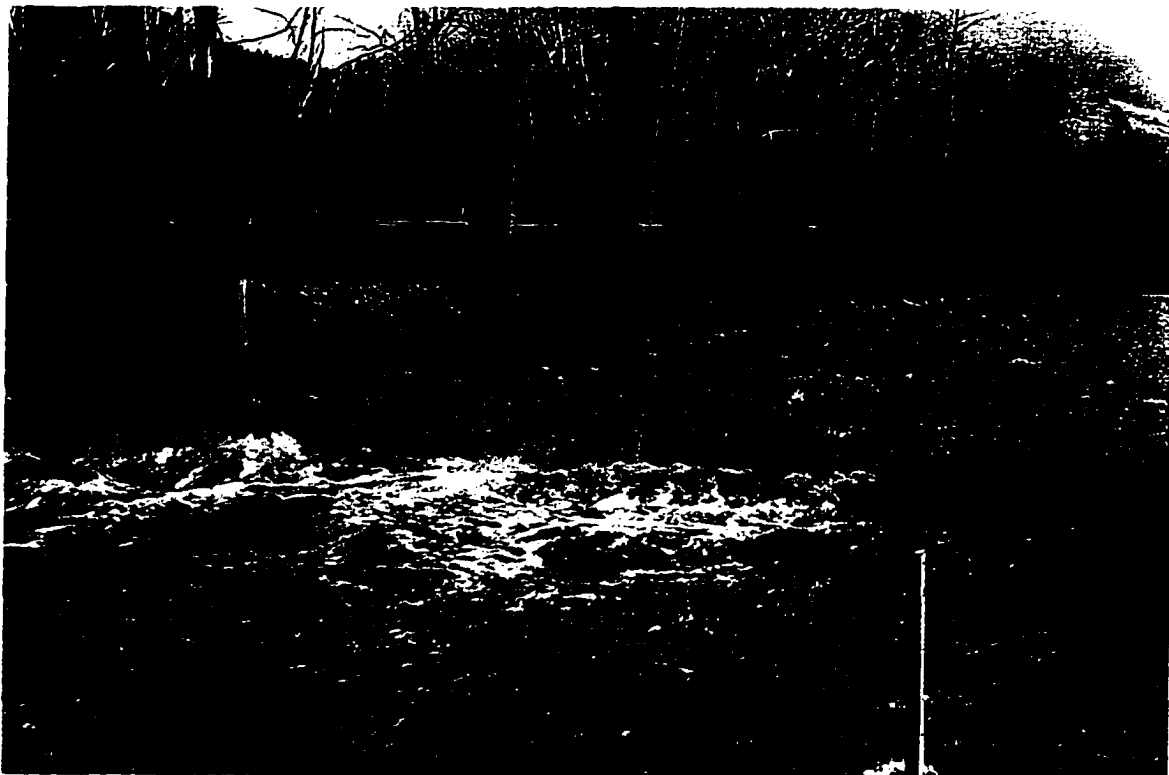
Figure 5.1 Large frame-net bed load sampler with steel pipe frame and nylon netting (top). Sampler in position on the log sill and secured to the bridge (bottom).

5.1.1 Aperture size

The most significant attribute of a coarse bed load sampler is the size of the sampler opening, or aperture, through which the bed load must pass before entering the storage component. A major problem with the Helley-Smith sampler is that the 76x76 mm or 152x152 mm aperture sizes available will not allow capture of the larger particles present in gravel bed streams. Flume studies by Hubbell (1987) using a 76 mm square orifice indicated a trap efficiency of about 100% for only the small particle sizes from 0.5-32 mm. Even with the larger 152 mm square orifice, the maximum particle size that can be captured is limited to about 150 mm. Gravel bed streams commonly have particle size distributions that extend into the cobble (64-256 mm) and boulder (>256 mm) size fractions. Dupuyer Creek contains particle sizes ranging up to 400 mm. The large frame-net sampler is able to capture all of the particle sizes present, including those in the boulder size range.

5.1.2 Proportion of flow width sampled

Related to the aperture size is the proportion of the flow width that is sampled when the sampler device is in position. The greater the width of the sampler opening, the greater the proportion of flow width sampled. The large frame-net sampler opening width of 1000 mm far exceeds the 60 mm or 120 mm opening width for the Helley-Smith, and is therefore a much more efficient sampling device for coarse bed load which may be highly variable across the channel width.

5.1.3 Sampler-stream bed contact

Stream beds composed of coarse sediments present an uneven surface on which the sampler mouth can not achieve flush contact. Some bed load will therefore pass beneath the sampler, or the sampler may scoop sediment. The large frame-net sampler was designed so that it could be positioned below a log sill installed in the stream bed (Figure 5.2). All of the bed load must then pass over this sill and into the sampler opening, maximizing the sampler efficiency.
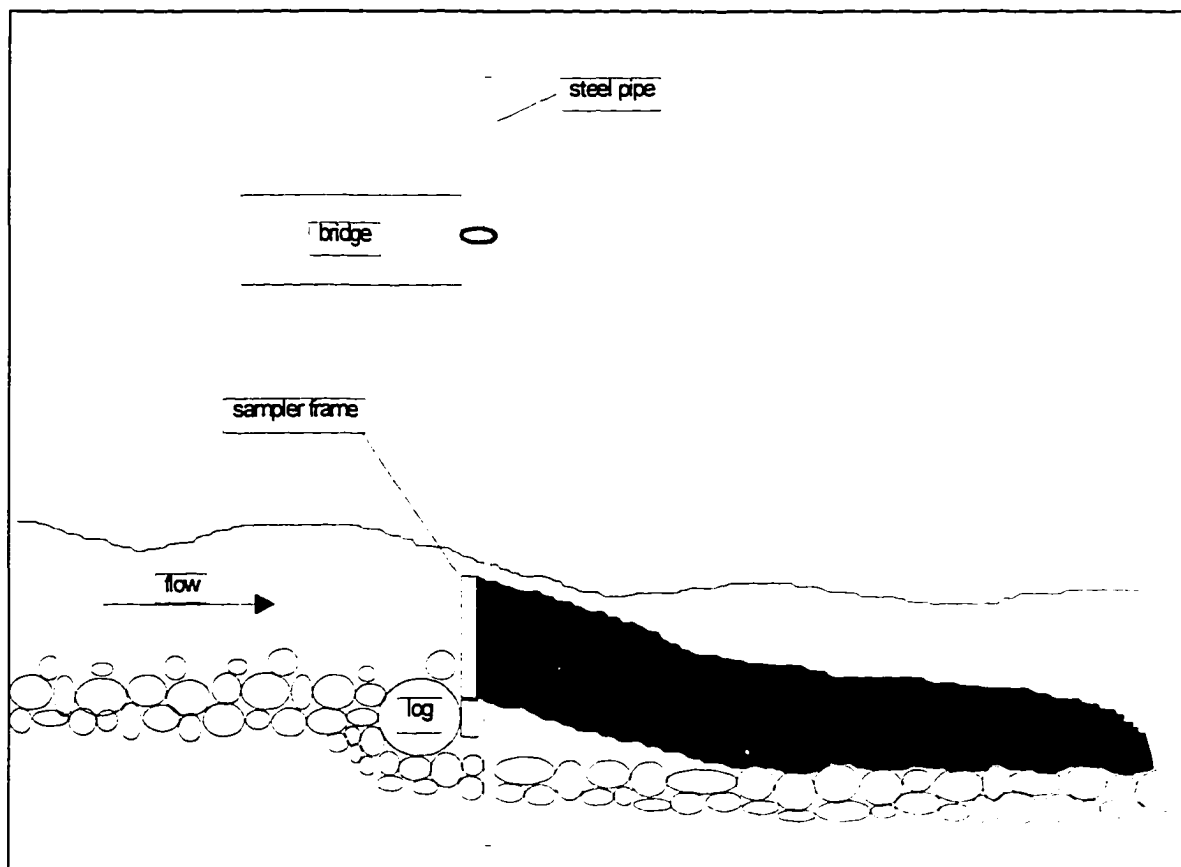
Figure 5.2 Schematic illustration of the bed load sampling at Dupuyer Creek with the large frame-net sampler. The sampler frame sits flush on the log sill, and is released by removing one of the steel support pipes. The second pipe is hidden behind the one shown.

5.1.4 Maintaining sampler position in high flows

Flow velocities are high in gravel bed streams when bed load transport is active. Consequently hand-held samplers are unmanageable because the fluid drag forces are too strong to be overcome by the operator. The Helley-Smith with its fine net mesh presents very high drag, and was in-operable in Dupuyer Creek for coarse bed load sampling. Fish-type Helley-Smith samplers are difficult to control, so that sampler position is often hard to predict. The large frame-net sampler is positioned against two steel pipes driven into the stream bed (Figure 5.2). Precise positioning can be achieved and the sampler can be operated in high flow velocities of over 3 m/s.

5.1.5 Flow disturbance

As with any sampling device, there is concern that the process being sampled is disturbed by the presence of the sampler in the flow. The large frame-net sampler with its large aperture size and 32 mm net mesh minimizes flow disturbance and any interference in the bed load transport process. However, the installation of the log sill in the stream bed had a greater influence on the local hydraulics. The step in the stream bed creates a zone of super-critical flow followed by a series of standing waves at higher flows. Local adjustment in the stream bed took place during the early stages of the first bed load moving flood, after which the channel was adjusted to the presence of the nick point. Immediately above the sill the channel gradient was slightly reduced, while below the sill a new scour pool developed. Once this adjustment had been made, there was no reason to

suspect that bed load processes were being changed in terms of rate of movement and size characteristics.

5.1.6 Operation of the bed load sampler

Operation of the large frame-net sampler requires two persons, or preferably three when obtaining larger sample sizes. Once sampling was complete, one of the steel pipes was removed to release the sampler frame from position. Rope attached to the sampler frame was used to maneuver the sampler onto the gravel bar downstream of the sampling point. The streamflow and submerged buoyancy of the bed load sample help in this process. Very large samples could be winched from the stream bed, but this dramatically increases the time required to empty and reposition the net, reducing the amount of time in a given period for which bed load is being sampled.

Two persons operating the sampler, without the benefit of a winching system, could still obtain eight 2 minute samples or six 4 minute samples over the period of an hour. Therefore, the sampler could be in position collecting bed load for 16-24 minutes in every hour, with a rapid turn around time of only 6 minutes required to release, empty, and reposition the net. Sample duration ranged from 1 minute during peak bed load activity, to 60 minutes during marginal bed load activity, with a mean sample size of 40 kg and a maximum of 242 kg. Without knowledge of the prevailing bed load rate at the start of each sampling session, some experimentation was required to find a sample duration that would give manageable sample sizes.

5.1.7 Trap efficiency of the sampler net

The large frame-net sampler with a 32 mm mesh is designed to trap the largest particles in motion, while allowing the finer fraction of the bed load to pass through. The advantage of this strategy is that sample duration can be increased to capture a greater sample mass of the coarse bed load fraction without overloading the sampler net. Consequently information is lost regarding the finer bed load fraction, and total rates of bed load movement can only be estimated. However, this compromise is necessary when the primary purpose of sampling is to establish flow competence. If the main objective was to measure total bed load rates, then finer net mesh sizes could be employed with the large frame-net sampler.

With a net mesh size of 32 mm there is the possibility that some particles with b-axes of 32 mm may still pass through the net. In the analysis of the bed load samples, trap efficiency is assumed to be 100 percent for particles 38 mm or larger in the b-axis dimension. It was found that as the sampler net fills with coarse bed load, a point is reached when significant numbers of particles <32 mm are captured because the presence of larger particles in the net prevents the smaller ones from passing through. Once the net trap efficiency rises in this manner, the sample size increases dramatically as a greater proportion of the total bed load is captured. Coarse bed load is therefore sampled more efficiently if sample durations are kept short enough that this over loading of the net does not occur. The net can then be removed from the channel and emptied more rapidly, increasing the amount of time over which coarse bed load is being sampled.

5.1.8 Sampling strategy

An inherent characteristic of the bed load transport process is that sediment moves in pulses or waves, even during steady flow conditions (Leopold and Emmett, 1976; Ergenzinger and Custer, 1983; Reid et al., 1985; Iseya and Ikeda, 1987; Kuhnle and Southard, 1988; Dinehart, 1989; Gomez et al., 1989). A single sample of 1-2 minutes may not contain the largest particles in motion under the prevailing flow conditions. Therefore, series of samples were taken over periods of 1-2 hours during which flow conditions remained steady. To validate the flow competence criteria, the largest particles captured for each sample series were paired with the mean flow condition during that time. This strategy ensures that the flow condition is linked more closely to the largest particles in motion at any given time.

The floods on Dupuyer Creek tended to have steep rising limbs, followed by extended and more gradual falling limbs during which the majority of samples were taken. One concern with bed load sampling for flow competence evaluations is that the largest particles captured are already in motion, and may perhaps have been entrained at an earlier much higher flow (Reid and Frostick, 1984). This concern arises particularly on steeper falling limbs of flood hydrographs after a sharp peak has occurred. If this were the case, then particle sizes trapped would be paired with a critical flow condition which was too low, and flow competence would be over-predicted.

The way in which bed load moves downstream determines whether this is a real problem or not. Unfortunately our knowledge of the bed load process precludes any firm conclusion. The evidence suggests that bed load moves in a series of steps and collisions.

interrupted by periods of time when the particles are caught in stable locations. As streamflow decreases, the larger particles are more likely to find stable pocket locations, reducing the transport rate for that size fraction. Significant transport of larger particles set in motion by earlier high flows does not seem likely with this scenario for bed load movement. In this case, hysteresis effects are not considered significant, and the threshold of entrainment is assumed to be close to the threshold of deposition.

Another possible concern is that sediment supply dynamics can create hysteresis effects in bed load transport relationships (Leopold and Emmett, 1976; Bagnold, 1977; Bathurst, 1987b). Available sediments may be exhausted on the rising limb of the flood hydrograph, so that bed load transport rates are significantly lower on the falling limb. Conversely, large volumes of sediment may only be released from storage once a critical flow is reached, so that transport rates are highest on the falling limb of the flood. These effects are unlikely to dominate in Dupuyer Creek where there is an unlimited supply of sediment from the mobile bed, gravel bars, and actively eroding banks.

5.1.9 Sieving bed load samples

All bed load samples were hand sieved in the field with Gilson screens of 25, 38, 51, 64, and 76 mm sizes, with particles larger than 76 mm measured by ruler along their b-axis. The three largest particles in each sample were always measured along their b-axis by ruler. As far as possible, even phi size classes were used to establish the particle size distribution, but class boundaries were controlled in part by the available sieve sizes. For the June flood bed load samples, the 25 mm size sieve was abandoned because capture in

the 25-38 mm size range was incomplete with a sampler-net mesh of 32 mm. All the bed load data and size distribution analyses were therefore expressed for bed load 38 mm in size or larger, for which the sampler net capture was 100 percent. After sieving, the mass of particles in each size class together with the mass of each of the three largest particles was determined using a hanging spring balance. For particles larger than 38 mm, the number of particles in each size class was also counted.

5.2 Tracer Experiment

Tracer experiments compliment bed load sampling because they give an indication of distance of travel during bed load transport. The influence of the complete flood event, including peak flows, can be studied for selected particles of known size. The main difficulty with tracer experiments is the recovery of tracer particles from the stream bed when high rates of scour and fill have led to deep burial.

By placing tracers in the stream bed in different areas of the study reach, spatial patterns of entrainment can be investigated. In this study, tracer placement was limited to riffles and runs because the hydraulic equations in the entrainment criteria can only model the flow conditions in these reaches. The assumption of uniform flow is certainly not valid through pool features which are associated with bends in the stream channel. The role played by riffle-pool sequences in bed load entrainment and transport processes remains unclear (Sear, 1996). Therefore, to test the existing entrainment criteria, riffle and run features were the sole focus of investigation.

5.2.1 Tracer selection and marking

Tracer particles larger than approximately 50 mm in b-axis diameter (substrate D_{50} and larger) were removed from the channel margins downstream from where bed load was sampled. Particles were not taken from beneath the water as these were coated with algae growth after the low flow season, and could not be painted easily. The particles were taken to a lab, scrubbed clean, and painted with a polyurethane paint which is relatively resistant to abrasion. To distinguish between two different placement techniques, half of the tracers were painted yellow and the other half painted red. Each individual tracer could also be distinguished through numbering. All particles were numbered with black paint, weighed, and the three axes measured. Size distributions for the yellow and red tracers were almost identical, following a similar pattern to the coarse substrate fraction on the riffles of the study reach.

5.2.2 Tracer placement technique

One problem encountered in tracer studies is that tracers placed in the stream bed by hand may be either more or less likely to be entrained than particles deposited by streamflow. Where tracer particles protrude further into the flow than the surrounding matrix, they are more exposed to entrainment forces than naturally deposited particles and thus occupy relatively unstable pockets. Generally it is not possible to recreate particle embededness when placing tracers, so tracer particles are more prone to entrainment.

Tracers were placed upstream from the sampling bridge location, along two riffle sections as illustrated in Figure 5.3. The locations of all tracer particles were mapped so that the distance of travel for each could be calculated when recovered after high flows. Two different placement techniques were used to examine the effect on tracer movement in the subsequent flood; individual placement, and cluster placement. Tracers positioned individually were carefully placed into pockets in the stream bed, often in place of a particle removed to create a pocket. This allowed the tracers to be integrated into the stream bed with minimal disturbance to the pre-existing roughness. Rows of ten particles were positioned across the full low flow channel width, with particles 0.6 m apart. Rows of individual tracers alternated with rows of clustered tracers, with rows spaced at 5 m intervals (26 rows in total). Clustered tracers were placed in three evenly spaced clusters across the channel, a cluster of four in the center, and a cluster of three on each side. The clusters could not be incorporated into the existing gravel matrix as easily as the individually placed tracers, and consequently the clusters were more exposed to entrainment forces.
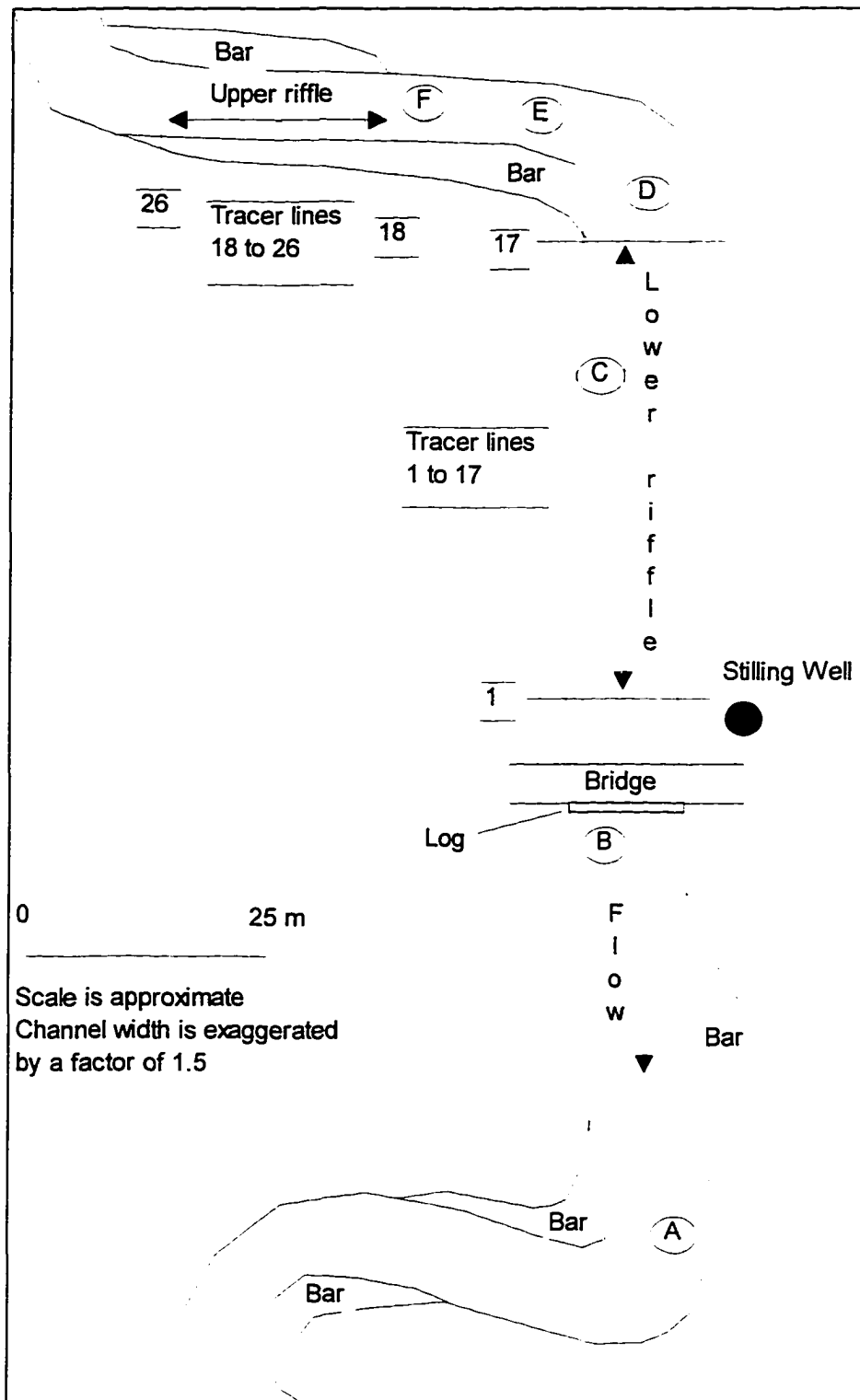
Figure 5.3 Map locating the 26 lines of tracer particles in the study reach. Each line contained 10 particles. Tracers placed individually on odd line numbers, and in clusters on even numbers . Lines 1-17 are in the lower riffle, and lines 18-26 in the upper riffle.

5.3 Flow Measurement

Flow velocities were measured with a Price AA current meter. When flows could be waded, the current meter was attached to a wading rod with readings taken every 30 cm across the channel. At flows when velocities were too high to wade, the current meter was attached above a 14 kg sounding weight and operated using a cable and hand reel from the sampling bridge. Velocities were measured at 0.6 flow depth to give an estimate of average velocity in the vertical for each measurement point (Rantz et al., 1982). Errors in estimating discharge were perhaps greater at the higher flows when the cable and sounding weight were used and depth was more difficult to measure. Also difficulties were caused by organic debris during high flow measurements. Frequent clearing of grass and roots was necessary to ensure the current meter rotated freely, and at extreme flows large floating debris and trees were a major hazard.

Due to high stream bed mobility and instability in the channel cross-section, frequent discharge measurements were taken during high flows to keep track of possible changes in the stage-rating curve. A clear shift in the rating curve resulted from channel widening in the June flood, and because of this instability the discharge was measured on every occasion that bed load samples were taken.

5.4 Slope Measurement

Water surface slope is an important hydraulic variable which is rarely measured in space and time at field sites during sediment transport (Prestegaard, 1983). Squaw Creek, Montana, is one location where detailed slope measurements have been made (Custer, 1992). The same 'slope-tube' technique was used to measure slope at Dupuyer Creek. Clear hosing was laid longitudinally along the stream bed, close to the bank, from the staff gage to a point 27 meters upstream. The upstream end was turned to face downstream, and anchored to rebar driven into the stream bed. At the downstream end, the hose was raised out of the stream and attached to the staff gage. The difference in height between the water level in the tube and the level of flow on the staff gage was the change in head. Slope was calculated by the head difference divided by the distance between the upstream end of the tube and point where the tube was raised at the staff gage.

Accurate and consistent readings of water surface slope were made impossible due to constant fluctuations in the level of the water in the raised tube. This problem was also experienced to some degree at Squaw Creek (Custer, personal communication, 1994). Rapid fluctuations in flow velocity may have been the cause of the problem. There were also difficulties caused by scour and deposition along the length of the slope-tube. Therefore, surveyed reach average stream bed slope was used in all flow competence analyses (1.0 percent slope throughout period of study).

5.5 Channel Surveys

Field survey techniques used in the channel long profiles and cross sections closely followed those suggested by Harrelson et al. (1994). Both sighting and laser levels were used, with measurements taken at least every 0.3 m and at all breaks of slope. All elevation measurements are expressed in relation to a permanent benchmark, a concrete pier with rebar spike located close to the stilling well, which is given an elevation of 30.48 m (100 ft.).

5.6 Channel Substrate Surveys

The commonly accepted method used to characterize the size distribution of channel bed materials in gravel rivers is the Wolman pebble count (Wolman, 1954). A sample of 100 particles is selected randomly from the population of particles exposed on the channel bed surface, with sample points determined by a grid system. The b-axis of each particle is measured. The intermediate b-axis is the dimension that determines the smallest sieve size class through which the particle will pass. Since this investigation examined the entrainment of particles from the channel bed surface, it seemed appropriate to sample the surface layer of the bed using the pebble count method. However, there are several variants on the pebble count procedure, with considerable variability between replicates of a method, between methods, and between operators (Marcus et al., 1995; Wohl et al., 1996; Kondolf, 1997). The question of which method to use to determine the

substrate size distribution for flow competence evaluations has not been addressed directly in the literature.

The Wolman pebble count procedure has been criticized on account of the inherent bias towards larger particle sizes due to the larger surface area they present on the channel bed (Leopold, 1970). The procedure is biased towards larger particles when considering the numbers of particles present in the stream bed which occupy the different size classes, but in describing the proportion of the channel bed area occupied by the different size classes the pebble count procedure is unbiased. No adjustment was made to the pebble count procedure here, because characterization of the substrate in terms of the area of the channel surface occupied by various size classes makes the most sense in flow competence analyses.

Two types of pebble count were performed over the study reach. The first type took a systematic sample of pebbles from specific zones in the main riffle; upper riffle, mid-riffle just upstream of the sampling bridge, and lower riffle. These zones or facies exhibited homogeneous particle size characteristics. One hundred particles were selected by traversing the bankfull channel width ten times, measuring ten particles per traverse, with each traverses separated by 0.5 m. This method gave an idea of the spatial variation in the size distribution of the substrate over the riffle where bed load was sampled. The second type of pebble count was undertaken over the whole reach, to obtain an estimate of the substrate size distribution at the reach scale. The reach scale pebble count was undertaken over several hundred meters of channel, encompassing five riffles and five pools upstream from the sampling bridge. One thousand particles were measured in this

larger scale stratified pebble count. The pool/riffle ratio was determined through pacing, and the proportions were used to dictate the number of pebbles measured in pools versus riffles. The number of particles measured in each riffle was proportional to the length of that riffle. Equal numbers of particles were measured in the pools as they were approximately the same size. Ten particles were selected in each traverse of the bankfull channel width, until the desired number of particles had been measured for each pool or riffle.

6. RESULTS AND DISCUSSION

6.1 Flood Events Sampled

Two major flood events took place in the spring of 1995 (Figure 6.1). Both of them transported large volumes of coarse bed load which could be sampled with the large frame-net sampler. The flood which began on May 6th was the first occasion on which flow had risen significantly above the winter base flow, and was the first high water of 1995. Discharge rose rapidly from less than 1 m^3/s to 9.2 m^3/s over a 24 hour period, then dropped to around bankfull (7 m^3/s) for the next two days before slowly tapering off. Diurnal snowmelt patterns were absent, as high flows were driven mainly by prolonged rains which became intense over the 5th, 6th and 7th of May. Bed load was sampled over the entire falling limb of the flood hydrograph. The bar plot reveals the general trend of decreasing maximum particle size with falling flows. During bed load transport the suspended sediment load was visibly high, and the stream bed could not be observed. By May 10th coarse bed load dropped to extremely low rates, and on May 11th Helley-Smith sampling (76 mm square orifice) was just possible at the lower flow velocities and depths. However, only small amounts of very fine gravel and sand were captured and effectively the bed load transport process had stopped after four days of high activity. Subsequent snowmelt produced some diurnal peaks, but these were short lived and did not transport significant bed load.

50
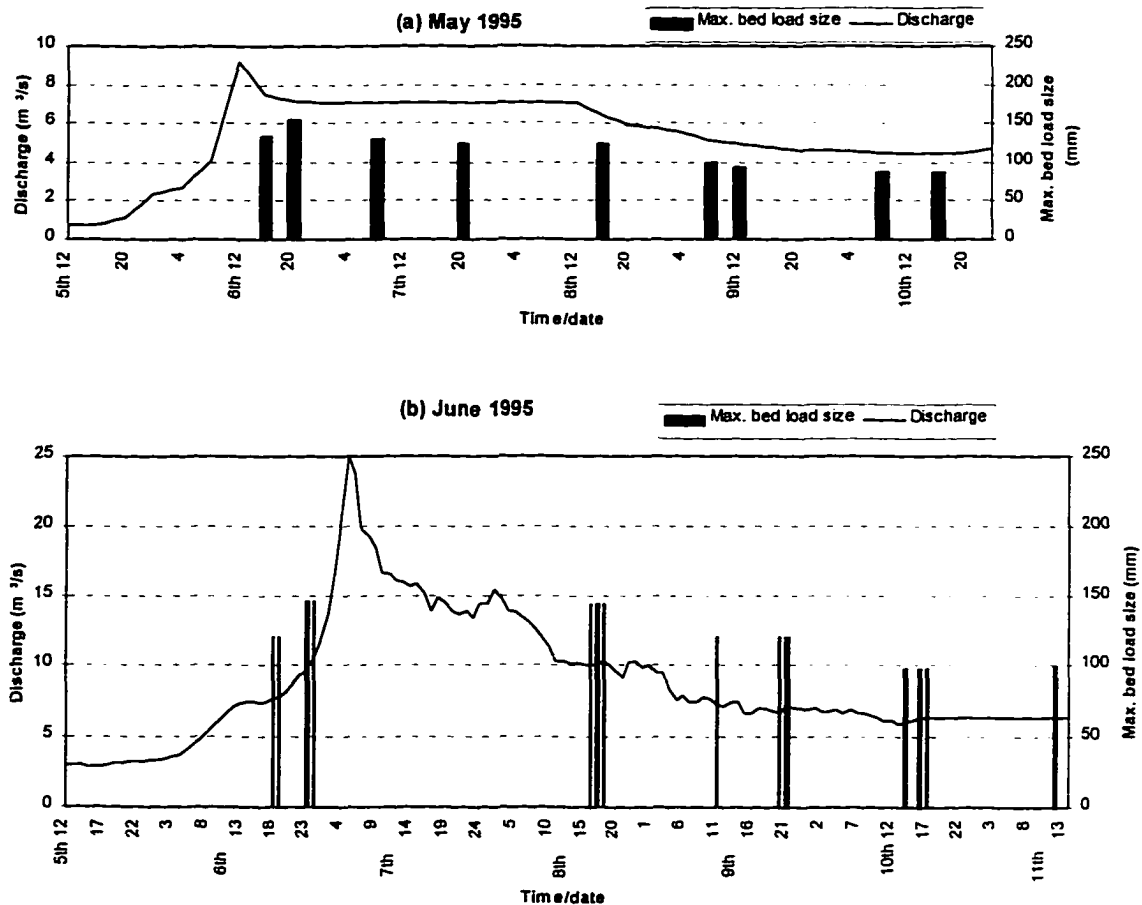
Figure 6.1 Flood hydrographs for May and June events, 1995. Maximum bed load particle size, represented by the columns, decreased on the falling limbs of the floods.

Heavy frontal precipitation in early June produced a flood of much greater magnitude (Figure 6.2). The flood began on June 6th with a steep rise from 3 m³/s to 25 m³/s, almost three times the peak of the May flood and about 3.5 times bankfull. Time to peak was again about 24 hours, but this time flows exceeded bankfull for four days rather than two. The initial dominant peak was followed by a steady decline, interrupted only by minor peaks before leveling off at about 6.5 m³/s.

Figure 6.2 High flow and suspended sediment levels on June 7th at the sampling bridge, shortly after the flood peak (top). Downstream view of main study riffle with bridge, and gravel bar submerged on the right (bottom).

Bed load transport was well underway when sampling began on the June 6th rising limb, and continued for over five days. Intense rain turned to snow early on June 7th, and rapid bank erosion at many locations led to visible increases in suspended sediment. Unfortunately the peak flow was not sampled because of hazardous sampling conditions. Flows of 15 m^3/s on June 7th were sufficient to damage, and eventually scour out, one of the sampler support pipes. Bank collapse on the outside of actively migrating channel bends led to entrainment of whole trees in the torrent. When sampling could be resumed, a trend of decreasing maximum particle size with falling flows was again observed.

6.1.1 Stage-rating curve relationships

Flow measurements were taken when ever bed load was sampled (Appendix A), because of the possibility of changes in the channel cross section and associated changes in the stage-rating curve. A single rating curve sufficed for the May flood (Figure 6.3a), but during the peak flows of the June flood, channel widening of over one meter altered the rating curve, and a new curve was established for the remainder of the June high flows (Figure 6.3b). These plots demonstrate the good stage-discharge relationships obtained (regression R-squared values are 0.99 and higher). This allowed relatively good estimates of discharge for the different levels of stage when bed load was sampled. All flows above 5 m^3/s had to be measured from the sampling bridge using the sounding weight and cable reel. Larger measurement error is possible at these higher flows (see methods). However, the rating curve for May indicates only slightly greater scatter at

higher flows, and the June curve shows the high flow measurement to be in good agreement with the trend set by lower flow measurements.

(a) Stage - discharge curve until 6/7/95

$y = 20.11x^{2.22}$
$R^2 = 0.99$

(b) Stage - discharge curve 6/7/95 onwards

$y = 25.60x^{1.63}$
$R^2 = 0.998$
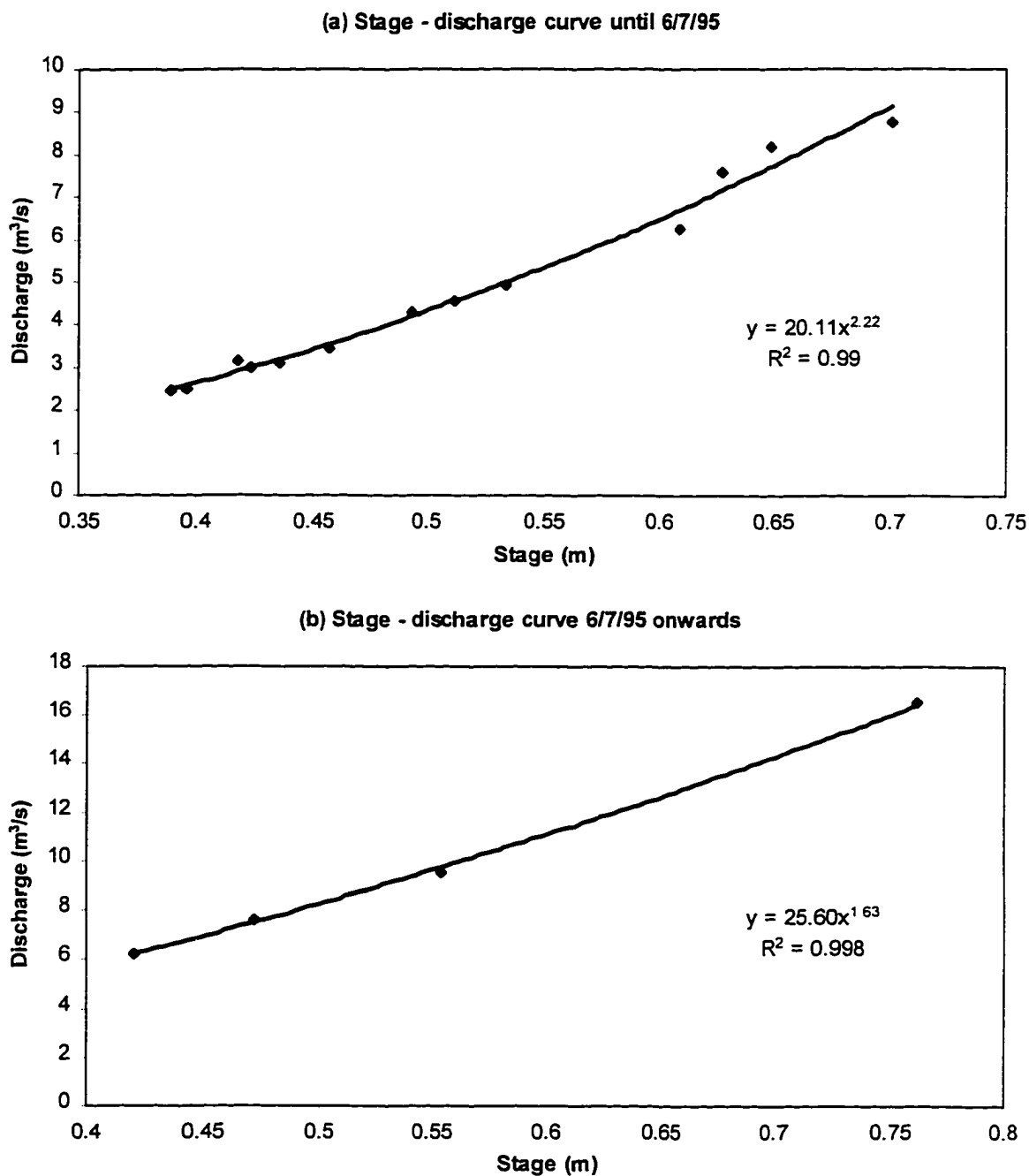
Figure 6.3 Stage - discharge curves for the flood season of 1995. Channel widening early on June 7th caused a shift in the relationship.

Discharge per unit width was calculated by dividing the estimated cross sectional discharge by the flow width where bed load was sampled. Because of the increase in flow width with rising stage, and the channel widening through bank erosion, channel discharge and unit discharge are treated as two separate variables. Relationships will differ when either channel discharge or unit discharge is plotted, and it is important to recognize the distinction between the two in the subsequent flow competence analysis.

6.2 Bed Load Data Set

A total of 120 bed load samples were taken during the May and June floods (Figure 6.4). A total of 4600 kg in mass was sampled during a sampling time of 488 minutes. Discharge sampled ranged over 4.5-11 m^3/s, and maximum particle sizes ranged from 35-175 mm. In the May flood, all 54 bed load samples were taken after the peak flow and on the falling limb of the flood hydrograph. However, in the June flood 27 bed load samples were obtained on the rising limb, with the remaining 39 samples taken on the falling limb, allowing the investigation of possible hysteresis patterns in transport. Due to the speed with which flood levels rise, it was not possible to sample the point at which coarse bed load transport began. However, the cessation of coarse bed load transport was captured on the falling limb of the May flood. Complete details of all individual samples are presented in Appendices B1-B4, while data for the sample groups are summarized in Tables 6.1 and 6.2.
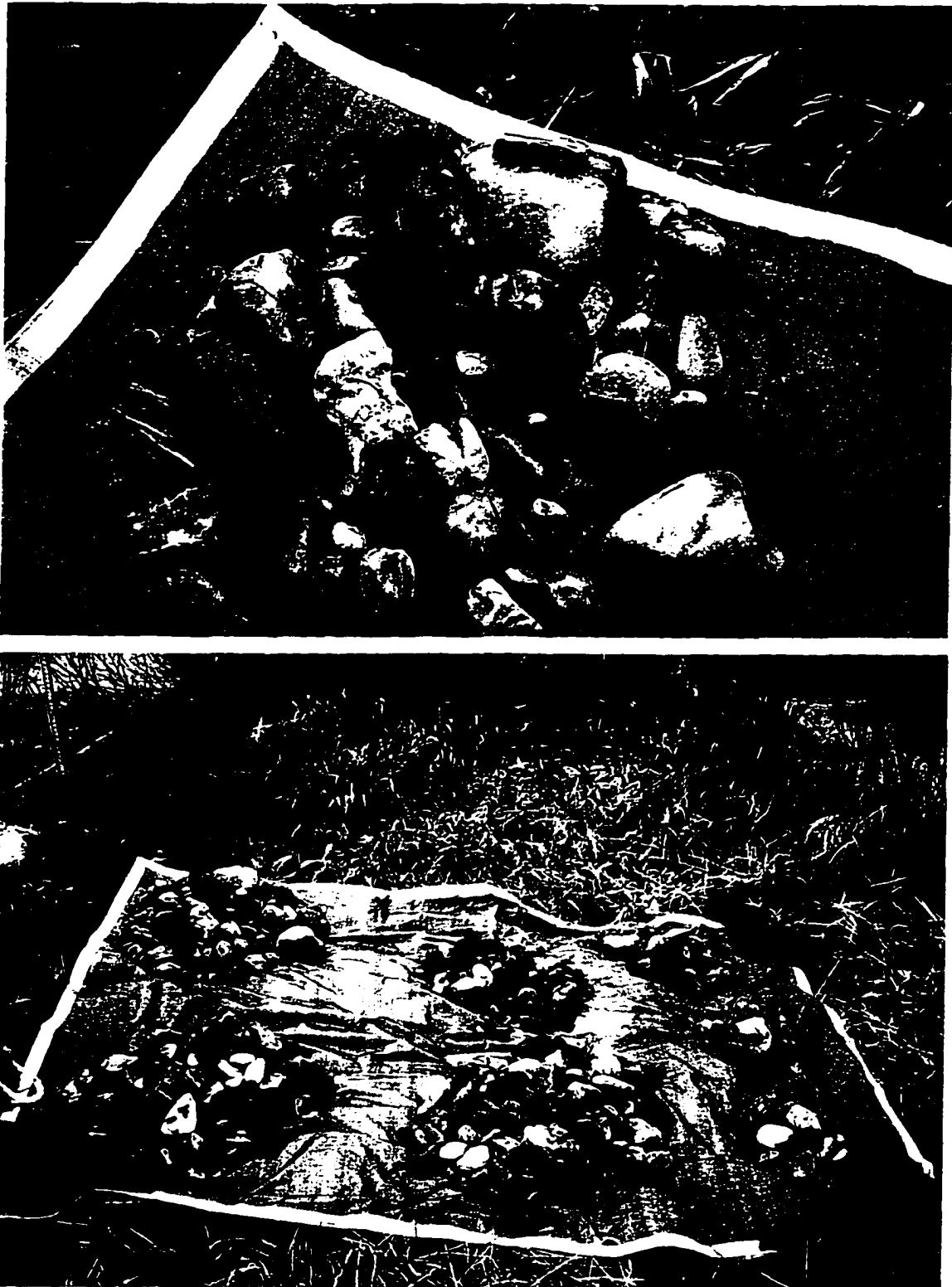
Figure 6.4 Single coarse bed load sample taken during the May flood. Penknife for scale indicates the large number of cobbles (top). Variable bed load sample sizes taken during steady discharge, May flood, due to pulsing nature of bed load transport (bottom).

Table 6.1 Characteristics of the bed load sample groups, and discharge conditions

Sample group number	Individual samples in each group	Date & time of sampling	Sampling time (minutes)	Sample mass (kg)	Range in discharge (m³/s)	Mean discharge (m³/s)
1	1-7	May 6, 15-1700	13	127	7.2-7.8	7.48
2	8-10	May 6, 20-2100	8	228	7.1-7.3	7.22
3	11-19	May 7, 09-1100	36	186	6.8-7.2	7.05
4	20-26	May 7, 19-2100	14	202	6.7-7.1	6.90
5	28-39	May 8, 15-1800	26	184	6.0-6.4	6.27
6	40-45	May 9, 09-1100	28	77	5.0-5.3	5.14
7	46-49	May 9, 14-1600	56	102	4.8-4.9	4.86
8	50-54	May 10, 11-1800	140	28	4.6-4.7	4.63
9	55-69	June 6, 18-2000	30	229	7.6-8.3	7.95
10	70-81	June 6-7, 22-0100	24	296	9.6-11.0	10.26
11	83-95	June 8, 16-1900	15	296	9.6-10.7	10.14
12	96-105	June 9, 11-2100	40	202	7.0-7.7	7.30
13	106-114	June 10, 14-1700	48	227	6.0-6.5	6.32
14	115-120	June 11, 12-1300	24	99	6.4-6.6	6.51

Table 6.2 Particle size characteristics of the bed load sample groups, and hydraulic flow conditions

Sample group number	Bed load particle sizes † D_{max}	D_{95}	D_{50}	Bed load rate >38 mm (kg/m/min.)	Unit discharge (m²/s)	Shear stress (N/m²)	Flow depth (m)
1	135	-	-	9.78	0.98	56.2	0.57
2	155	108	59	-	0.91	55.3	0.56
3	131	113	50	5.17	0.89	54.7	0.56
4	175	114	50	14.41	0.87	54.1	0.55
5	123	82	49	7.08	0.79	51.7	0.53
6	100	74	48	2.76	0.65	47.3	0.48
7	94	69	47	1.81	0.61	46.1	0.47
8	88	80	48	0.20	0.58	45.2	0.46
9	120	99	53	7.62	0.93	57.7	0.59
10	146	124	60	12.32	1.20	64.9	0.66
11	144	112	55	19.70	1.11	62.5	0.64
12	121	89	50	5.05	0.81	52.3	0.53
13	98	78	50	4.73	0.72	48.5	0.49
14	100	93	52	4.11	0.74	49.3	0.50

† For the coarse bed load fraction >38 mm only

6.2.1 Characteristics of coarse bed load transport

May 1995 flood

Bed load transport rates, by size fraction for each sample, decrease over the falling limb of the flood (Figure 6.5a). Bed load rates drop to a relatively low level soon after the peak flow on May 6th for reasons which remain unclear, and rebound on May 7th before continuing a declining trend. As would be expected from their greater abundance in the stream bed, and their apparent greater mobility, the finer size fractions display the highest transport rates. High transport in the 64-90 mm and 90-128 mm size fractions is particularly noticeable in the first sample group, although no transport is detected in the coarsest 128-180 mm fraction. The two subsequent sample groups at slightly lower flows are the only ones in which transport is detected in the 128-180 mm fraction. By the time flows have dropped to 0.65 m²/s, transport is largely restricted to particles less than 64 mm in size, and at 0.58 m²/s coarse bed load transport has almost totally ceased. A hand-held Helley-Smith sampler with 76 mm square orifice was just manageable at this flow. The Helley-Smith sampling captured particles up to 35 mm in size and showed very low transport rates.

The percentage of total sample mass is shown for each of the various size fractions during the May flood (Figure 6.5b). As flows decrease on the falling limb of the flood, the proportion of bed load in the finer 38-51 mm fraction increases while the proportion above 64 mm declines. Interestingly, the proportion of sampled bed load in the 51-64 mm
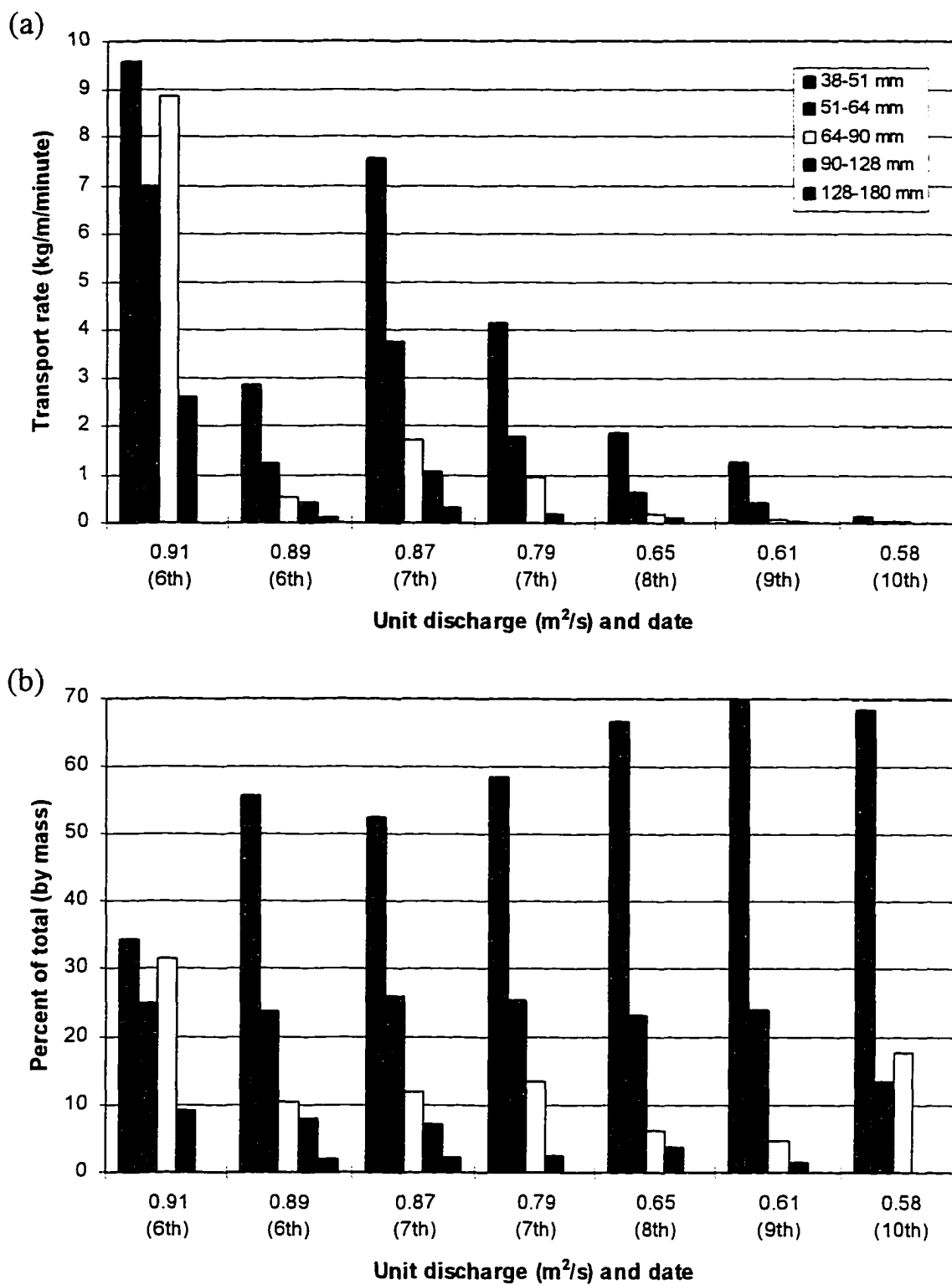
Figure 6.5 May 1995 flood, for each sample: (a) Bed load transport rates by size fraction (b) Percent of bed load sample within each size fraction (>38 mm only).

fraction remains relatively constant. The size distribution of the bed load is shown to vary with discharge.

June 1995 flood

Bed load sampling on both the rising and falling limbs of the June flood shows some evidence of hysteresis behavior in transport rates (Figure 6.6a). Maximum transport rates for the 38-90 mm size fraction occur after the peak flow sampled. Maximum transport rates for the coarser 90-180 mm size fraction do coincide with maximum discharge. Transport rates for the 64-128 mm fraction are markedly elevated at the two highest flows sampled, and transport in the 128-180 mm fraction is only detected at these highest flows. As flows decline on the falling limb of the flood, transport rates drop significantly, but stabilize in the 0.72-0.81 m²/s flow range.

The proportions of total bed load in each size class follow similar patterns to those of the May flood (Figure 6.6b). The trends show that bed load during higher flows contains greater proportions in the coarse 64-180 mm fraction, while proportions decrease in the finer 38-51 mm fraction. Again, the size distribution of the bed load varies with discharge.

Comparison between May and June floods

The greater magnitude of the June flood produced not only higher bed load transport rates, but also a greater proportion of that bed load in the coarser size fractions. This can be illustrated by examining the proportional transport rates of the various size fractions.
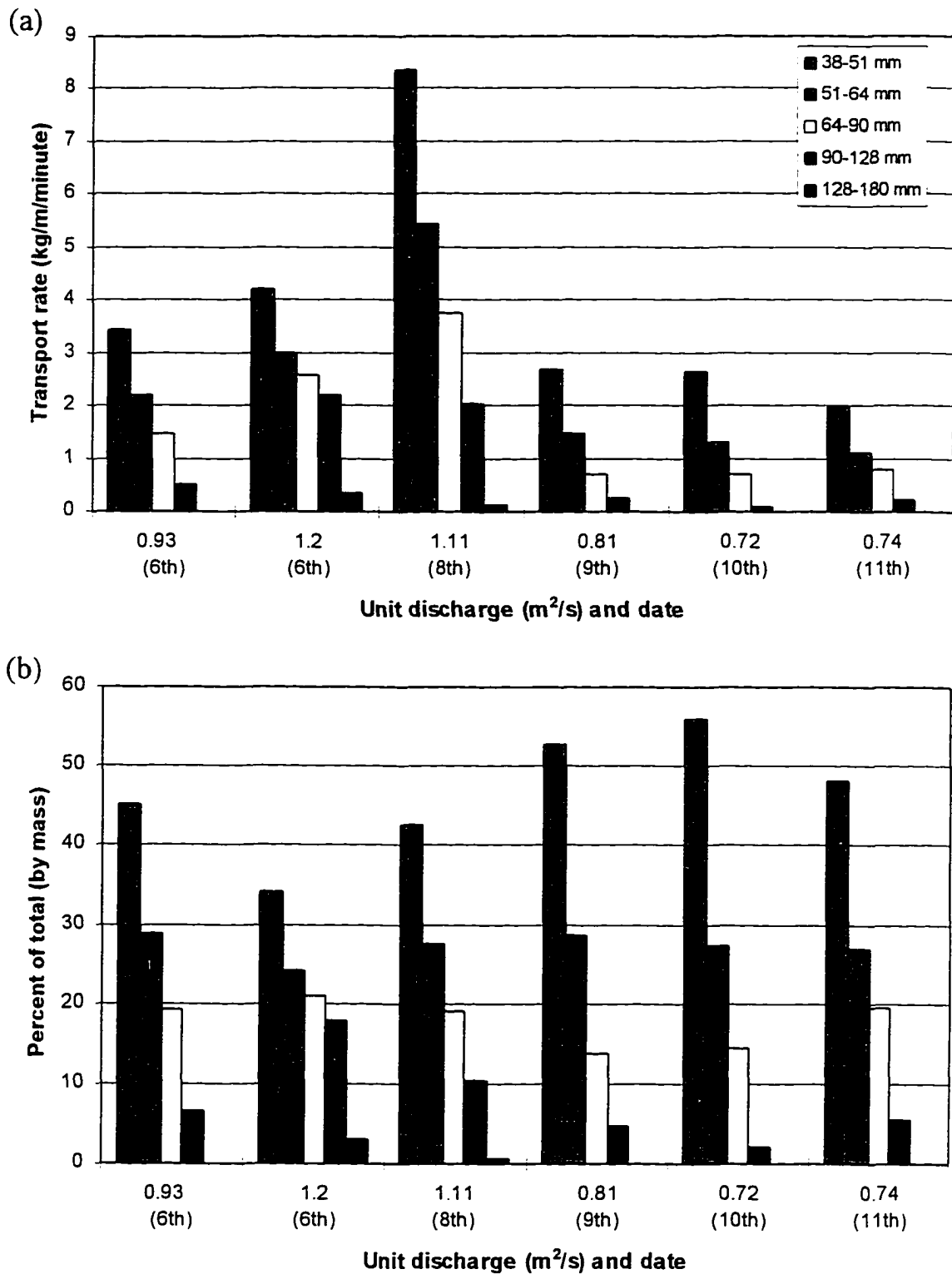
Figure 6.6 June 1995 flood, for each sample: (a) Bed load transport rates by size fraction (b) Percent of bed load sample within each size fraction (>38 mm only).

The May flood transports 50-70% of the relatively fine 38-51 mm fraction, compared to 45-55% for the June flood. The larger 51-64 mm fraction comprises approximately 25% of total sampled bed load for both floods, while transport of the 64-90 mm fraction is markedly higher in the June flood at around 15-20% as compared to about 10% in May. The proportion of coarse bed load in the 90-128 mm fraction never exceeds 10% in the May samples, but during the highest flows sampled in June this proportion reaches 18%.

6.2.2 Bed load rating curves

The plot of all individual bed load samples of transport rate against unit discharge shows a high degree of scatter due to the pulsing and unsteady nature of the bed load process (Figure 6.7a). The data show that sampled bed load rates can drop to low levels when the sampling period falls between such pulses. Rates typically vary by one order of magnitude, but can vary as much as two orders of magnitude at any discharge. Separate regression lines for the May and June data show clear positive relationships between bed load rate and unit discharge.

The analysis of sample groups extends the sampling duration from the 1-4 minute range typical of individual samples to a range of 15-60 minutes or more. This ensures mean sampled transport rates are less influenced by individual bed load pulses, and dramatically reduces the scatter in the bed load rating curve, especially for the lower flows below 0.85 m^2/s (Figure 6.7b). At discharges above 0.85 m^2/s, variability increases because sample duration may be insufficient to smooth out pulsing effects.
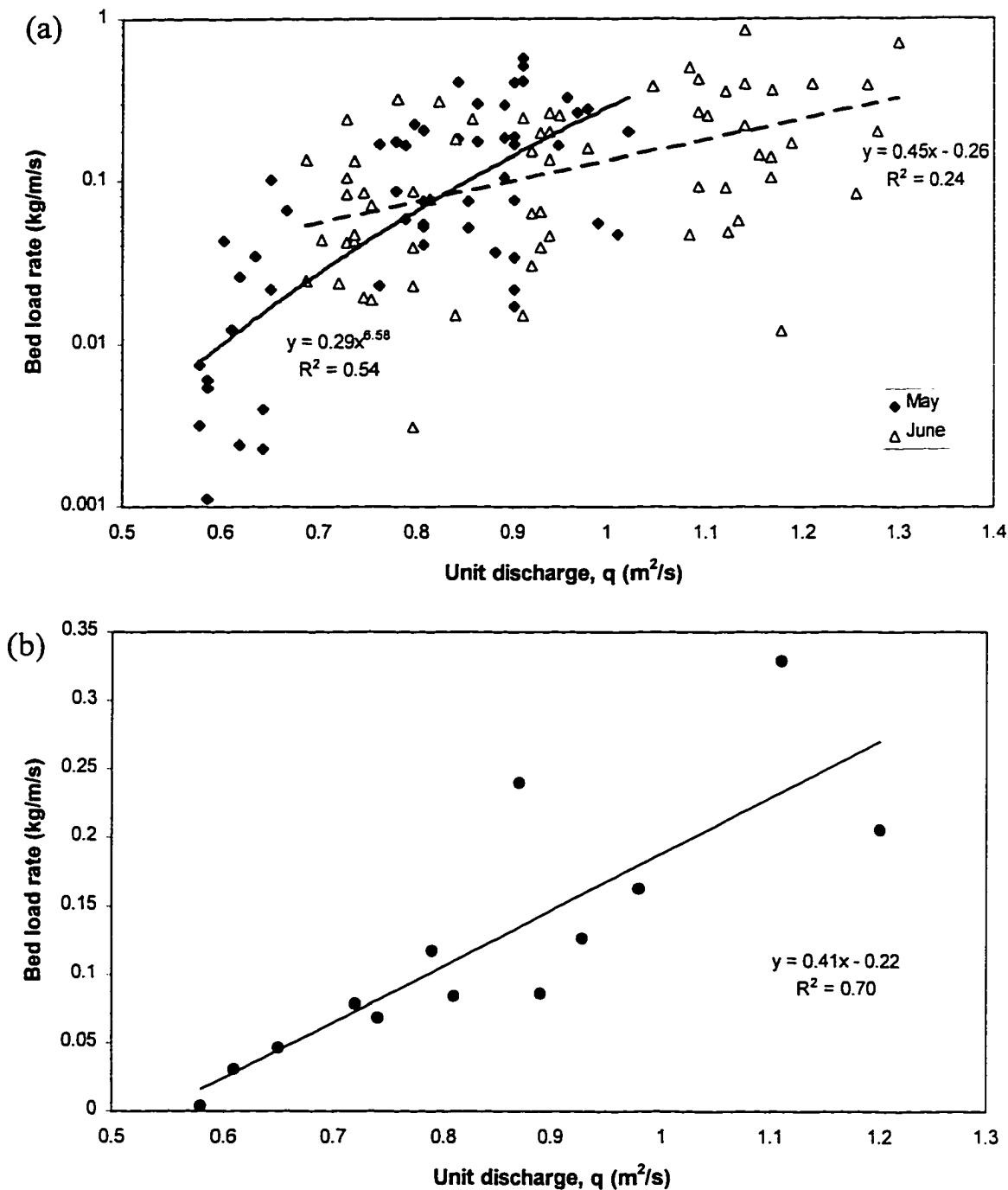
Figure 6.7 Coarse bed load rating curves (>38 mm only): (a) Individual samples for May and June floods with separate regression lines, (b) Sample groups with regression line.

Bed load sample groups can also be analyzed in terms of rate of transport of the various size fractions, and how this changes with discharge. Figure 6.8a illustrates the

rating curves by individual size fraction for both floods. Power regression lines fit the coarser size fractions particularly well. A similar fractional rating curve analysis is presented in Figure 6.8b, but this time bed load rates are expressed in terms of the number of particles per unit width and time rather than the mass of the particles. This analysis leads to the same conclusion that the coarsest bed load fractions become more dominant with increasing flows.

6.2.3 Comparing substrate to bed load size distributions

Equal mobility in the bed load process can be examined by comparing the relative rates of transport across different size fractions with the proportions in which they occur in the channel substrate. For example, if ten percent of the channel substrate occupies a given size fraction, one would expect ten percent of the bed load to also occupy this size fraction if there is equal mobility in transport. Such a comparison is not easy because of the different sampling techniques employed for the static channel substrate versus the moving bed load. Substrate Wolman pebble count data contains information regarding the proportions of particle numbers within different size fractions, which is different from the proportions of particle mass within each size fraction. Therefore, only bed load transport rates in terms of the numbers of particles captured in each size fraction may be compared with the substrate pebble count data.
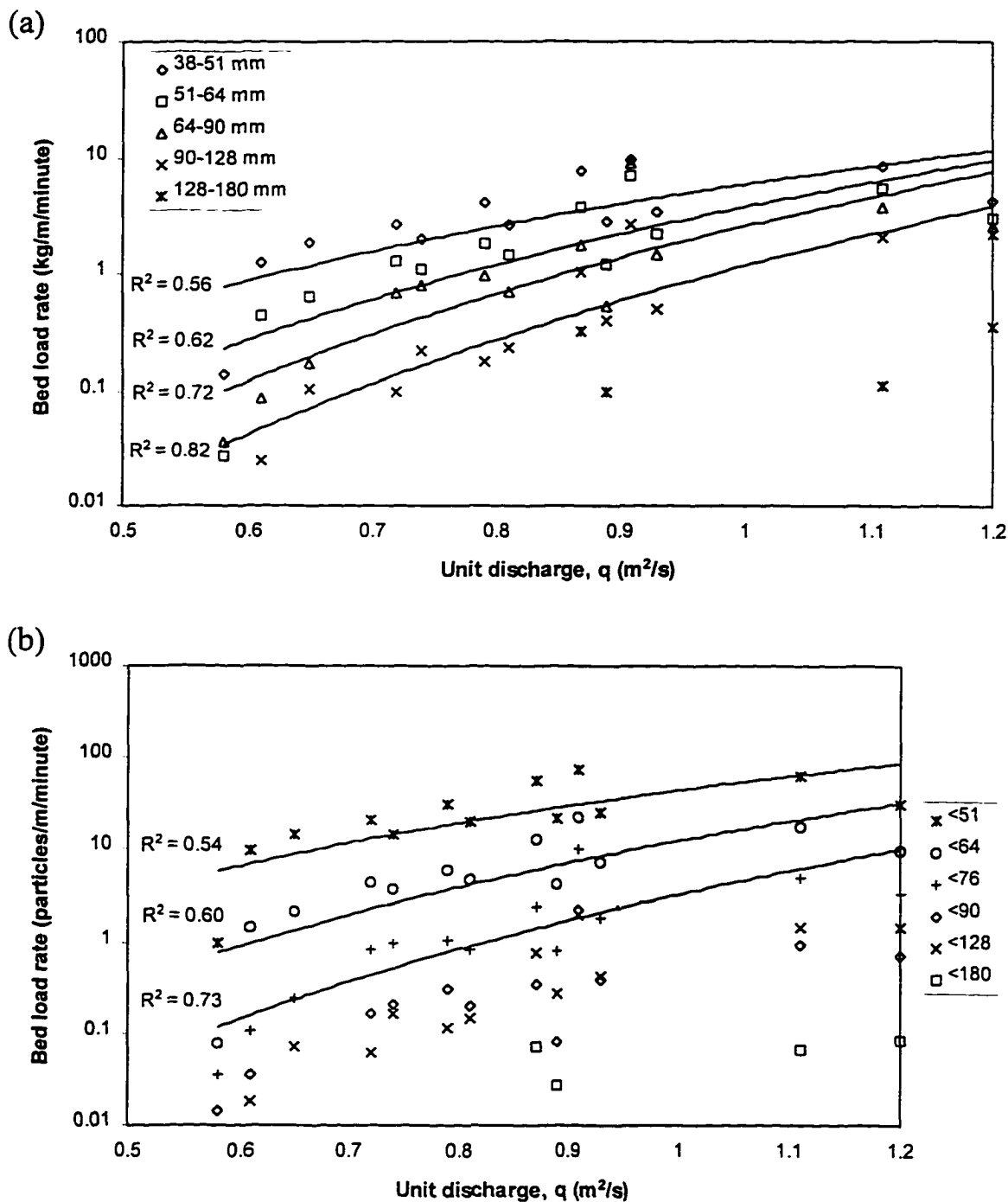
Figure 6.8 Bed load rating curves by size fraction. Power regression lines fitted to size fractions without zero values: (a) Particle mass transport rates, (b) Particle number transport rates.

Figures 6.9a and 6.9b show the relative proportions of the sampled bed load particles across size fractions for each of the sample groups. Also plotted are the proportions for the channel substrate as determined by pebble count procedures. While a pebble count procedure will give a slightly coarser size distribution than for the square sieving technique used on bed load samples, the differences in the figures are far greater than can be explained by this alone. For both the May and June flows sampled, the smallest size fraction is being transported in preference to the largest three fractions through size selective transport processes.

In the 38-51 mm size fraction there is large over-representation for all the bed load samples when compared to the substrate. Between 67% and 89% of the bed load sampled in the 38-180 mm range lies in the 38-51 mm fraction compared to only 23% for the substrate. This suggests size selectivity and the preferential entrainment and transport of particles in the 38-51 mm size range. The 51-64 mm size fraction is the only one where transport rates are in close proportion to the relative abundance in the substrate, at around 15-20%. The 64-90 mm range is clearly under-represented in the bed load samples, especially for those taken during the lower flows, and this pattern continues into the largest size fractions. Pebble counts indicate 28% of the substrate (in the 38-180 mm fraction) lies in the 90-128 mm range, while the figure for the bed load never exceeds 3-4%. Similarly 9% of the substrate occupies the 128-180 mm range, but the bed load proportions remain between zero and a fraction of one percent. The evidence strongly supports a dominance of size selective bed load transport across the full range of flows
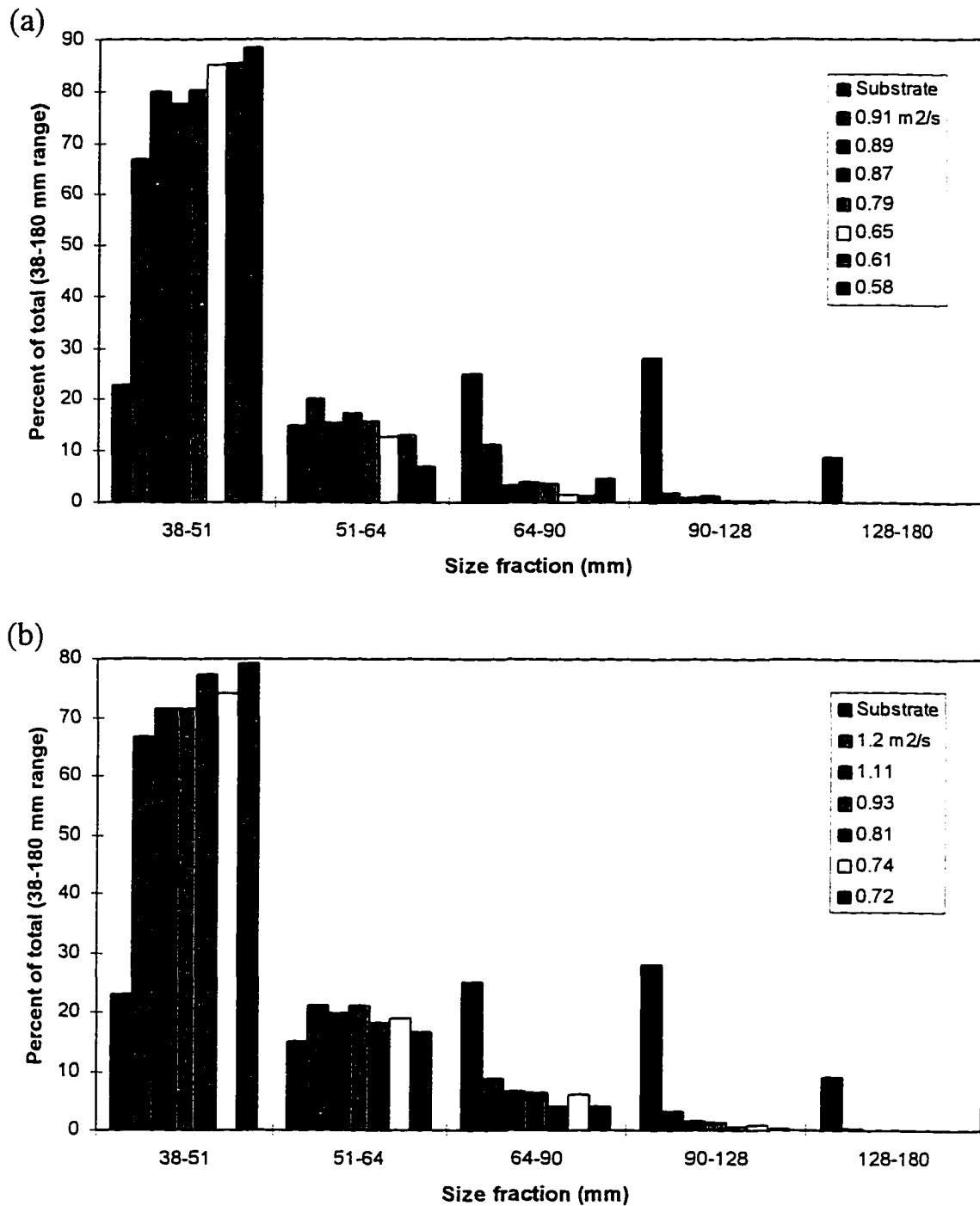
Figure 6.9 Comparison of channel substrate and bed load size distributions in the 38-180 mm range: (a) May 1995 samples, (b) June 1995 samples. Legend entries give the unit discharge for each sample. Coarse fractions of the substrate are under-represented in the bed load samples, even at the highest flows sampled.

sampled. A trend can also be seen where the bed load becomes slightly less size selective at the highest flows sampled.

6.2.4 Sensitivity of bed load size distribution to discharge

Particle size distribution plots for the sample groups also reveal the pattern of coarsening bed load with increasing flows. Figures 6.10a and 6.10b show these size distributions for all bed load greater than 38 mm in diameter, for the May and June floods respectively. The last sample group in the May flood is omitted because of the marginal rate of coarse bed load occurring at a time when transport had effectively ceased. Although there is some departure from the trend, the size distribution curves shift to the right with increasing discharges for both the May and June floods, demonstrating that bed load coarsens at higher flows. In each flood the bed load sample taken at the highest flow has the coarsest size distribution, and conversely the bed load sample taken at the lowest flow has the finest size distribution. This trend also supports selective transport.

Bed load particle size percentiles can be extracted from the size distribution data, and plotted against unit discharge to examine alternative flow competence relationships for particular sizes (Figure 6.11). Regression lines can be fitted to these relationships, with R-squared values which suggest the regression models could be used for predictive purposes. The plot shows that it is not only the maximum bed load particle size which is sensitive to discharge, but the complete size distribution of the bed load. For the bed load samples, the D_{50}, D_{95}, and D_{max} all increase in size with discharge. The relationship is
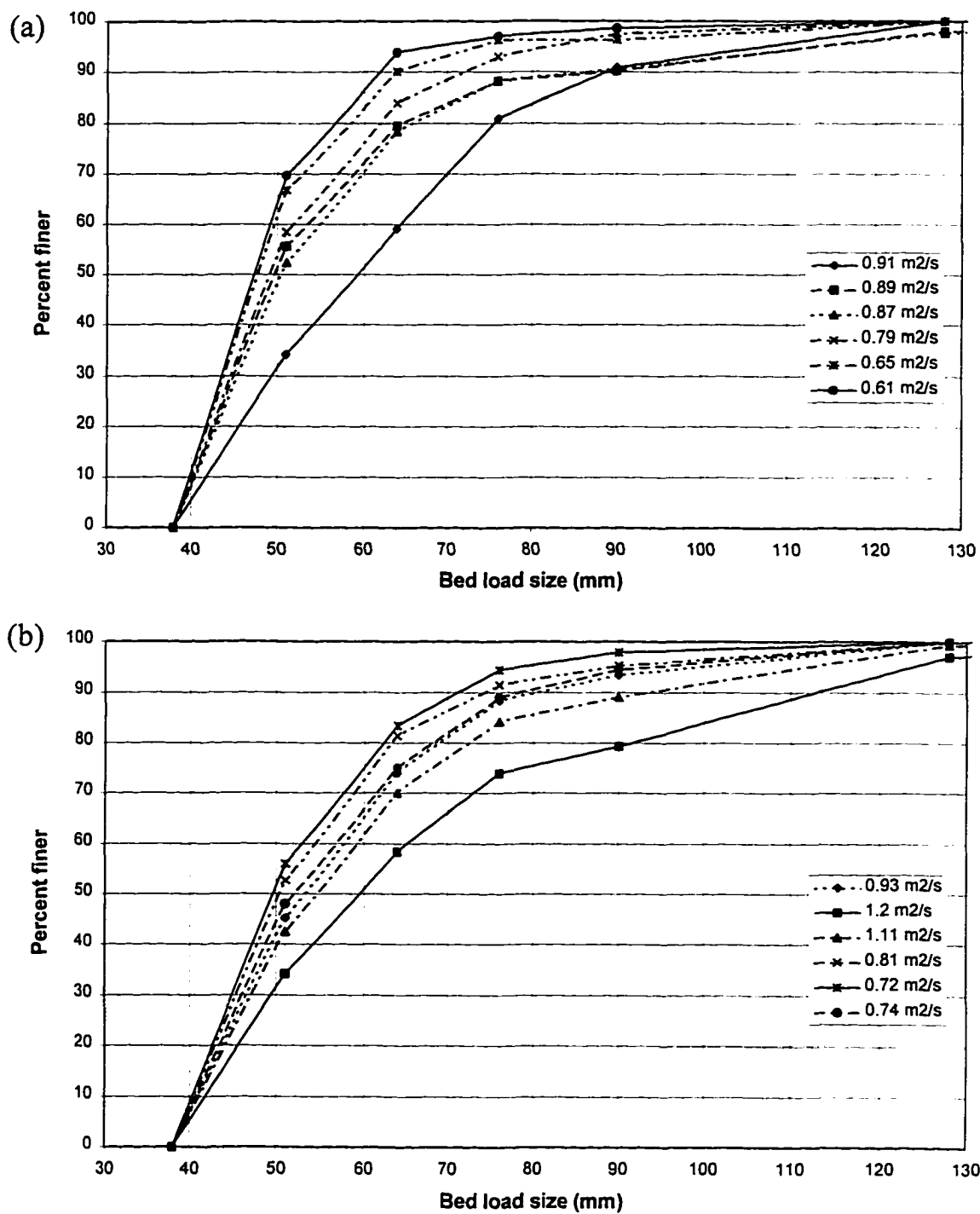
Figure 6.10 Variation in the bed load size distribution with unit discharge (>38 mm fraction): (a) May 1995 samples, (b) June 1995 samples. For both May and June, there is a trend of coarsening bed load with increasing discharge.
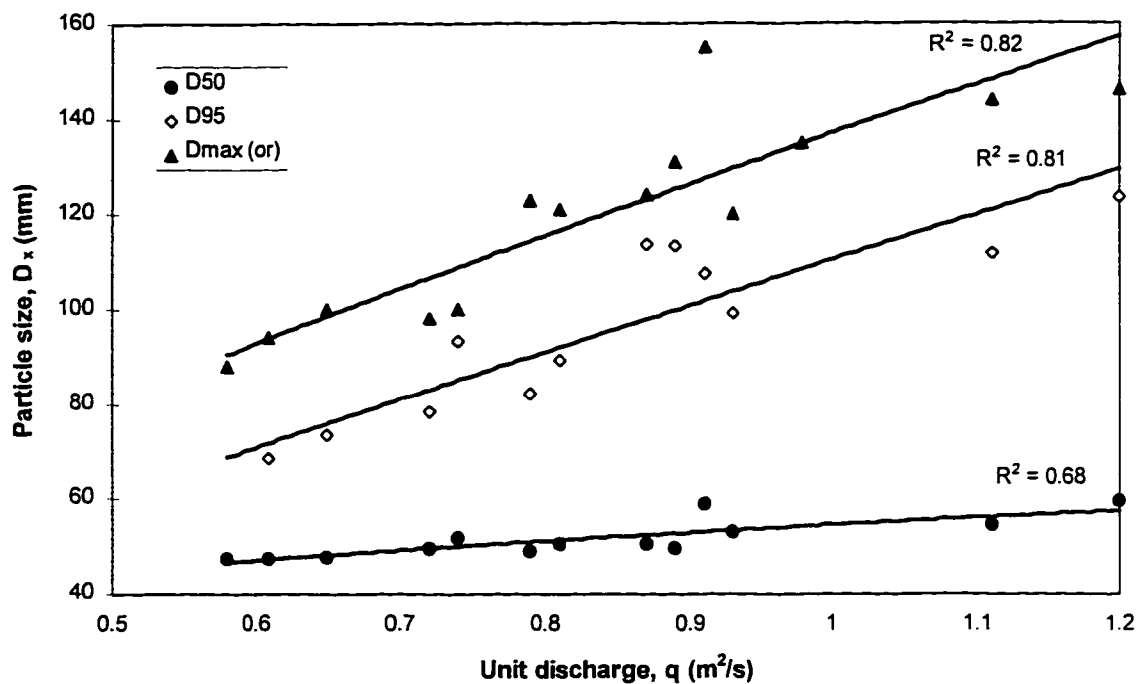
Figure 6.11 Power regression relationships between bed load particle size percentiles and unit discharge. The high R-squared values indicate that flow competence relationships can be established for median (D_{50}) and coarse (D_{95}) bed load percentiles, as well as maximum particle sizes (D_{max} - outlier removed).

stronger for the D_{max}. This result suggests that flow competence relationships are valid in this stream channel, not only for the maximum particle sizes, but also the more central and less extreme size distribution percentiles. A more complete analysis of flow competence is presented in the next chapter.

6.3 Particle Tracers

6.3.1 General observations

Widespread bed load movement during the May flood led to a high degree of tracer activity, but the high suspended sediment levels prevented direct observation of their movement. Tracer recovery began on May 10th when the suspended sediments had dropped sufficiently, and continued until the occurrence of the next flood on June 6th. After the first flood, 71 (27%) of the original tracers were recovered, with a further 26 (10%) recovered after the second flood. These two groups of recovered tracers had to be considered separately. The first, larger group, experienced only the May flood, and the smaller, second group, experienced the May and June floods.

Two related factors account for the low recovery rate of tracers in this stream channel. First, the high rates of bed load transport cause high levels of abrasion which can strip the particles completely clean of their tracer paint. These tracer particles are then indistinguishable from the rest of the channel bed and will not be recovered. Secondly, the high rates of scour and fill associated with the active bed load process results in many tracers becoming buried in the channel bed, either in situ without any transport, or after traveling some distance. Tracer particles may go through a cycle of entrainment, deposition, burial, and then re-exposure several times during a flood event. Those buried at the time when bed load transport ceased will not be found. The vast majority of tracers found after the first flood had been entrained and transported some distance, with only 3 yellow (placed individually) tracers and one red (placed in cluster) tracer found in their

original position. All tracers found after the passage of both floods had been transported some distance.
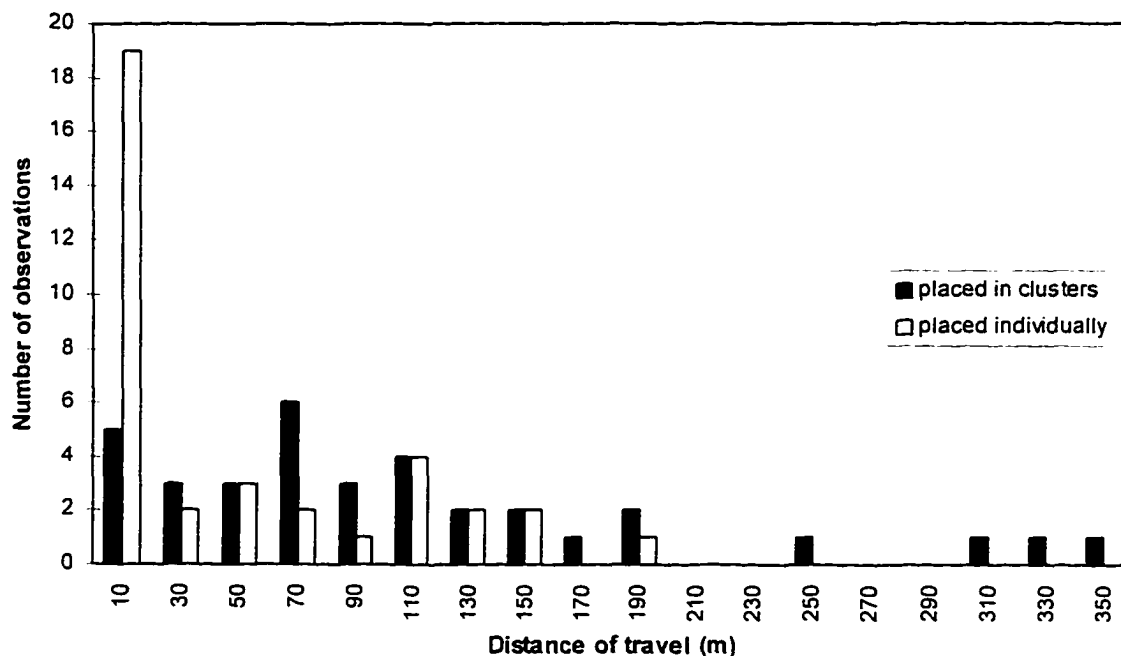
Figure 6.12 Distance of travel for tracers recovered after the May 1995 flood. Tracers placed in clusters were found to travel up to 350 m in some cases. Tracers placed individually tended to travel less far, and never exceeded 200 m.

Overall mean distance of travel for both tracer types recovered after the May flood is 83 m. For tracers placed in clusters, the mean travel of 110 m is twice the mean of 54 m for individually placed tracers. The distribution of tracer travel distances is different for each of the two types of tracers (Figure 6.12). Observations peak in the 0-20 m range for individually placed tracers, while the peak range for tracers placed in clusters is much higher at 60-80 m. This indicates that the method of tracer placement in the channel bed has a major influence on the resultant entrainment and distance of travel. One reason for this difference in mobility could be that the placement of tracers in clusters produced

larger protrusions from the original stream bed. These less stable arrangements were entrained at an earlier point in time which enabled them to travel further. Another reason might be that with four tracer particles clustered in the channel center for each row, they were more prone to entrainment than the individually placed tracers spread across the full channel width. However, when the relationship between travel distance and original position in the channel is examined, there does not seem to be any obvious increase in mobility for tracers placed nearer the channel center (Table 6.3). Where several tracers were recovered from the same original row, those placed towards the banks moved similar distances to those placed close to the channel center.

Tracers which had not traveled very far, or which were partly buried, tended to retain a good coverage of paint. Patterns of abrasion on tracer particles provided interesting indications regarding their movement characteristics and positions occupied in the channel bed. For example, several particles were only abraded on one side with the paint on the opposite side barely touched. This indicates that the particle, if moved, was in motion for only a short period of time, spending the majority of time stationary in a stable position at the stream bed surface while high bed load activity scoured the paint from its upper side. Sections of the channel bed can therefore remain stable even while rates of bed load transport are very high.

The long profile survey shows general thalweg deposition of 15-20 cm occurred during the May flood over the upper riffle, with thalweg scour of 10-20 cm prevailing over the lower main riffle. Just below the upper riffle there was also very deep scour and fill, and these channel dynamics partly explain the patterns of recovery of the tracers. The

very low recovery rate for tracers placed on the upper riffle could be attributed to particle burial in the dynamic pool zone immediately downstream. However, two of the longest travel distances were recorded by tracers from the upper riffle. This suggests earlier entrainment of tracers on this riffle, greater travel distances, and higher abrasion of the paint as another reason for low recovery. The lower riffle is much more stable, with less pronounced scour and fill contributing to the higher recovery rates.

One tracer recovered after the June flood had traveled 900 m, more than twice as far as the maximum 360 m of travel measured for the May flood. However, the mean distance of travel for the other 25 tracers recovered after the June flood was only 86 m, which barely exceeds the 83 m for the May flood alone. It would be expected that particles which had experienced the second and larger June flood in addition to the May flood should have traveled much further on average. In fact, 18 of the tracers recovered after the June flood were those positioned in clusters, and considering only these tracer types the mean travel distance actually drops from 110 m to 89 m. Tracers recovered after the June flood, which were not found earlier after the May flood, may have been deeply buried in the stream bed. Although subsequently re-exposed, their burial and removal from transport resulted in lower travel distances.

6.3.2 Evidence of stochastic and chaotic behavior in transport

Comparison of the travel distances of tracers recovered which had originally been placed close together gives some interesting insight into the bed load process (Table 6.3). In some cases a similarity in transport distances between neighbors is found, but in other

cases there is dramatic dispersion in the transport paths of one time neighbors. Neighboring tracers in the same row or in the same cluster were found to travel both very similar distances in some situations, and in others to travel very different distances. Examples of each of these situations are described as follows.

Table 6.3 Plan view of tracer travel distances for particles recovered after the May flood, in reference to their original tracer row location in the stream bed. Tracer rows are numbered, with -c added for cluster placement, and -i added for individual placement

Tracer row	Left bank (looking upstream)								Right bank	
		Distance of travel (m)								
26-c		0								
25-i								24.1		
24-c									74.1	
23-i										
22-c				360, 336, 53.1						
21-i			59.5	125						
20-c		43.3		33.1						
19-i		186								
18-c										
17-i			13.4	15.5		66.2				2.4
16-c		94.1, 146		12.5						
15-i	6.1		2.4	11.9	28.1				151	77.6
14-c				35.1, 141					137, 69.7	
13-i	0		1.2			118				
12-c		83.1		137, 55.2					186	
11-i	0.9	138	18.3							
10-c		105, 109, 0.3		31.4, 304					102	
9-i			110			110	95.6			104
8-c		185		60.5					15.9, 243	
7-i		4.1		156						
6-c		6.7							179, 119	
5-i		7.1		9.8						
4-c		85.8		63.9					60.8, 76.1	
3-i	55.9	19.7							49.5	0
2-c										
1-i	13.6				5.3				0	1.5

Similarity in transport between neighbors. In row 4 (clustered), four tracers were recovered with travel distances ranging only between 61-86 m. In row 9 (individual), four tracers were recovered with travel distances ranging only between 96-110 m, and just upstream in row 10 (clustered) three more tracers moved close to 100m.

Dispersion in transport between neighbors. In row 10 (clustered), there was a high recovery rate of tracers, with travel distances ranging from 0.3-304 m. Entrainment of the left hand cluster in this row led to two tracers traveling 105 m and 109 m, while the third tracer moved just 0.3 m. Breakup of the center cluster led to one tracer traveling 31 m, while another traveled 10 times as far (304 m). Entrainment of the right hand cluster in row 8 led to one particle traveling 16 m with another traveling 243 m. Mobilization of the center cluster in row 22 left one particle traveling 53 m, while two others traveled 336 m and 360 m. These sharp differences in travel distances between particles placed in contact with each other in the same cluster could not be explained in terms of their relative sizes. In half the cases the smaller tracers did move the greater distances, but in the other half the larger tracers outran the smaller ones.

6.3.3 Distance of travel relationships

When the tracer attributes of b-axis diameter, mass, and sphericity are plotted against distance of travel, weak negative trends indicate that smaller, lighter, and more rounded particles tend to travel further although the range in scatter is wide (Figures 6.13a and 6.13b). There are very little differences between the relationships for individual and
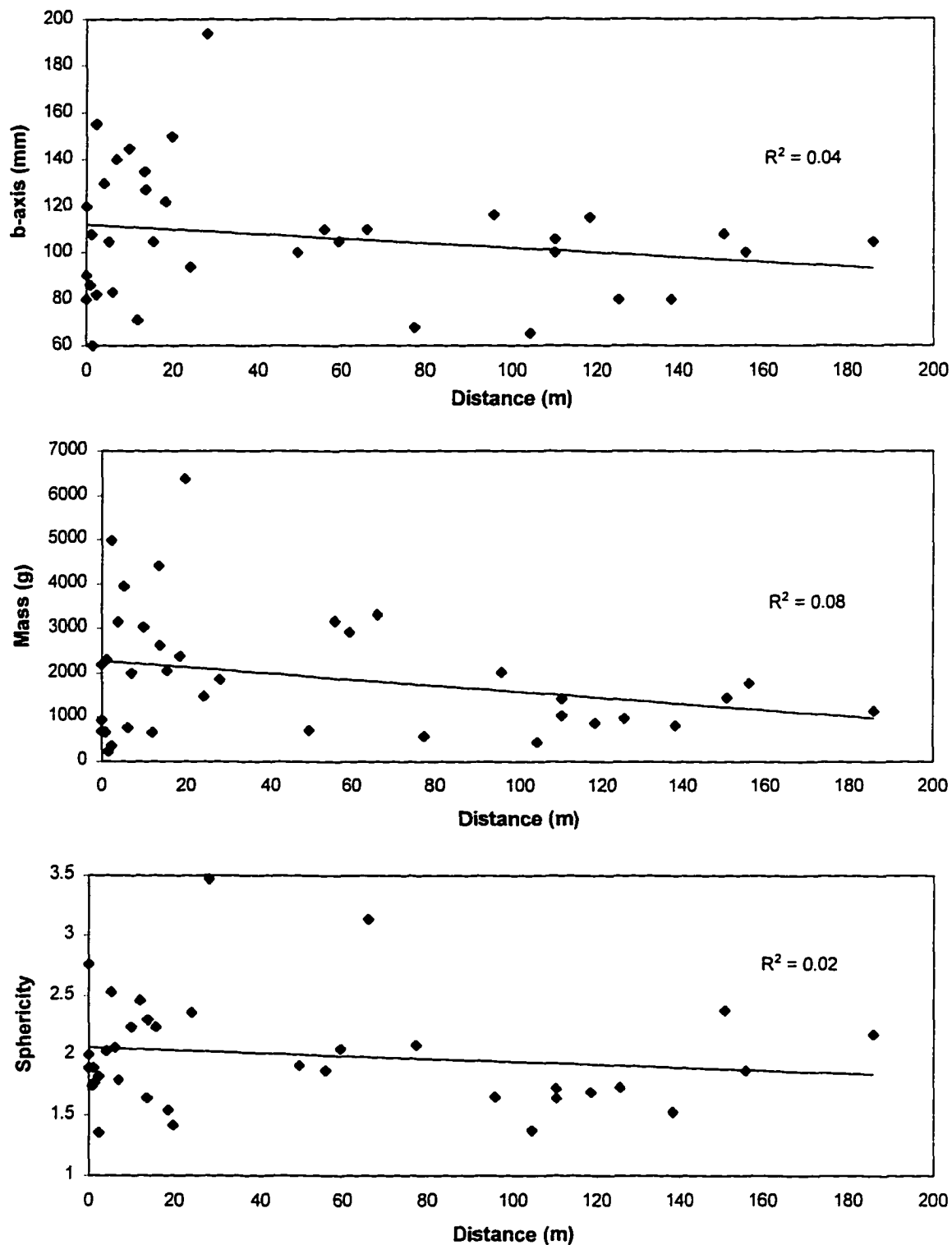
Figure 6.13a Individually placed tracers - distance of travel relationships for particle b-axis, particle mass, and particle sphericity from the May flood.
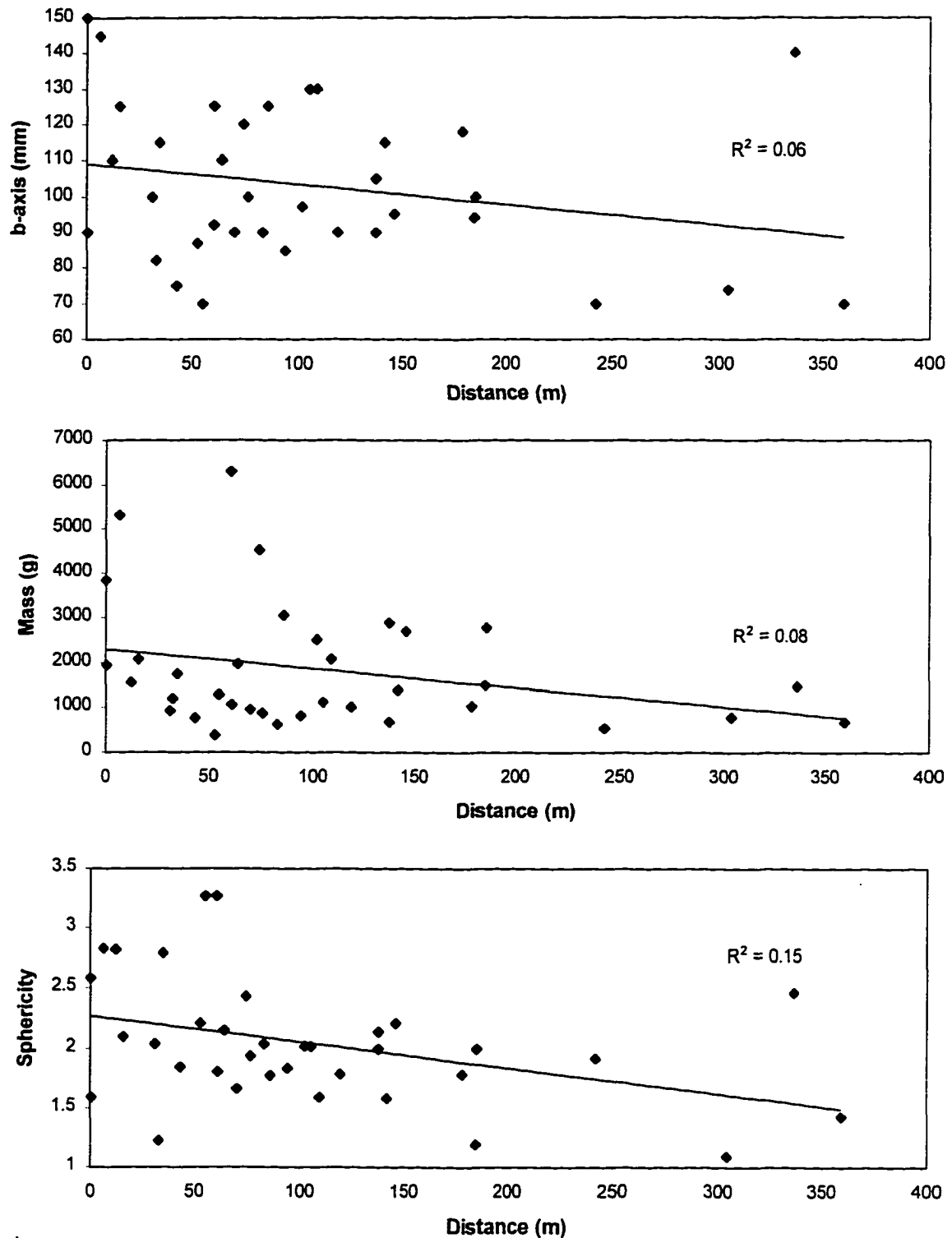
Figure 6.13b Clustered tracers - distance of travel relationships for particle b-axis. particle mass, and particle sphericity from the May flood.

clustered tracers. The tracers which traveled the greater distances do tend to be the smaller, lighter, and more rounded particles, but these characteristics do not always lead to high travel distances. Many small and rounded tracers move relatively short distances as well, probably due to their burial at some stage, and this produces the wide scatter on the distance of travel plots. Smaller and more rounded particles have a greater potential to travel longer distances, but this potential may not be achieved if the particle comes to rest in a stable pocket location or becomes buried. Although more easily entrained in transport because of their lower mass, it could be argued that smaller particles are more likely to subsequently find stable pockets in the stream bed, reducing the difference in mobility between different size particles. The results of the tracer experiment indicate no dependence of transport distance on size during bed load transport for the particles recovered after the May flood.

6.3.4 Tracer size distributions

Particle size distributions for the tracers placed individually and the tracers placed in clusters are very close to each other (Figure 6.14). None of the smallest tracer particles below 60 mm in size where recovered, and the plot shows the distributions for recovered tracers to be coarser than the original population. This is probably the result of smaller particles being more difficult to recover from the stream bed, producing a slight bias in the recovered sample towards coarser particles. The smaller particles which traveled the furthest are also more likely to have experienced greater abrasion, leaving less paint for identification. However, even taking this bias into account would not greatly improve the

weak trends in the distance of travel plots, because of the large number of small tracers

that were found to move short distances.
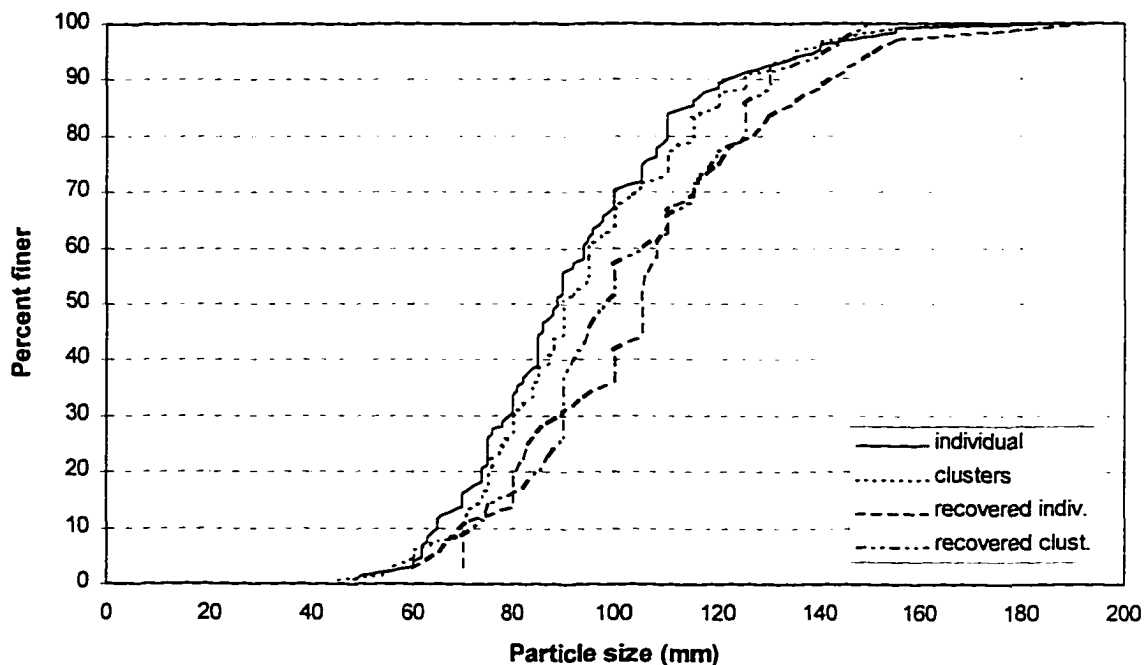
Figure 6.14 Size distribution of individual and clustered tracers positioned on the stream bed, and the size distribution of the tracers recovered after the May flood.

Although the recovered populations are small, the size distribution for the individually placed tracers seems slightly coarser than for the tracers placed in clusters. However, the significant difference in mean travel distances between the two types of tracers can not be attributed to this small difference in particle size distribution. Tracer positioning method appears to influence the subsequent entrainment and distance of travel.

6.4 Channel Surveys

Bank erosion, scour and fill, and the movement of pools were all visibly evident after the occurrence of the first flood in May 1995. Subsequent re-survey of the channel long profile and cross sections confirmed that major channel changes had taken place during this bankfull flow event. The June 1995 flood produced similar adjustments in the stream channel, even though this second flood was several times bankfull in magnitude.

6.4.1 Long profile channel changes

Dramatic scour and fill changes are well illustrated in the long profile surveys of the channel thalweg (Figure 6.15). During the May flood, deposition of up to 0.6 m occurred in pools A and E at the base and top of the study reach, while the two upper pools D and E migrated downstream about 6 m. Pool D almost completely filled after 0.3 m of deposition, and pool E just upstream scoured by 0.3 m. Throughout the central riffle section, there appears to have been overall scour along the thalweg of 0.1-0.2 m. The installation of the log sill introduced a nick point in the profile, with a corresponding plunge pool B below, but the overall reach slope remained constant at one percent.

The June flood produced similar changes in the channel thalweg, although it was several times the magnitude of the May flood. A new pool F was established at the top of the study reach after nearly 0.75 m of scour. The next two original pools D and E continued to migrate downstream, but this time the upper pool E filled 0.15 m and decreased in size while the lower pool D scoured over 0.3 m and became re-established.

Immediately downstream of the pools at the top of the main riffle is a zone of deposition. The main riffle experienced net deposition during the June flood, ranging up to 0.2 m in the area upstream of the sampling bridge. Another new pool C was established, this time towards the top of the main riffle. The small pool below the plunge pool B completely filled, as did pool A after a further 0.2 m of deposition, while a new deep pool formed below the study reach.
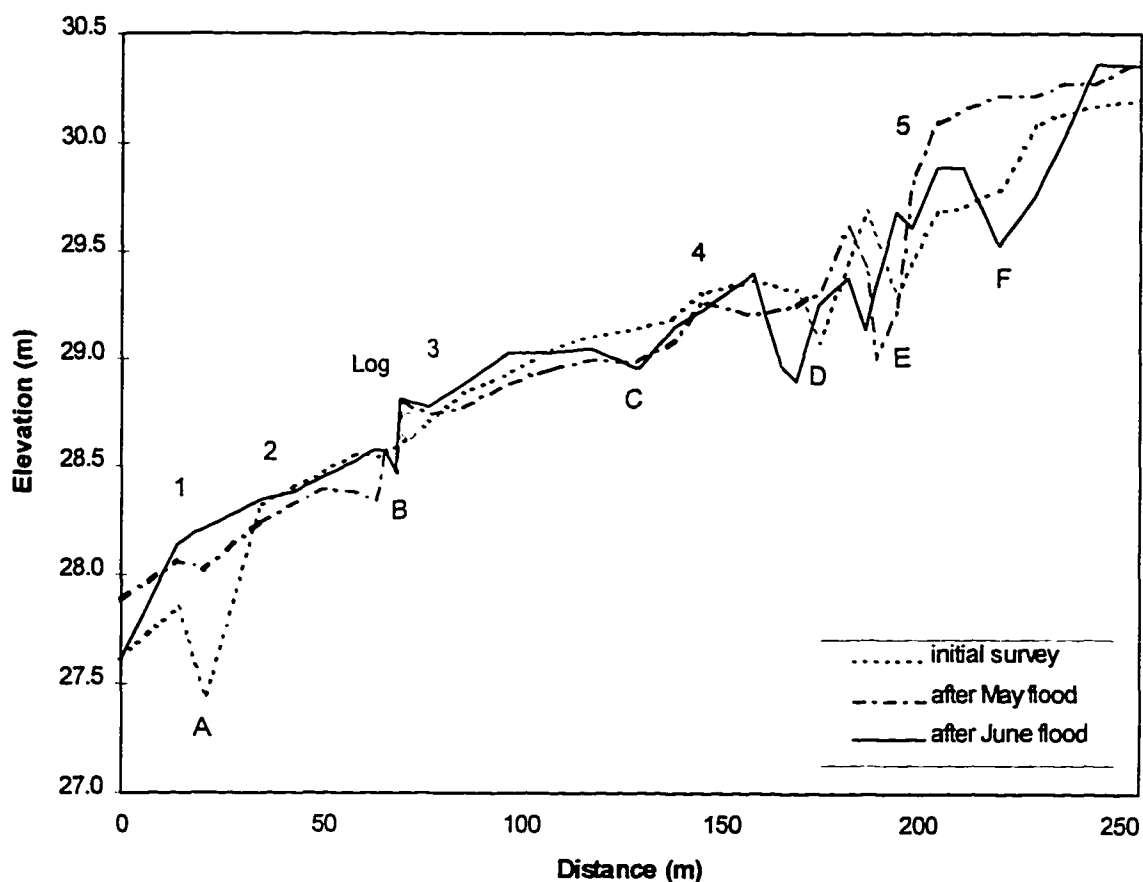
Figure 6.15 Thalweg long profile surveys for Dupuyer Creek, 1995. Labeled numbers 1-5 refer to the surveyed cross sections (Figure 6.16), and letters A-F refer to pool features.

6.4.2 Cross sectional channel changes

Cross sections 1 and 5 experienced the largest changes over the course of the two floods (Figure 6.16a/6.16b). Both of these cross sections are on channel bends in or near pool sections which are shown to be the most dynamic based on the long profile surveys. Cross section 1 is located on the bend below the sampling bridge (Figure 4.4). The left bank at this cross section retreated rapidly in both floods, 2 m in May and a further 1.5 m in June, while deposition across the entire channel width completely filled the pool producing a wider shallower channel.

Cross section 5 is upstream where the channel is particularly wide, and includes a large gravel bar feature which is only submerged at high flows. The main channel against the left bank of the cross section showed increasing deposition, although the deepest point did not change in elevation by more than 0.15 m. In contrast to cross section 1, bank erosion was minimal with just 0.3 m lost from the left bank during the first flood, and no further retreat after the second. Most of the scour and fill took place towards the
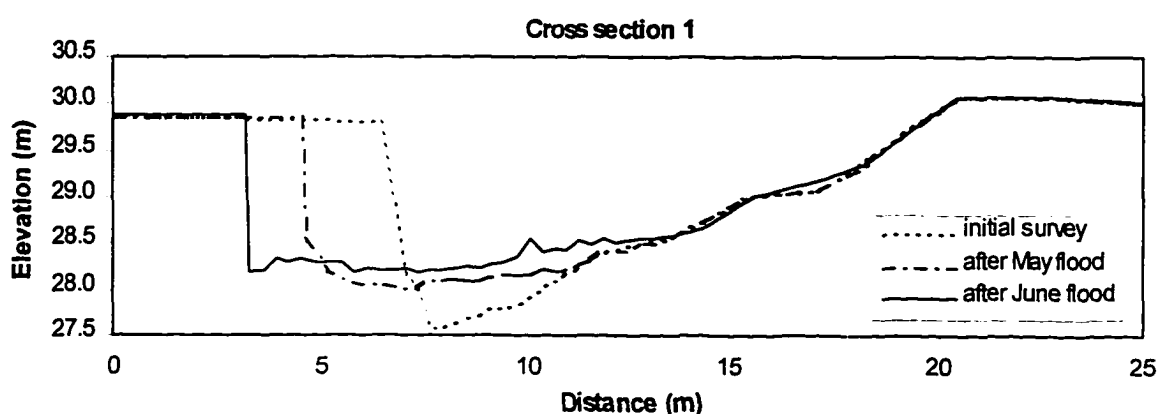
Figure 6.16a Cross section 1 surveys for Dupuyer Creek, 1995. Cross sections 2-5 shown overpage in Figure 6.16b. All axes are set to the same scale.
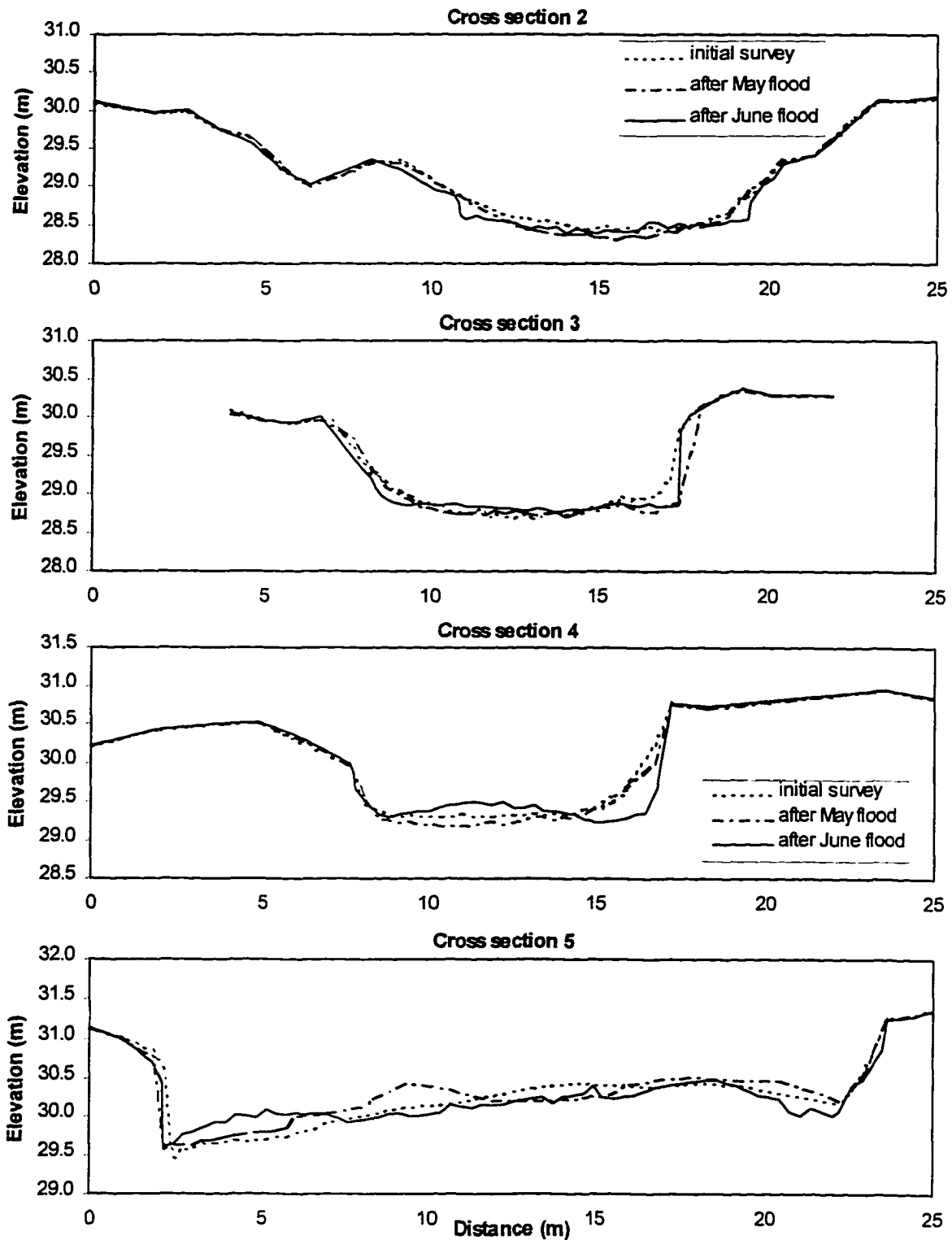
Figure 6.16b Surveys of cross sections 2-5 for Dupuyer Creek, 1995. Cross section 1 shown on previous page in Figure 6.16a. All axes are set to the same scale.

right side of the low flow channel, and across the full width of the channel bar. Bar deposition dominated after the May flood, while scour was dominant during the June flood removing up to 0.5 m of bar deposits. Both banks remained very stable even though large changes took place across the entire channel bar and thalweg.

Cross sections 2, 3, and 4 are on lower, middle, and upper sections respectively of the main straight riffle. These cross sections experienced 1.2-1.5 m of channel widening together with scour and fill. Cross sections 2 and 3 showed a widening and flattening of the channel bed. Here the channel became more flume-like in character, with scour and fill generally less than 0.15 m. In contrast cross section 4, which is only 15 m or so below pool D close to the upper bend, showed a different pattern of change. After initial scour during the May flood, a mid-channel bar formed in response to 0.3 m of deposition from renewed scour of pool D. This caused the main thalweg to shift to the right bank and erode this bank in the process.

6.4.3 Overview

These observations demonstrate that significant channel scour and fill occurs in Dupuyer Creek on a regular basis during bankfull floods or larger events. The elevation of the thalweg fluctuates from one flood to the next, alternating between scour and fill such that new pools may be created while others are filled. Interactions and feedback processes between flow hydraulics and the stream bed must contribute to this fluctuating pattern in the channel system which may be exhibiting dynamic equilibrium behavior.

Differences in scour and fill between adjacent pools and riffles must be the result of changing local hydraulic conditions which in turn influence the movement of bed load from one pool or riffle to the next. The channel bed is likely extremely dynamic during these flood events. The re-surveys at lower flows simply reveal the configuration of riffles and pools at the point when significant bed load transport ceased.

6.5 Channel Substrate Surveys

Repeat pebble counts on the main study riffle before, in between, and after the two floods of 1995 show significant temporal variation in substrate size distribution (Figure 6.17a). After the first flood the changes were slight, and the D_{50} and D_{84} remained almost constant at 60 mm and 112 mm respectively. However, after the second flood the riffle size distribution became finer, and the D_{50} and D_{84} decreased to 48 mm and 106 mm respectively. These temporal variations at the same mid-riffle location are similar in magnitude to the spatial variations found across the upper, middle, and lower riffle sections, where D_{50} varied between 45-63 mm and D_{84} between 100-112 mm (Figure 4.5). Although sample error explains some of this variation, downstream migration of relatively coarse and relatively fine channel substrate zones may be occurring, perhaps related to the pulsing dynamics of the bed load transport process (see discussion below on transport mechanisms).

The substrate size distribution of the main study riffle is slightly coarser than the size distribution of the study reach as a whole. This is due to the absence of major pools and
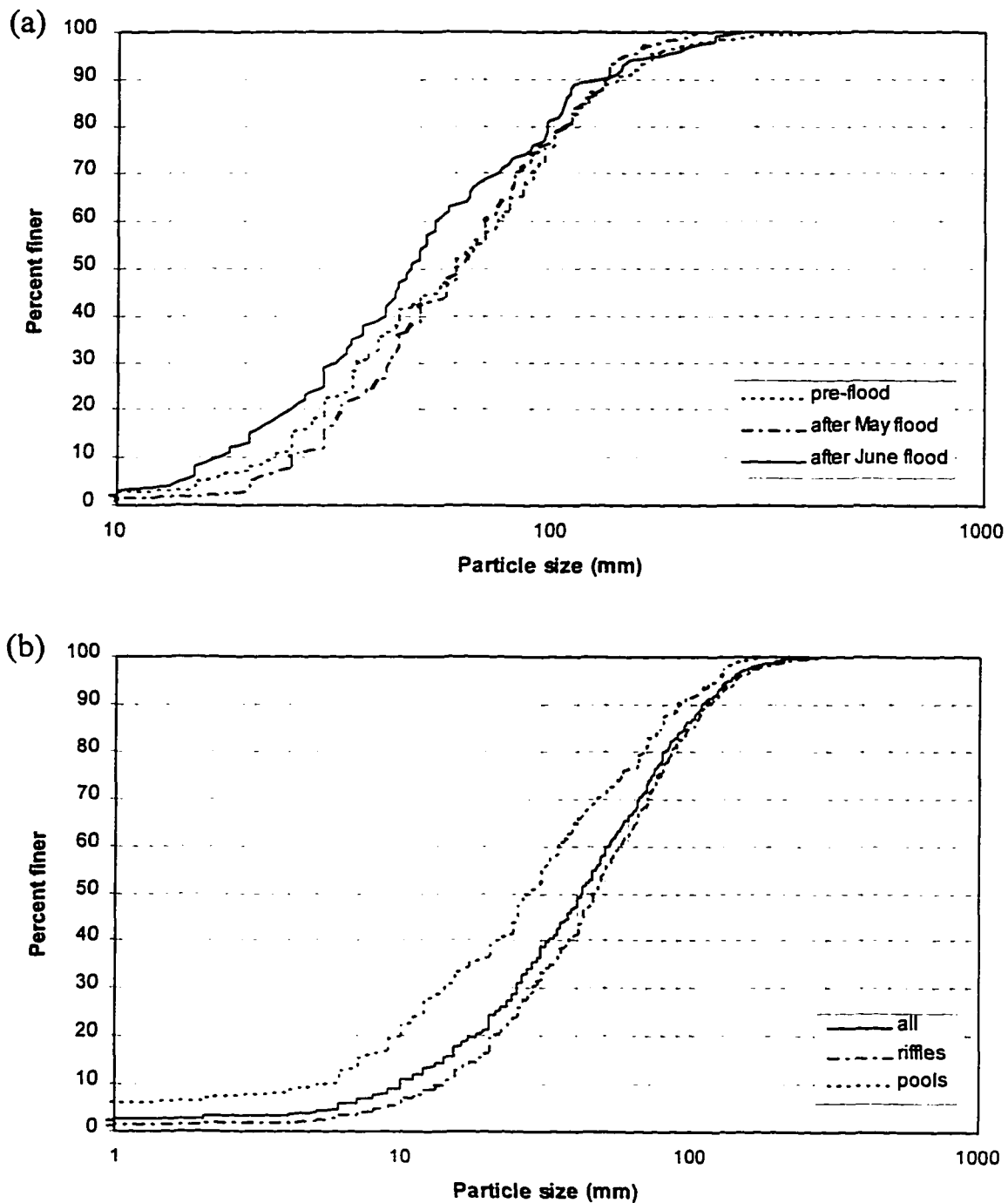
Figure 6.17 (a) Temporal variation in the particle size distribution at the riffle upstream of the sampling bridge. (b) Particle size distribution for the study reach as a whole, after the floods of 1995.

the limited deposits of fine gravel in the main riffle. The pool/riffle ratio for the reach scale pebble count is 24% pool and 76% riffle, which is typical for the main fork of Dupuyer Creek. The size distribution for pools alone is notably finer than that for riffles due to local deposits of fine gravel in the pools (Figure 6.17b). The median particle size for pools is 27 mm, compared to 45 mm for riffles and 42 mm for the reach as a whole.

6.6 Mechanisms of Bed Load Transport

Rates of bed load transport in Dupuyer Creek were shown to fluctuate by one or two orders of magnitude, even during steady flow conditions, as other workers have found (Emmett, 1976; Leopold and Emmett, 1976, 1977; Ergenzinger and Custer, 1983; Custer et al., 1987). Several mechanisms of bed load transport have been observed or suggested which could explain the variability in the process. Bed load transport may occur by the migration of dune or sheet-like bed forms (Kuhnle and Southard, 1988; Whiting et al., 1988; Gomez et al., 1989; Dinehart, 1989, 1992a, 1992b; Pitlick, 1992), as kinematic waves of particles in a slow-moving traction carpet (Langbein and Leopold, 1968; Gomez, 1983; Reid et al., 1985), or through pulses related to turbulent flow cells during unsteady flood flows (Ergenzinger et al., 1994). The dominant bed load transport mechanism could vary from one stream channel to another depending on channel size and slope, the size distribution of the channel substrate, and sediment supply characteristics, although this has yet to be investigated.

In Dupuyer Creek, the variability in the bed load transport rates was accompanied by variability in the size distribution of the individual bed load samples. The patterns of variation in the fractional transport rates could have been the result of longitudinal sorting of bed load by size, as found by Iseya and Ikeda (1987) in a flume study, and by Dinehart (1992a) in field measurements. The nature of the bed load pulsing was plainly heard from the pattern of collisions of bed load particles against the metal sampler support pipes. Bed load pulses occurred over a range of time-scales, from a few seconds to several minutes. Often, the high frequency pulses were superposed on background low frequency pulses. This pattern may have been the result of migrating bed forms, with smaller dunes superposed on larger dunes (Dinehart, 1992a). However, unsteady flow conditions and the development of turbulent flow cells and variable bed roughness could also account for the pattern of bed load pulses (Ergenzinger et al., 1994). Whether bed forms, or flow cells, or both are present in Dupuyer Creek, the data show clearly that there remains a strong hydraulic control on the bed load transport process. This allows the concept of flow competence to be explored in detail in the following chapter.

7. FLOW COMPETENCE ANALYSIS

7.1 Shear Stress Criterion

7.1.1 Maximum particle size relationships

Flow competence analyses are most commonly based on relationships between flow shear stress exerted at the stream bed and the maximum particle size entrained in bed load transport. The Shields criterion (Shields, 1936) is the most widely used method of predicting thresholds in bed load initiation:

$$\tau_{ci} = \theta_{ci}(\rho_s - \rho)gD_i \tag{1}$$

where τ_{ci} and θ_{ci} are, respectively, the critical shear stress and Shields dimensionless parameter to entrain a particle of diameter D_i (m), ρ_s and ρ are the densities of sediment and water respectively (kg/m^3), and g is the acceleration due to gravity (m/s^2). Mean cross sectional shear stress, τ (N/m^2), is most easily estimated using du Boys formula:

$$\tau = \rho gRS \tag{2}$$

where ρ is the fluid density (kg/m^3), g the acceleration due to gravity (m/s^2), R the hydraulic radius (m), and S the water surface slope. In the wide and relatively shallow flows within the trapezoidal cross section of the study riffle, the hydraulic radius can be

90

approximated by mean flow depth. Andrews (1983) suggested the mean flow depth should be calculated only across that portion of the channel bed which is active in transporting bed load. In larger rivers, there may be regions such as those close to the banks where flows are too shallow and/or too slow moving to transport bed load. At the sampled cross section on Dupuyer Creek the trapezoidal shape enabled active bed load transport across almost the entire width. Only the outer meter against each bank was considered inactive and excluded from the mean depth calculations.
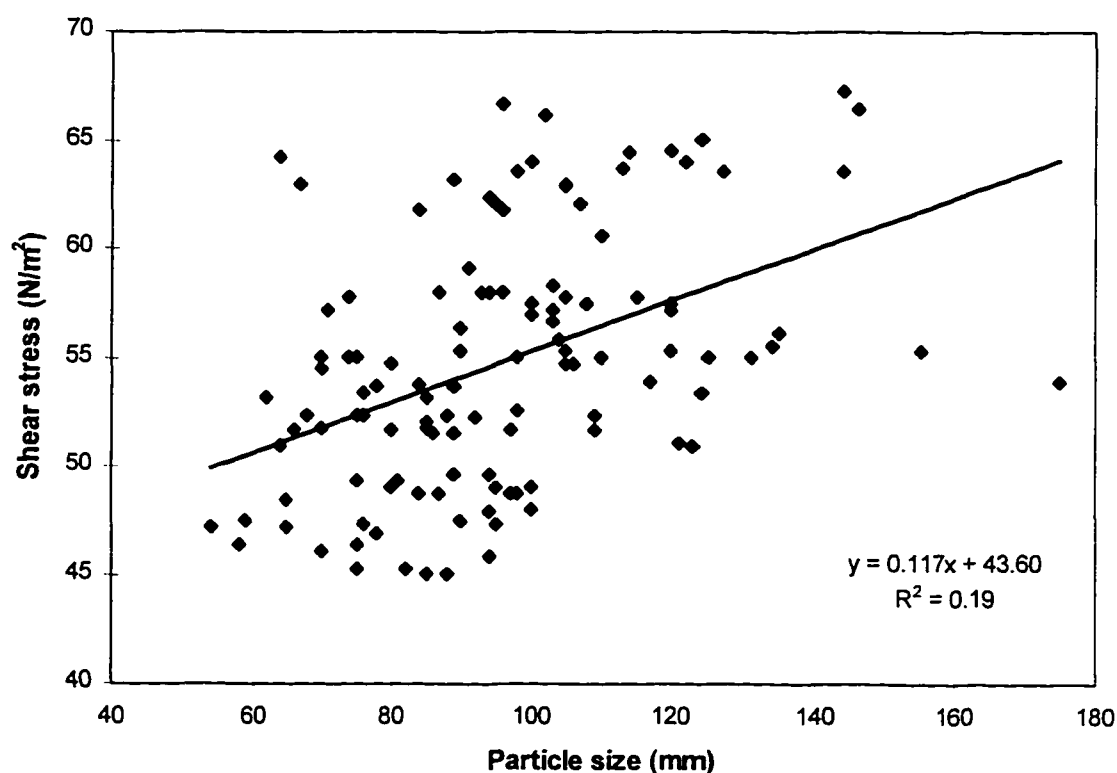
Figure 7.1 Relationship between flow shear stress and the maximum particle size for all 120 individual bed load samples taken over the May and June floods, 1995.

When the largest particle size in each individual bed load sample is plotted against the estimated mean shear stress, a wide range in scatter is seen (Figure 7.1). The pulsing

nature of the bed load means that any single sample may not contain the largest particle size in transport under the prevailing flow conditions. The largest particles move in pulses with an interval which often exceeds the manageable sample duration. Unsteady transport of coarse bed load, together with the practical constraints on sample sizes which can be removed from the stream bed, necessitates the aggregation of series of smaller individual samples into larger sample groups.

The relationship between maximum particle size in each sample group and the mean shear stress shows considerably less scatter, and a power regression line can be fitted with an R-squared value of 0.63 (Figure 7.2). For higher shear stresses and particle sizes there is a noticeable increase in the scatter of the data. The slope of 0.41 for the relationship indicates a greater dependence of critical shear stress on absolute particle size than previously reported by authors (Table 7.1).

Variation in the dimensionless shear stress coefficient appears to be related to relative particle size in the manner suggested by Andrews (1983). A power regression relationship can be fitted (Figure 7.3, $R^2 = 0.77$) to determine the constant θ and the slope x in the equation:

$$\theta_{ci} = \theta(D_i/D_{50})^x \qquad (3)$$

To estimate the constant θ, which represents the critical dimensionless shear stress for the median particle size, did require extrapolation beyond the sampled data range. However, the
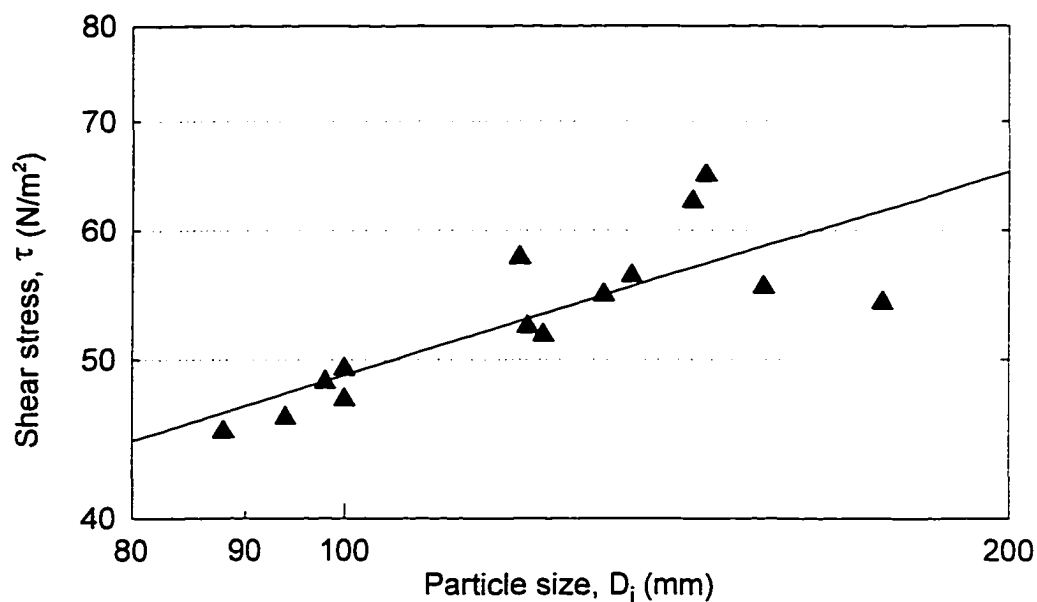
Figure 7.2 Critical shear stress against the maximum particle size entrained for the sample group data. Power regression plots as straight line with log-log scales ($R^2 = 0.63$).
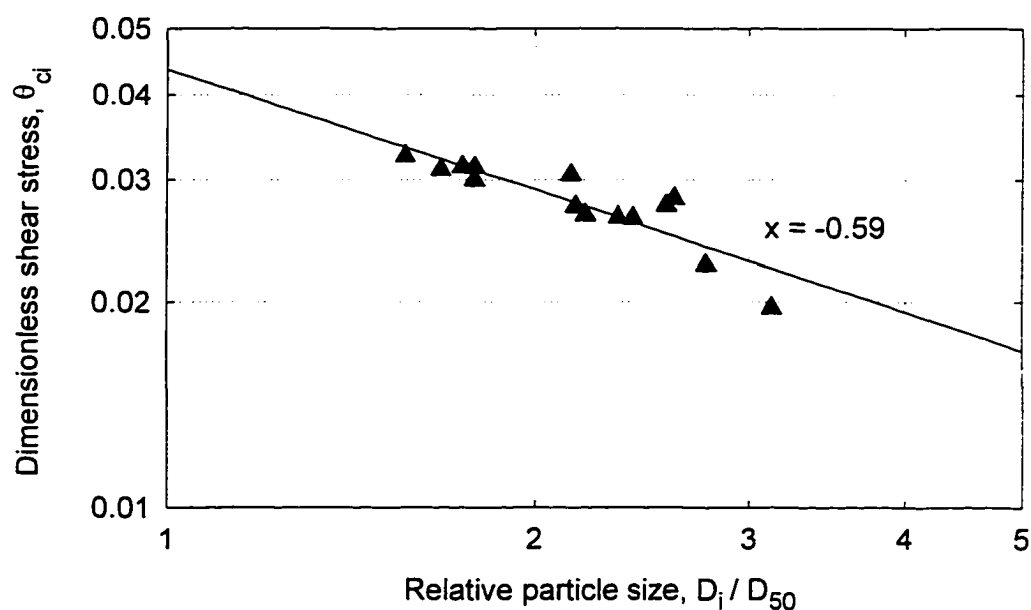
Figure 7.3 Critical dimensionless shear stress against relative particle size. Slope of power regression line ($R^2 = 0.77$) gives a value of -0.59 for x in equation (3). The dimensionless shear stress at relative particle size 1.0 gives a value of 0.044 for θ in equation (3).

obtained value of 0.044 for θ is only slightly lower than values found by workers on other rivers (Table 7.1). Other studies have found the value of x to be around -0.7 or larger, while the -0.59 for Dupuyer Creek indicates slightly greater size selectivity in the bed load process. Despite this, use of appropriate published values for θ and x would give reasonable predictions of bed load thresholds.

Table 7.1 Values of θ and x in $\theta_{ci} = \theta(D_i/D_{50})^x$ (from Petit, 1994)

θ	x	D_{50} (mm)	D_i/D_{50}	Reference
0.088	-0.98	1.3-25	0.045-4.2	Parker et al. (1982b)
0.083	-0.87	54-74	0.3-4.2	Andrews (1983)
0.045	-0.68	20	0.4-5.9	Milhous (1973) in Komar (1987)
0.045	-0.68	20	0.5-10	Carling (1983)
0.045	-0.71	7.5	0.67-5.33	Hammond et al. (1984)
0.089	-0.74	23-98	0.1-2	Ashworth and Ferguson (1989)
0.047	-0.88	73	0.04-1.2	Ferguson et al. (1989)
0.049	-0.69	18-32	0.15-3.2	Ashworth et al. (1992)
0.044	-0.59	56	1.57-3.13	This study

7.1.2 Sensitivity to estimated particle sizes

Useful flow competence analysis is dependent on accurate estimates of the stream bed size distribution and the maximum particle sizes entrained in bed load transport across a range in flow conditions. The modeling of particle hiding and exposure relies upon a good estimate of the stream bed median particle size, while the maximum particle sizes captured in bed load sampling are critical in defining the flow competence relationship. It is therefore prudent to examine the sensitivity of parameters in the shear stress criterion to different estimates of these characteristic particle sizes in Dupuyer Creek.

In the Methods section it was suggested that a surface-area based pebble count is the correct procedure for estimating the stream bed size distribution and median particle size in flow competence analyses. However, there is considerable variability in the exact technique used in the field to select the particles for measurement, and different variants of the pebble count will produce different results (Marcus et al., 1995; Wohl et al., 1996; Kondolf, 1997). At the current time there is no consensus as to which form of pebble count should be employed in a flow competence analysis. Here the effect of using a stream bed D_{50} estimate from a reach scale pebble count (42 mm) is compared to that obtained with a pebble count restricted to the riffle where bed load was sampled (56 mm). The reach scale pebble count gives a finer stream bed size distribution due to the inclusion of finer deposits around pool regions and certain bar features which are absent from the sampled riffle.

If the flow competence at the sampled cross section is dependent on the local stream bed size distribution, then an added complication is the possible variation in local size distribution over the passage of a flood hydrograph. Pebble counts can only be undertaken at relatively low flows both before and after a flood. As a result there is no information on the stream bed size distribution while bed load transport is active. With active bed load, it would seem highly probable that changes in stream bed size distribution will occur in response to the size characteristics of sediment supplied from upstream, and due to sizes left during winnowing in response to selective transport. These factors produce difficulties when determining the D_{50} in flow competence modeling.

When sampling for the maximum particle size in transport there is concern that extreme values and outliers can distort the flow competence relationship and render it unreliable (Komar and Carling, 1991; Wilcock, 1992). To address this concern some workers have taken the mean of the largest three to five particles captured to represent the maximum size in transport (Carling, 1983). In this analysis, flow competence was examined for the following definitions of maximum particle size (Figure 7.4):

D_{max} - Absolute maximum particle size captured in each sample group

D_{max} (or) - Absolute maximum particle size captured in each sample group, but with the removal of a suspected outlier from one sample group (175 mm particle diameter in group 4)

D_{max} (3) - Mean of the three largest particles captured in each sample group, excluding the same suspected outlier

Table 7.2 Sensitivity of model coefficients and constants to the values assumed for maximum particle size in transport, D_i as defined above, and stream bed D_{50} in; (a) The relationship between shear stress τ and maximum size in transport D_i and; (b) The relationship between critical dimensionless shear stress θ_{ci} and relative particle size D_i/D_{50}

	(a) $\tau = aD_i^b$			(b) $\theta_{ci} = \theta(D_i/D_{50})^x$			
D_i	a	b	R^2	θ (D_{50}=56)	θ (D_{50}=42)	x	R^2
D_{max}	7.24	0.41	0.63	0.044	0.052	-0.59	0.77
D_{max} (or)	4.05	0.54	0.79	0.040	0.046	-0.46	0.73
D_{max} (3)	2.94	0.62	0.85	0.040	0.045	-0.38	0.69

Note: By definition, b-x = 1

Table 7.2 shows that the relationship between shear stress, τ, and maximum particle size, D_i, improves when first the outlier is removed, and then the mean of the three largest

particles is considered. However, the corresponding relationships for the dimensionless shear stress, θ_{ci}, show a slight decrease in the R-squared value. The coefficient x in the dimensionless shear stress equation is particularly sensitive to the definition of maximum particle size in transport. Removing the outlier and taking the mean of the three largest particles produces a flow competence relationship with even greater size selectivity, moving further away from values obtained by other workers (compare to Table 7.1). This shift is further illustrated in Figure 7.4 which shows a steeper regression line for the mean of the three largest particles.

Flow competence relationships based on the single largest particle in each sample are very sensitive to the influence of outliers. More consistent results may be achieved if the mean of the three largest particles captured is used to model flow competence. It is interesting to note that values for the second largest particle size were very close to the mean values of the three largest particles, giving almost identical flow competence relationships. The value of θ, the dimensionless shear stress coefficient for the median particle size, is by definition dependent on our estimate of this particle size, but also our estimate of maximum size in transport as shown in Table 7.2. However, less certainty can be placed on the estimates of θ, compared to x, because they were derived by extrapolation outside of the range in particle sizes sampled. Observations of bed load suggest the relationship may not extend down into these smaller particle sizes.
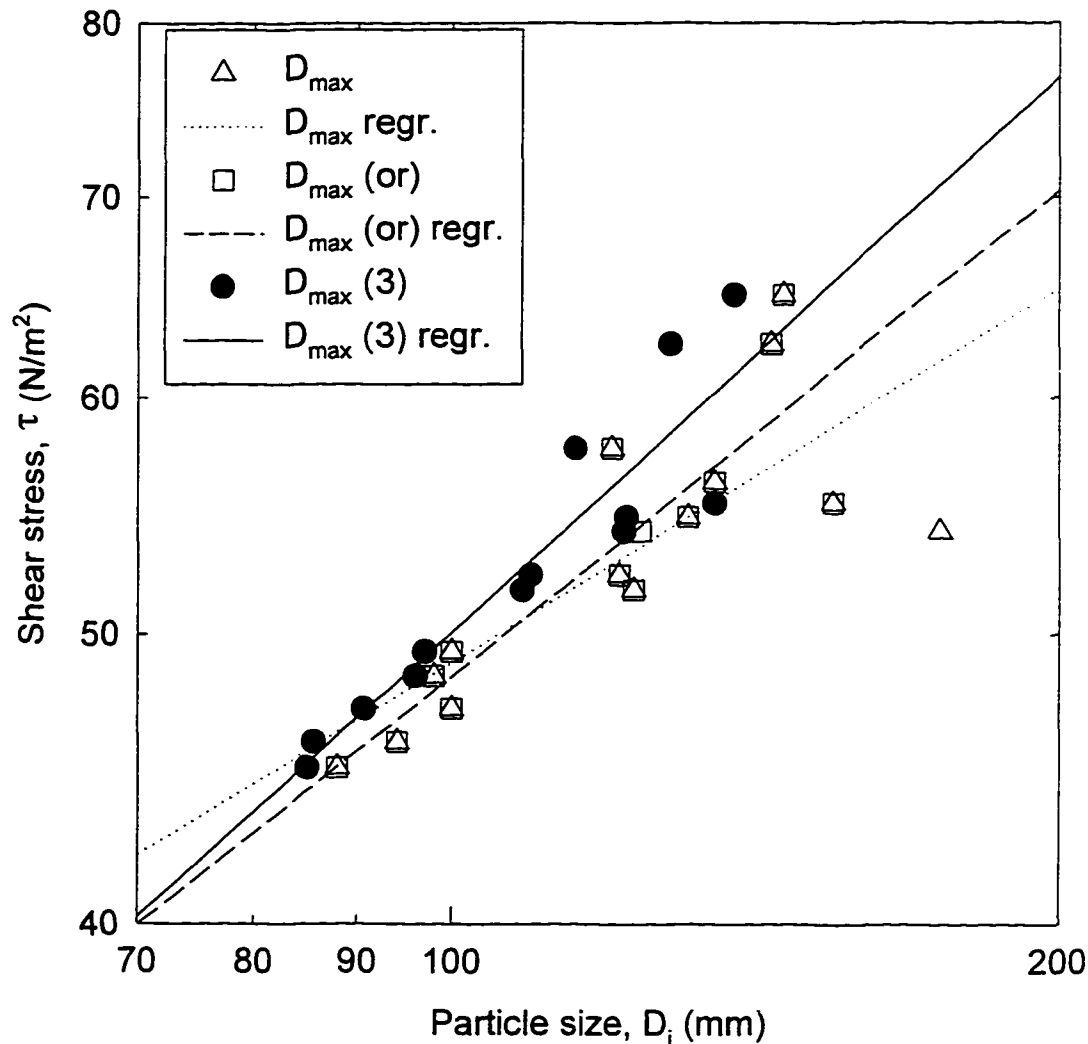
Figure 7.4 Flow competence relationships of the form $\tau = aD_i^b$ for; D_{max} = maximum particle size; D_{max} (or) = maximum size with outlier removed; D_{max} (3) = mean of the three largest particle sizes.

7.1.3 Bed load percentile relationships

In determining flow competence, sample size and scaling problems associated with using an extreme value of the transport grain-size distribution has led to the consideration of alternative definitions (Wilcock, 1992). Flow competence may be defined for the bed load size distribution as a whole, such as the median particle size in transport or some

coarse percentile that is established by a reasonable number of grains. Komar and Carling (1991) examined flow competence relationships in terms of changing grain-size percentiles with varying flow stresses:

$$\tau = aD_x^b \tag{7}$$

where τ is the shear stress required to bring the bed load percentile x to a given size. This analysis was undertaken with the Dupuyer Creek data by determining bed load size distribution percentiles for each sample group as a whole, ranging from D_{50} to D_{max}. Regression analysis was used to determine the coefficients a and b, and the results are summarized in Table 7.3 along with the Oak Creek data of Milhous (1973) as analyzed by Komar and Carling (1991).

Table 7.3 Regression coefficients of the Dupuyer Creek and Oak Creek data for $\tau = aD_x^b$ where τ is the flow stress (dynes/cm^2) and D_x is the diameter (cm) of a percentile of the sieved bed load size distribution or the maximum particle sizes transported

D_x	Dupuyer Creek			Oak Creek		
	a	b	R^2	a	b	R^2
D_{50}	86	1.12	0.62	350	0.11	0.68
D_{60}	106	0.94	0.65	335	0.13	0.72
D_{70}	114	0.86	0.69	315	0.15	0.76
D_{75}	111	0.85	0.73	-	-	-
D_{80}	139	0.71	0.74	286	0.19	0.80
D_{90}	162	0.57	0.83	241	0.26	0.81
D_{95}	182	0.48	0.76	209	0.30	0.69
D_{max} (3)	121	0.62	0.85	-	-	-
D_{max} (or)	140	0.54	0.79	-	-	-
D_{max}	188	0.41	0.63	166	0.36	0.65

Only the D_{max} regressions on the Dupuyer Creek and Oak Creek data produce similar relationships in terms of the coefficients a and b, and the R-squared values. Although direct comparison of absolute values for the bed load percentiles can not be made because of the truncation of Dupuyer Creek data at 38 mm, the trends in how the regression coefficients vary can be compared. Moving to smaller bed load percentiles in the Dupuyer Creek data, values for a and b rapidly diverge from those of Oak Creek with trends of opposite direction. For Dupuyer Creek the slope b increases towards smaller percentile sizes. This means that as shear stresses rise, finer bed load percentiles increase in size at a slower rate than the largest bed load particles. This is intuitive for a stream which is dominated by size selective transport. The reason for the opposite trend in the Oak Creek data may be a result of the coarse pavement layer restricting size selective transport, and differences in the distribution skewness of stream bed material.

For Dupuyer Creek, the strongest relationship is seen between shear stress and the mean of the three largest particles ($R^2 = 0.85$), closely followed by the relationship for coarse bed load D_{90} ($R^2 = 0.83$). In Oak Creek the pattern is very similar, with lowest R-squared values for the D_{50} and D_{max} sizes and the strongest relationship for the D_{90} ($R^2 = 0.81$). This suggests that a coarse bed load percentile such as the D_{90} or the mean of the three largest particles would be the most suitable parameter to model in flow competence analyses. For Dupuyer Creek these coarse percentiles are also more sensitive to changes in flow stress than the bed load D_{50}, at least over the range in flows sampled. In other words, changes in flow shear stress produce a greater response in the maximum bed load particle sizes (D_{max} (3)) than the median bed load particle size (D_{50}).

7.1.4 Shear stress estimation from velocity observations

Boundary shear stress in the proceeding analysis has been estimated from flow geometry in the du Boys formula. With the data available, this provides the most appropriate estimate of mean cross sectional shear stress. However, local shear stress over a specific area of the stream bed can be estimated from observations of velocity above that portion of the bed, and by assuming a logarithmic velocity profile. Wilcock (1996) presents a good evaluation of the precision and accuracy of techniques available in estimating local bed shear stress from velocity observations. To achieve accuracy, multiple velocity measurements should be made in the vertical so that the velocity profile can be plotted, or the depth-averaged velocity calculated. Alternatively, a single near-bed velocity observation may be used which only requires a logarithmic velocity profile near the stream bed.

Flow velocity measurements taken at Dupuyer Creek were made to estimate discharge during bed load movement. Appendix A contains these velocity observations in the form of cross sections for all flow measurements taken during the May and June floods. Due to time constraints and conditions of variable flow, only single velocity observations were made in each vertical across the channel at 0.6 times flow depth (d) below the surface to give an estimate of depth-averaged velocity U. The accuracy of the following shear stress estimates is therefore dependent on the validity of the assumption that velocity at 0.6d approximates the depth-averaged velocity. For nearly uniform flow in a wide channel with only grain-scale roughness an appropriate expression relating U and local bed shear stress τ_L is:

$$U/u_* = 1/k \ln(h/e \, z_0) \tag{8}$$

where shear velocity, $u_* = (\tau_L/\rho)^{1/2}$, ρ is fluid density, k is von Karman's constant (taken to be 0.40), h is flow depth, e is the base of the natural logarithms, and z_0 is the bed roughness length (all in SI units). An independent estimate of z_0 is required. For gravel bed rivers, z_0 is approximated by $0.1D_{84}$ (Wilcock, 1996).

The alternative method, which may be used with just a single near-bed velocity observation, is similar in form to (8):

$$u/u_* = 1/k \ln(z/z_0) \tag{9}$$

where u is the velocity observed at height z above the bed. However, this method does not apply in the case of large relative roughness (D_{84}/h greater than approximately 0.2), for which wakes dominate the entire flow field and the vertical velocity profile is non log linear. For the flows sampled in Dupuyer Creek, relative roughness ranged from 0.17-0.24 such that (9) is not always a suitable method.

Equation (8) was therefore used to establish cross sections of local bed shear stress from depth-averaged velocity estimates at 0.6d (Figures 7.5a/7.5b). High variability in estimated shear stress over each flow measurement cross section is a result of the variable velocity fields. Spatial variability in the velocity fields is caused by the immediate influence of individual grains and grain clusters in the shallow flows with
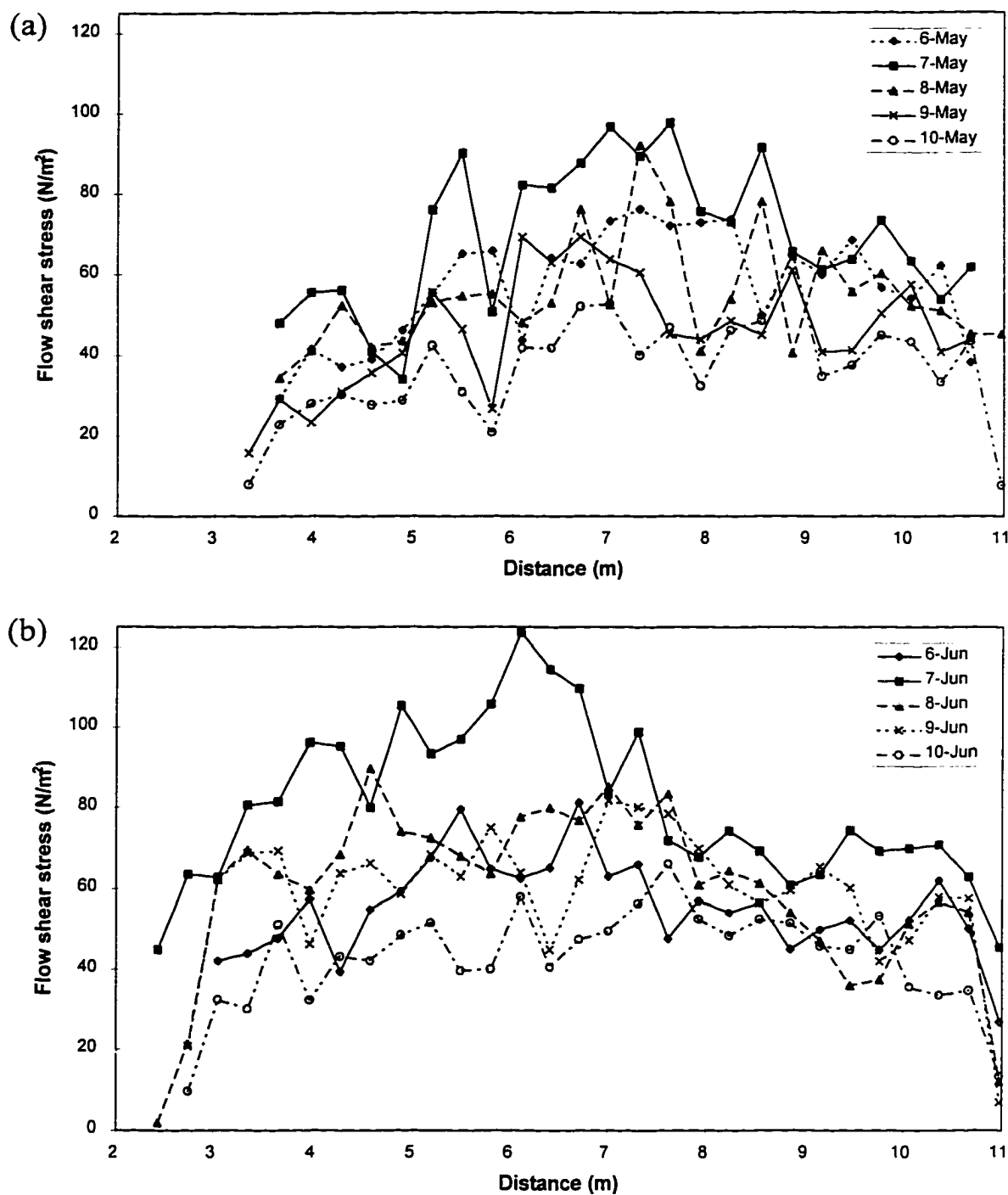
Figure 7.5 Estimates of local bed shear stress over the channel cross section from velocity measurements made with Price AA current meter at 0.6 depth; (a) May 1995 flood; (b) June 1995 flood. Velocity cross sections are located in Appendix A.

large relative roughness. High bed roughness and a corresponding high variability in flow depth produces more variability in shear stress over a cross section. Values generally range between 40-80 N/m^2 and remain high across most of the channel width. only dropping off at the far edges close to the banks. These high values across most of the channel width result from the relatively simple trapezoidal geometry of the cross section with little variation in flow depths, and helps to explain why bed load transport was active across the majority of the flow width.

Mean cross sectional shear stress was calculated from the cross sections in Figures 7.5a/7.5b and the mean shear stress for each sampling period was estimated. Sampled bed load grain size was not paired with estimated local bed shear stress because of the stochastic nature of the entrainment process, and the fact that sampled bed load was entrained upstream of the point where velocities were measured. Spatial variability and the unsteady nature of the flow make it necessary to consider mean cross sectional shear stresses in flow competence analyses.

Figure 7.6 compares the two flow competence relationships when shear stress is estimated from velocity observations and the du Boys method. For the relationship between shear stress and maximum particle size entrained, a slightly better relationship is obtained when shear stress is estimated from velocity observations (R^2 = 0.77 versus 0.63), while the slope of the relationship is very different (0.77 versus 0.41). The much higher slope indicates greater size selectivity in the entrainment process and is even further removed from values of 0.3 and lower reported by previous workers. The shear stress estimates from velocity observations were used to examine the relationship
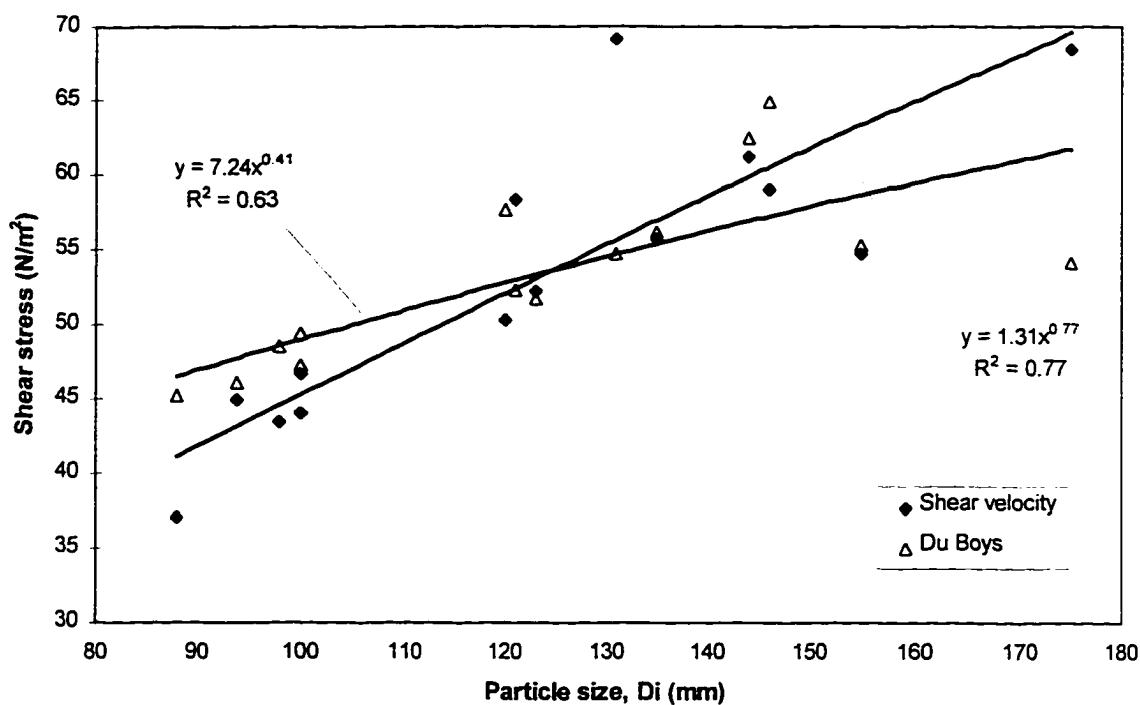
Figure 7.6 Comparison of flow competence relationships when shear stress is based on velocity measurements (shear velocity, equation 8) and depth-slope measurements (Du Boys, equation 2).

between critical dimensionless shear stress and relative particle size in equation (3). The slope of the regression line is low (0.23) and the relationship is very weak ($R^2 = 0.24$). This suggests that the hiding and exposure effect as modeled by Andrews (1983) in equation (3) may not be significant. Even when the bed roughness estimate is changed by reducing the D_{84} estimate from 109 mm to 100 mm, or when method (9) is applied, the flow competence coefficients remain much the same as above.

Before any hasty conclusions are made regarding the apparent insignificance of the hiding and exposure effect, the accuracy of the shear stress estimates based on a single 0.6d velocity observation must be considered. No independent check was available to test the assumption that mean velocity was approximated at 0.6d, which could be a major

source of error. The shallow flows and large relative roughness in Dupuyer Creek make it unlikely that reliable estimates of mean velocity can be obtained with a single measurement at 0.6d (Wilcock, personal communication, 1996). Also, estimating the roughness length, Z_0, using $0.1D_{84}$ may be inappropriate in the presence of bed forms which greatly increase the roughness (Dinehart, 1992a).

7.2 Unit Discharge Criterion

7.2.1 Maximum particle size relationships
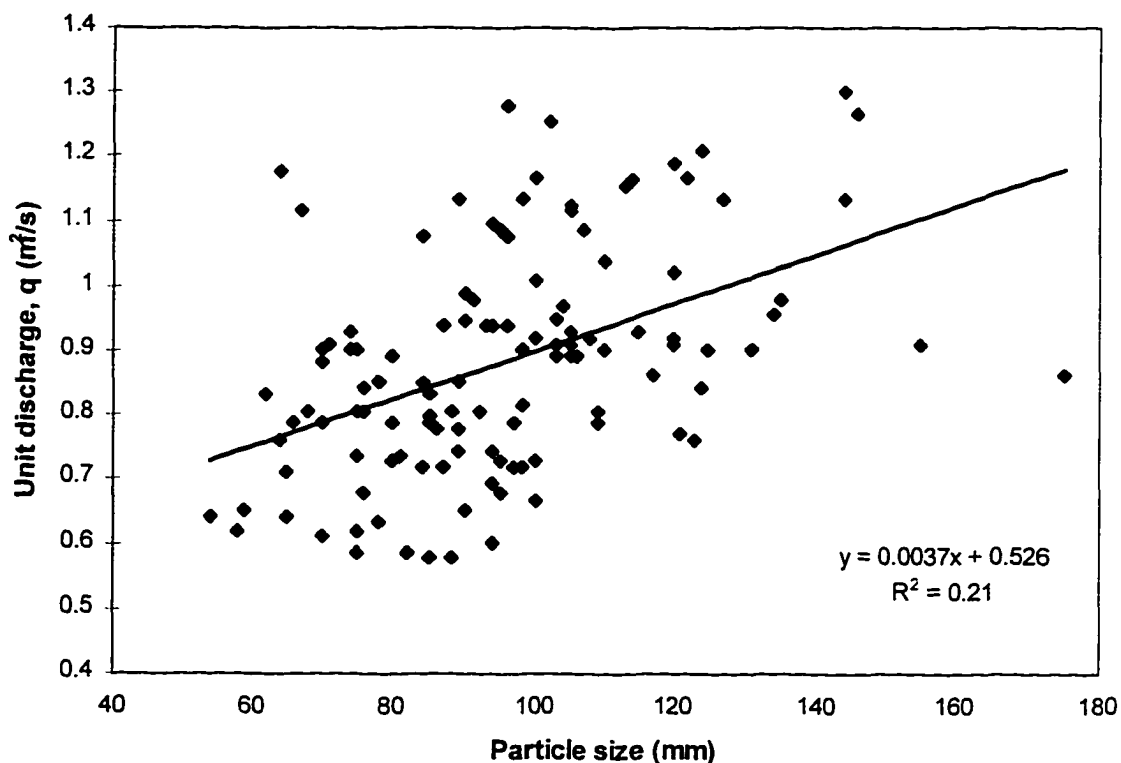
Figure 7.7 Relationship between unit discharge and the maximum particle size for all 120 individual bed load samples taken over the May and June floods, 1995.

When the largest particle size in each individual bed load sample is plotted against the estimated unit discharge, a wide range in scatter is seen with a similar pattern to the shear stress plot (Figure 7.7). This is because both unit discharge and shear stress parameters were estimated from stage-rating curves. The relationship between maximum particle size in each sample group and the mean unit discharge shows much less scatter, and a power regression line is fitted with an R-squared value of 0.66 (Figure 7.8). Plotted in Figure 7.8 with the regression line is the relationship for uniform sediments as developed by Bathurst et al. (1987):

$$q_c = 0.15g^{0.5}D^{1.5}S^{-1.12} \tag{4}$$

where q_c is the critical unit discharge (m²/s) needed to entrain a particle of diameter D (m), g is acceleration due to gravity (m/s²), and S is the water surface slope. Bathurst (1987a) suggested that this relationship for uniform sediments can be used to predict the critical flow for entrainment of a reference particle size in mixed-sized sediments. Data from Dupuyer Creek can be used to test this relationship (Figure 7.8).

The reference particle size is defined by the intersection of the two lines representing the relationships for uniform sediments and field data, as shown in Figure 7.8. Bathurst (1987a) found the reference size to closely approximate the D_{50} of the stream bed distribution, which makes it possible to apply a similar hiding and exposure adjustment to that developed by Andrews (1983):

$$q_{ci} = q_{cr}(D_i/D_r)^b \qquad\qquad (5)$$

where the subscripts i and r relate to the particle size of interest and the reference size respectively, and b is the coefficient indicating the strength of the hiding and exposure effect. However, the empirical equation (4) for the reference particle size does not seem to apply to Dupuyer Creek, where the intersection occurs at 14 mm, a significant departure from the D_{50} of 56 mm. Equation (4) predicts the critical flow for entrainment of the D_{50} size to be 1.08 m^2/s which is more than twice the observed value of 0.43 m^2/s. Coarse bed material is entrained at much lower flows in Dupuyer Creek than the existing unit discharge criterion suggests.

The relationship between critical unit discharge and relative particle size is modeled through regression to determine the exponent b in equation (5), represented by the line gradient (Figure 7.9). The b value of 0.84 obtained for Dupuyer Creek is 2-4 times greater than those values found by Bathurst (1987a) for the Roaring River, again indicating a greater size selectivity in the bed load process in Dupuyer Creek. Comparison with published values summarized by Ferguson (1994) yields the same conclusion. The higher gradient in the critical unit discharge - particle size relationship is one reason why the relationships in Figure 7.8 intersect well below the measured D_{50}.
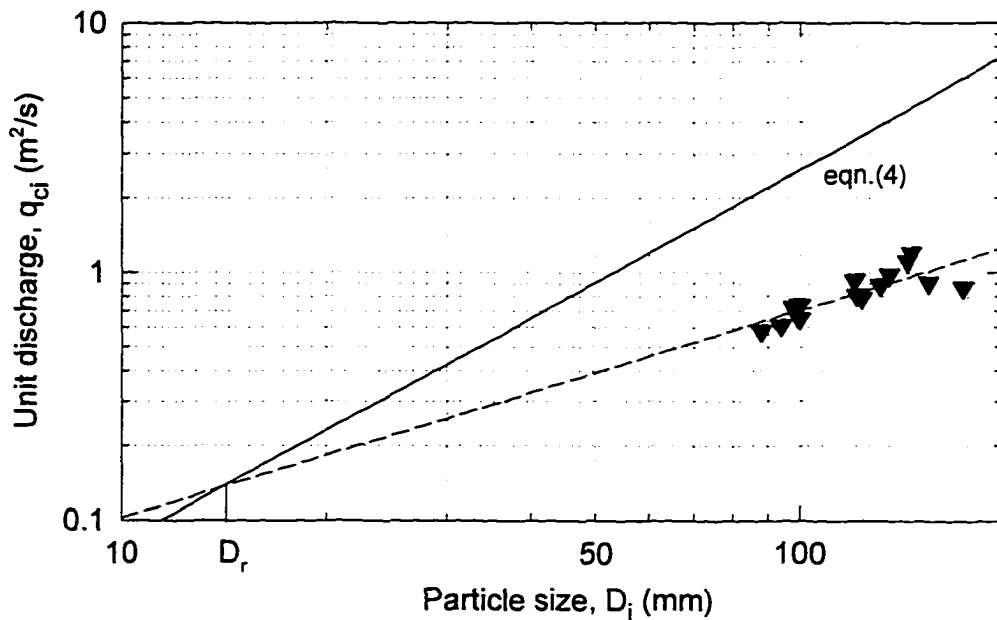
Figure 7.8 Critical unit discharge against the maximum particle size entrained for the sample group data (regression line $R^2 = 0.66$). Equation (4) represents the relationship for uniform sediments. The two relationships intersect at 14 mm, and not the D_{50} of 56 mm.
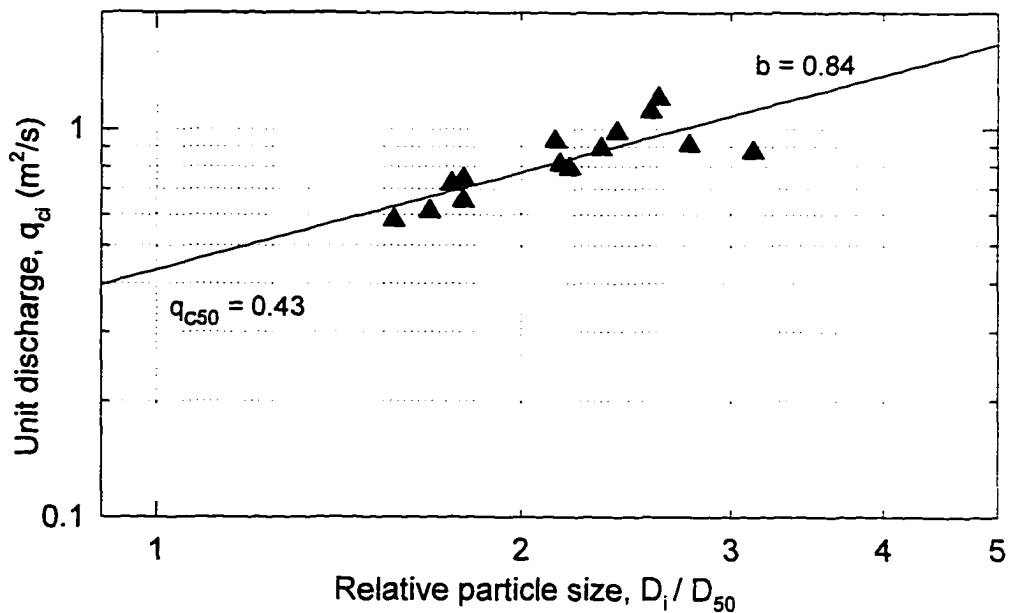
Figure 7.9 Critical unit discharge against relative particle size. Equation (5) is represented by the regression line, with slope, b = 0.84.

Bathurst (1987a) proposed the following relationship to estimate the b exponent in equation (5):

$$b = 1.5(D_{84}/D_{16})^{-1} \qquad\qquad (6)$$

where the greater the difference between the D_{84} and D_{16}, the stronger is the hiding/exposure effect and the smaller b becomes. A smaller value for b results from a relatively narrow range in discharge over which all particle sizes are brought into motion, indicating more equal mobility in the bed load process.

The relationship in equation (6) does not work well for Dupuyer Creek, giving an estimate of 0.36 for b compared to the 0.84 obtained from regression analysis. This may be because in different stream channels, factors other than the D_{84}/D_{16} ratio determine the degree of size selectivity in transport. Stream bed sorting and structure such as clustering, armoring, and imbrication may become more important. Dupuyer Creek is notable for the looseness of the stream bed particles and a lack of structuring. This could produce higher size selectivity by allowing smaller particles to be entrained from the loose substrate, whilst movement of larger particles remains marginal. A tightly packed substrate, or one that exhibits greater structure, increases the interdependence between particles and narrows the range in discharge over which all particles are entrained.

7.2.2 Sensitivity to estimated particle sizes

As with the shear stress approach, the modeling of particle hiding and exposure relies upon a good estimate of the stream bed median particle size, while the maximum particle sizes captured in bed load sampling are critical in defining the flow competence relationship. The sensitivity of parameters in the unit discharge criterion to different estimates of these characteristic particle sizes was therefore also examined with the Dupuyer Creek data. Again the effect of using a stream bed D_{50} estimate from a reach scale pebble count (42 mm) is compared to that obtained with a pebble count restricted to the riffle where bed load was sampled (56 mm). Flow competence was examined for the same definitions of maximum particle size:

D_{max} - Absolute maximum particle size captured in each sample group

D_{max} (or) - Absolute maximum particle size captured in each sample group, but with the removal of a suspected outlier from one sample group (175 mm particle in group 4)

D_{max} (3) - Mean of the three largest particles captured in each sample group, excluding the same suspected outlier

Table 7.4 Sensitivity of model coefficients and constants to the values assumed for maximum particle size in transport, D_i as defined above, and stream bed D_{50} in the relationship between critical unit discharge, q_{ci}, and maximum size in transport. $q_{ci} = q_{c50}(D_i/D_{50})^b$

D_i	b	R^2	$D_{50} = 56$		$D_{50} = 42$	
			q_{c50} for uniform sediments	q_{c50} from field data	q_{c50} for uniform sediments	q_{c50} from field data
D_{max}	0.84	0.66	1.08	0.43	0.70	0.34
D_{max} (or)	1.08	0.82	1.08	0.37	0.70	0.27
D_{max} (3)	1.22	0.89	1.08	0.36	0.70	0.26

In a similar pattern to the shear stress data, the flow competence relationship improves when first the outlier is removed and then the mean of the three largest particles is considered (R^2 increases from 0.66 to 0.89). The slope coefficient, b, increases from 0.84 to 1.22 indicating a greater range in flow is necessary to entrain a given particle size range, and approaching the value of 1.5 in the case of uniform sediments when there is no hiding and exposure effect (Figure 7.10). Estimates of b are not dependent on the estimate of substrate D_{50}, but they are shown to be very sensitive to how the maximum particle size is defined, and therefore to sampling techniques and strategy. This explains why values for b in the literature range so widely from 0.2 to 1.2, which can also be attributed to variation in the grain sorting and packing characteristics between stream channels. For the boulder bed Roaring River in Colorado, b is in the range 0.2-0.4 (Bathurst, 1987a), while for the gravel bed Oak Creek in Oregon a value of 1.22 is obtained (Komar, 1989, analysis of the data of Milhous, 1973). Values of b for the gravel and cobble bed Dupuyer Creek approach those of Oak Creek, depending on how maximum particle size is defined.

The observed flow competence relationships (Figure 7.10) do not intersect the suggested flow competence model for uniform sediments at a meaningful particle size for the application of hiding and exposure adjustments. The large disparity in values for q_{c50} between field observations and predictions for uniform sediments also illustrates the problem (Table 7.4). The intersection, which defines the reference particle size, occurs at very small particle sizes well below the substrate D_{50} and shows that the suggested model for uniform sediments can not be used for stream channels such as Dupuyer Creek.
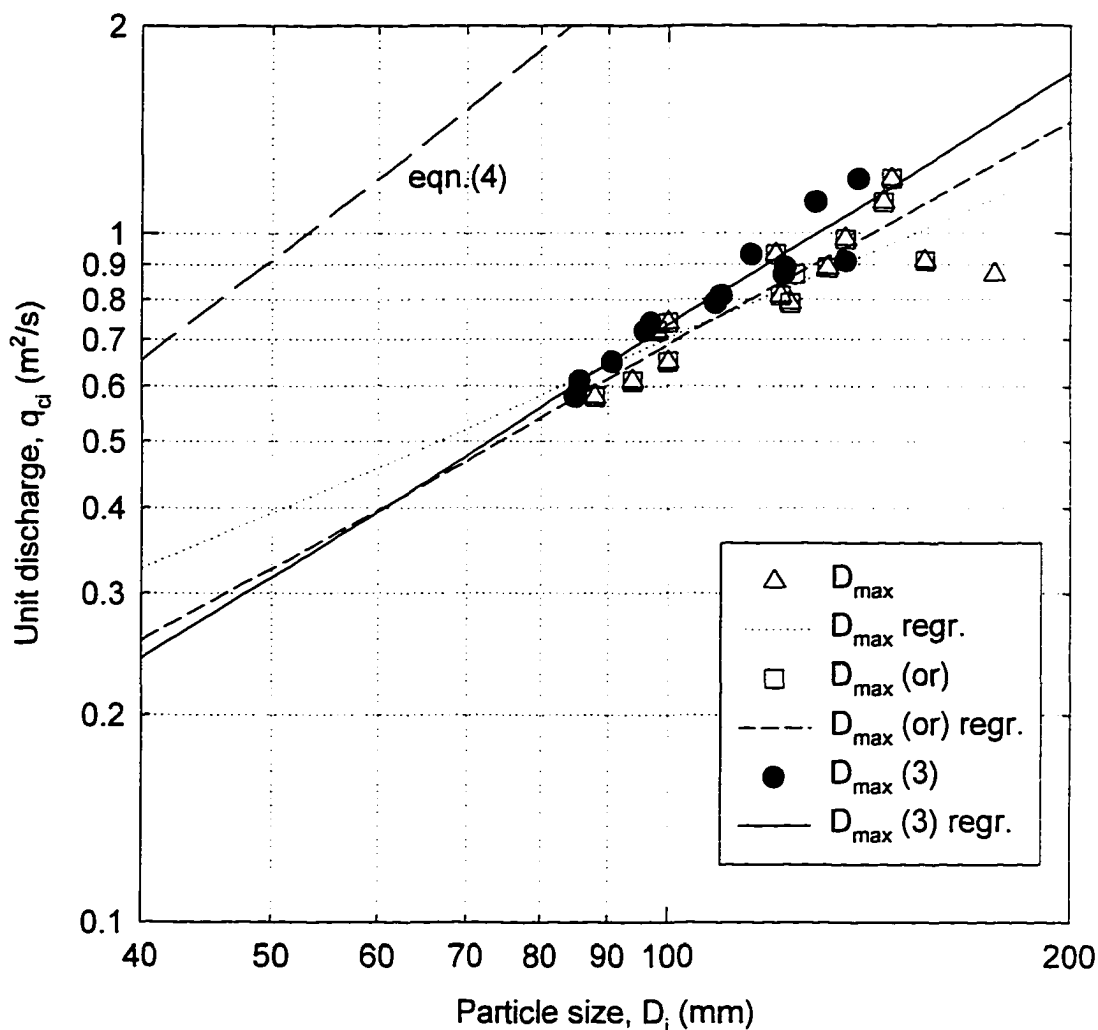
Figure 7.10 Flow competence relationships of the form $q_{ci} = aD_i^b$ for; D_{max} = maximum particle size; D_{max} (or) = maximum size with outlier removed; D_{max} (3) = mean of the three largest particle sizes. Equation (4) for uniform sediments also plotted.

7.3 Maximum Particle Mass Relationships

An alternative approach to flow competence analysis is to consider the individual mass of the largest particles in transport rather than their b-axes diameters. This option was explored by fitting simple power regression relationships to the particle mass data for

the sample groups, which can be compared to similar relationships in the conventional particle diameter approach. Flow competence was examined for the following definitions of maximum particle mass:

M_{max} - Absolute maximum particle mass captured in each sample group

M_{max} (or) - Absolute maximum particle mass captured in each sample group, but with the removal of a suspected outlier from one sample group (4.64 kg or 175 mm in group 4)

M_{max} (3) - Mean of the three heaviest particles captured in each sample group

These particle mass flow competence relationships show similar patterns to the particle size analysis and provide an interesting alternative perspective (Figure 7.11). However, Table 7.5 shows that the approach offers no advantage over the conventional particle size relationships which consistently achieve closer degrees of fit. This indicates that particle interactions and sorting due to size are more important than simply hydraulics alone and the ability of the flow to do work in transporting particle mass. There is also the difficulty in adjusting for relative particle size effects which cannot be translated simply to a relative particle mass adjustment.

Table 7.5 Comparison of the degree of fit for flow competence relationships based on particle mass versus those based on particle size. The R-squared values are given for power regression relationships

	Particle Mass		Particle Size	
	Shear Stress	Unit Discharge	Shear Stress	Unit Discharge
Max	0.50	0.57	0.63	0.66
Max (or)	0.57	0.63	0.79	0.82
Max (3)	0.72	0.79	0.85	0.89
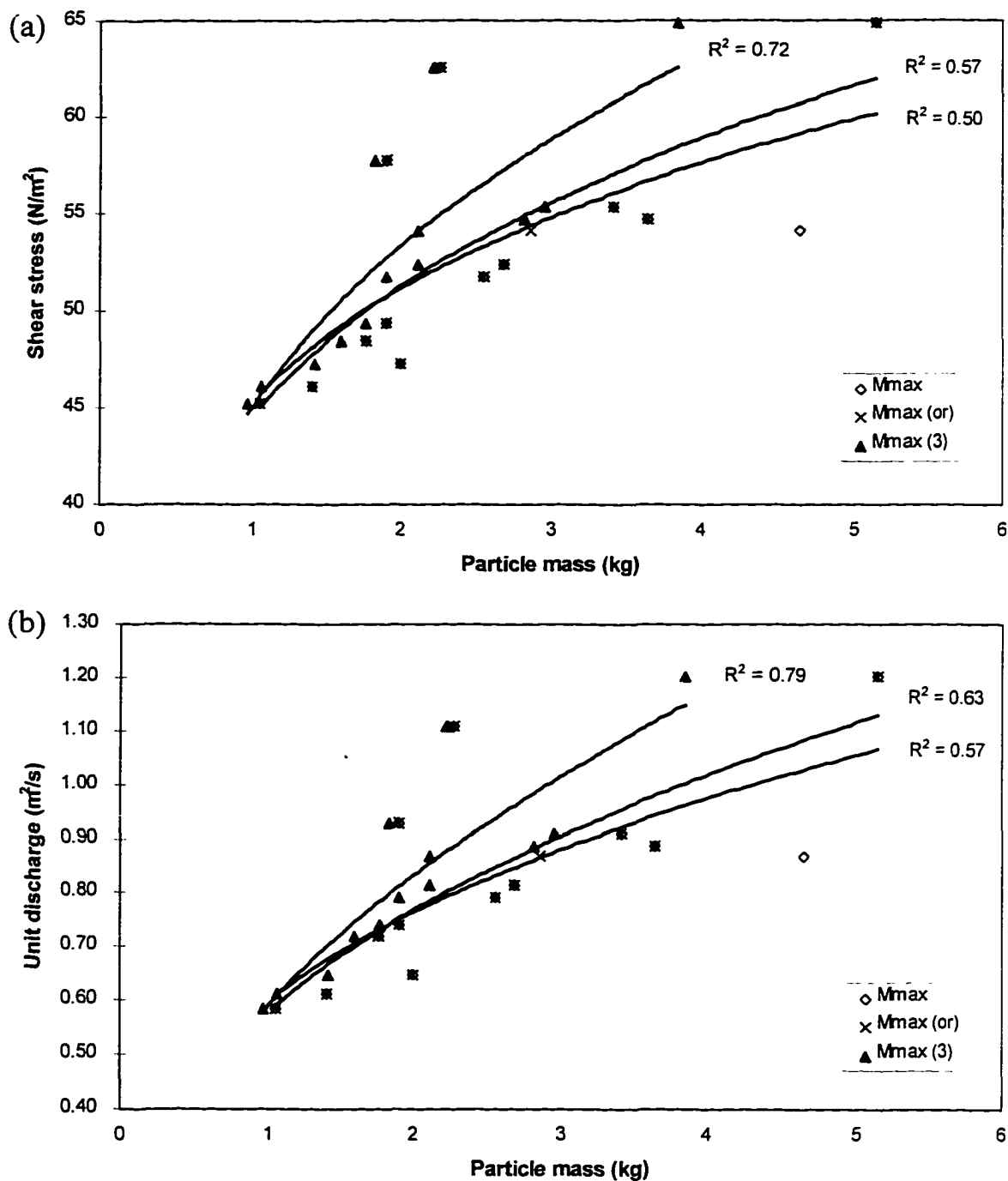
Figure 7.11 Particle mass flow competence relationships for (a) shear stress and (b) unit discharge as power regression lines where; M_{max} = maximum particle mass; M_{max} (or) = maximum mass with outlier removed; M_{max} (3) = mean of the mass of the three largest particles.

7.4 Sample Size Effects

Flow competence relationships have been examined here based on the largest grains found in bed load samples and on coarse percentiles of the bed load grain-size distribution. Wilcock (1996) criticized this classical concept of flow competence, and suggested the relationships are sensitive to the effect of sample size which tends to vary widely in sediment transport samples from natural flows. In a statistical analysis of the often cited data of Milhous (1973) from Oak Creek, Wilcock (1996) concluded the flow competence relationships may be attributed as much to sample size as to variation in flow strength. Reliable use of flow competence data therefore requires an adequate consideration of sample size effects.

The Dupuyer Creek bed load data do show correlation between sample mass and flow variables, with Pearson correlation coefficients of 0.81 and 0.83 for unit discharge and shear stress respectively (99% significance level). The correlations between sample mass and flow variables are inevitable because higher rates of bed load transport during high flows produce larger samples, even when sample time is greatly reduced. Flow competence relationships may be due, in part, to the fact that larger samples at higher flows have a greater probability of containing the larger particles towards the coarse tail of the bed load size distribution. This possible factor is expected to be indicated by correlations between sample mass and the bed load particle sizes sampled. Table 7.6 shows these correlations to be significant at the 99 percent level, with coefficient values not far below those for the flow variables.

Partial correlation coefficients can be used to determine the relationship between flow strength and bed load percentiles without the influence of sample size by controlling for this variable. The correlation coefficients are lower when calculated in this way, but many are still significant at the 99 percent level. This indicates that the flow competence relationships derived between flow strength (shear stress and unit discharge) and bed load particle sizes remain valid even after sample size effects are accounted for. Partial correlation coefficients improve greatly when the outlier observation is removed from the maximum particle size data series. Peak coefficient values occur with the bed load D_{90}, and indicate this variable might be the most reliable for flow competence modeling. Slightly higher coefficients are obtained with unit discharge, and suggest unit discharge has greater potential in flow competence modeling as compared to shear stress.

Table 7.6 Correlation and partial correlation coefficients to examine the effect of sample size in flow competence relationships based on the shear stress and unit discharge variables

Bed Load Percentile	Pearson Correlation Coefficients			Partial Correlation Coeffs. Controlling for Sample Mass	
	Shear Stress	Unit Discharge	Sample Mass	Shear Stress	Unit Discharge
D_{50}	0.79	0.81	0.65	0.61†	0.67
D_{60}	0.80	0.82	0.70	0.53†	0.59†
D_{70}	0.82	0.85	0.73	0.55†	0.63†
D_{75}	0.85	0.87	0.74	0.61†	0.69
D_{80}	0.85	0.88	0.70	0.68†	0.76
D_{90}	0.91	0.94	0.76	0.78	0.87
D_{95}	0.86	0.88	0.70	0.72	0.78
D_{max} (3)	0.91	0.92	0.84	0.66	0.70
D_{max} (or)	0.87	0.88	0.74	0.67	0.71
D_{max}	0.73	0.74	0.65	0.45†	0.48†

Note: All coefficients are at the 99% significance level, except for those denoted † indicating 95% significance level (one-tailed test)

7.5 Shear Stress versus Unit Discharge Criteria

The shear stress and unit discharge criteria are shown to perform quite differently when applied to the Dupuyer Creek data set. For maximum particle size relationships and coarse bed load percentiles, good flow competence relationships can be established with critical shear stress (equation 3). Variation in the dimensionless shear stress coefficient appears to relate to relative particle size in the manner suggested by Andrews (1983), although the significance of the hiding and exposure adjustment decreases towards smaller bed load percentiles. For maximum particle size relationships the values derived for x and θ in equation (3) are in close agreement with many other studies on gravel bed rivers.

With the unit discharge criterion (equation 4), a problem emerges. The assumption is that median particle sizes in mixed sediments are unaffected by relative particle size effects, so that equation (4) can be used to predict the critical unit discharge for entrainment of the D_{50}. Field evidence at Dupuyer Creek suggests that equation (4) can not be applied in this manner.

Bed load percentile sizes and maximum particle sizes are both highly correlated to the flow variables of shear stress and unit discharge, even after sample size effects are removed. The difficulty lies in determining suitable values for the constants and coefficients in the established empirical equations. In the shear stress criterion this entails setting values for x and θ in equation (3). In the unit discharge criterion, equation (4) needs re-development and establishment of a value for b in equation (5). The Dupuyer

Creek data suggests that for gravel bed streams it may be more difficult to determine suitable values in the unit discharge criterion. Therefore, in the absence of bed load sampling to validate flow competence relationships, the shear stress approach is recommended for the most reliable prediction of particle entrainment.

7.6 Application of Flow Competence Relationships

The Dupuyer Creek data set has been used to demonstrate the relative performances of the critical shear stress and critical unit discharge approaches in modeling flow competence. The purpose of flow competence modeling is to enable the following questions to be addressed for stream channels composed of mixed size sediments.

(A) For maximum particle sizes in transport:

(i) What critical flow condition is required to transport a given particle size?

(ii) What is the maximum particle size that will be transported at a given flow condition?

(B) For percentiles in the bed load size distribution:

(i) What critical flow condition is required to bring a given bed load percentile up to a given size?

(ii) What is the size attained for a given bed load percentile at a given flow condition?

The Dupuyer Creek data set illustrates that predictable flow competence relationships can be formulated and used to answer the above questions. However, it is important to stress that these relationships only apply to the range in flows and particle sizes for which they were developed. Observations of bed load transport behavior in Dupuyer Creek show that major discontinuities exist in flow competence relationships, such that extrapolation will lead to erroneous predictions (Figure 7.12). There appears to be a discontinuity at around 0.6 m^2/s or 45 N/m^2, at which point flow competence shifts from 35 mm to 88 mm (substrate D_{25} to D_{70}) for the maximum particle sizes in transport. This shift in flow competence may represent the threshold when riffle sediments are entrained, and bed load transport shifts from phase 1 to phase 2 (Jackson and Beschta, 1982). Interactions between different particle sizes on the riffles resulting from clusters, armor, or imbrication, appear to impart a degree of entrainment equal mobility for particle sizes 35 mm to 88 mm (substrate D_{25} to D_{70}). Although this range in particle sizes is mobilized at the same flow, the data show that bed load transport rates remain strongly biased in favor of the finer substrate size fractions. Transport rate equal mobility is never achieved in the Dupuyer Creek data set. The upper limit to the flow competence relationship is defined by the point at which the largest particles present in the stream bed are entrained in transport.
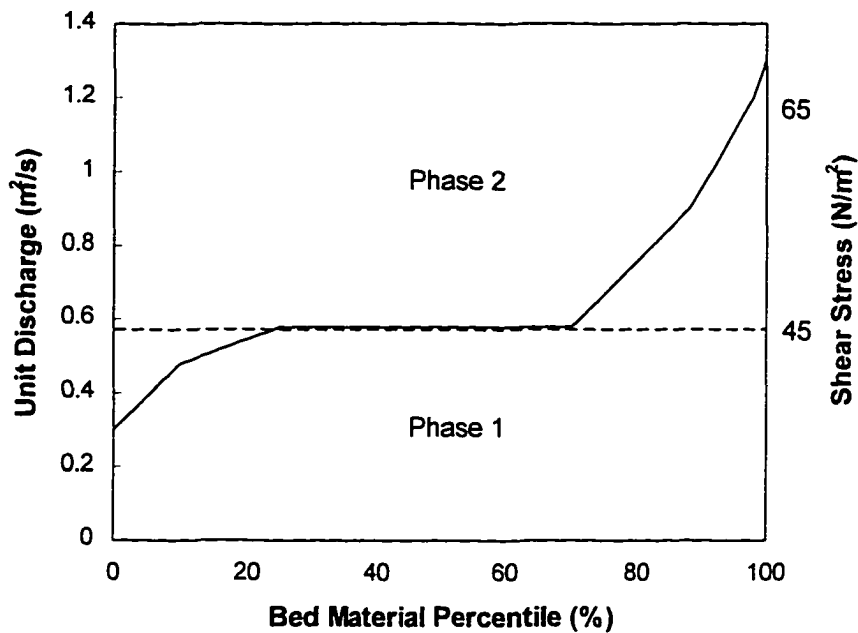
Figure 7.12 Proposed flow competence relationship for Dupuyer Creek, showing the maximum bed material percentile entrained for a given unit discharge or shear stress. The discontinuity, marked by the dashed line, represents the shift between phase 1 and phase 2 bed load transport. The unit discharge axis is linear, while the shear stress axis is non-linear.

Without an intensive bed load sampling scheme, the difficulty is in knowing where these discontinuities occur in the flow competence relationship, and in obtaining the correct values for the slope and intercept of this relationship. Limits to the application of flow competence models in streams where little or no coarse bed load sampling has been undertaken can be listed as follows.

(A) Identification of discontinuities in bed load transport behavior due to phenomena such as pavement layer break-up and re-stabilization, and bed form or cluster movement.

(B) Identification of the slope and intercept of flow competence relationships which may be strongly influenced by local stream channel characteristics.

(C) Accurate characterization of the stream bed size distribution.

Even when bed load sampling is undertaken, the maximum particle sizes obtained depend on the sampling device used and the sampling strategy followed. Determination of an optimum sample duration remains problematic due to the unsteady and pulsing characteristics of bed load transport. There is currently no consensus on suitable standards for bed load sampling and characterization of substrate size distributions in the development of flow competence relationships. The success of the portable large frame-net bed load sampler in this study demonstrates its potential as a standard instrument in defining flow competence relationships.

8. CONCLUSIONS

The study conclusions are listed in relation to the five original objectives as outlined in the third chapter.

8.1 Equal Mobility versus Size Selectivity

- Bed load size distributions for material 38 mm in size and larger (substrate D_{25}), obtained with the large frame-net sampler, reveal a trend of coarsening bed load with increasing flows. Within the range of flows (0.58-1.2 m^2/s) bed load transport is shown to be a size selective process.

- On the falling limb of the flood hydrograph, particles in the size range 35-88 mm (D_{25}-D_{70}) cease to move as bed load over a very narrow flow range (approximately 0.58 m^2/s). This range in particle sizes may therefore be described as equally mobile in terms of bed load entrainment.

- Bed load transport rates, measured in particle numbers for different size fractions, are not proportional to the abundance of each size fraction in the channel substrate size distribution. This provides further evidence of strong size selectivity in transport.

123

- The tracer study very weakly suggests that smaller, lighter, and more rounded particles travel further. Tracer recovery rates were too low to place any confidence in conclusions regarding equal mobility.

8.2 Shear Stress versus Unit Discharge Criteria

- Flow competence relationships can be usefully employed over the range in flows for which transport is shown to be size selective.

- Model constants and coefficients derived for the shear stress criterion are within the range of values published for other gravel bed streams, although with a slightly lower dependence on relative particle size and the hiding/exposure effect.

- Equation (4) in the unit discharge criterion cannot be used to predict entrainment of the median particle size. The equation constant and slope coefficient must be redefined for streams such as Dupuyer Creek if the unit discharge approach is used.

- The shear stress criterion is the only method which will produce reasonable estimates of flow competence. The evidence shows that the unit discharge criterion can not be widely applied to gravel bed streams.

8.3 Bed Load Percentiles as Indicators of Flow Competence

- Consideration must be given to the presence of outliers in developing flow competence relationships for maximum sampled particle sizes in transport. Removal of a single outlier in the Dupuyer Creek data set has a very large effect on the regression relationship for maximum particle sizes. Modeling the mean of the three largest particles sampled. $D_{max}(3)$, gives a more representative flow competence relationship.

- Sample size effects are shown to be strong for the maximum particle size data set including the outlier. Therefore, more reliable flow competence relationships will be possible by removing such outliers. Sample size effects are much reduced for the $D_{max}(3)$ variable, suggesting this could be the optimum size with which to model flow competence.

- Coarse bed load grain sizes such as the $D_{max}(3)$ variable are more sensitive to changes in flow strength than the median bed load grain size, and therefore are superior parameters for flow competence modeling.

- Significant flow competence relationships have been derived for a wide range of bed load grain sizes from the D_{50} to D_{max}. The most useful relationship will depend on the particular problem to which modeling is being applied.

8.4 Modeling Particle Mobility by Size versus by Mass

- Flow competence relationships developed for maximum particle mass entrained are not found to be superior to the standard particle size relationships. A particle mass approach to flow competence modeling is therefore not pursued any further. Theory regarding particle hiding and exposure relates to relative particle size and cannot be extended to relative particle mass.

8.5 Channel Change and Coarse Bed Load Transport

- Floods capable of moving coarse bed load produce major scour and fill of the thalweg, and channel migration at meander bends. Pool features are especially dynamic, migrating with the meander bends, and scouring and filling.

9. LITERATURE CITED

Andrews, E.D. 1983. Entrainment of gravel from naturally sorted riverbed material. *Geological Society of America Bulletin*, **94**, 1225-1231.

Andrews, E.D. and Nankervis, J.M. 1995. Effective discharge and the design of channel maintenance flows for gravel-bed rivers. In: Costa, J.E., Miller, A.J., Potter, K.P. and Wilcock, P.R. (eds.), *Natural and Anthropogenic Influences in Fluvial Geomorphology*, American Geophysical Union Monograph **89**, 151-164.

Andrews, E.D. and Parker, G. 1987. Formation of a coarse surface layer as the response to gravel mobility. In: Thorne, C.R., Bathurst, J.C. and Hey, R.D. (eds.), *Sediment Transport in Gravel-Bed Rivers*, John Wiley & Sons, 269-328.

Ashworth, P.J. and Ferguson, R.I. 1989. Size-selective entrainment of bed load in gravel bed streams. *Water Resources Research*, **25**, 627-634.

Ashworth, P.J., Ferguson, R.I., Ashmore, P.E., Paola, C., Powell, D.M. and Prestegaard, K.J. 1992. Measurements in a braided river chute and lobe (2). Sorting of bed load during entrainment, transport and deposition. *Water Resources Research*, **28**, 1887-1896.

- Bagnold, R.A. 1977. Bed load transport by natural rivers. *Water Resources Research*, **13**, 303-312.

Bathurst, J.C. 1987a. Critical conditions for bed material movement in steep, boulder-bed streams. In: Beschta, R.L. et al. (eds.), *Erosion and Sedimentation in the Pacific Rim*, IAHS Publication, **165**, 309-318.

Bathurst, J.C. 1987b. Measuring and modelling bed load transport in channels with coarse bed materials. In: Richards, K. (ed.), *River Channels*, Basil Blackwell Inc., 272-294.

Bathurst, J.C., Graf, W.H. and Cao, H.H. 1987. Bed load discharge equations for steep mountain rivers. In: Thorne, C.R., Bathurst, J.C. and Hey, R.D. (eds.), *Sediment Transport in Gravel-Bed Rivers*, John Wiley & Sons, 453-492.

Bettess, R. 1984. Initiation of sediment transport in gravel streams. *Proc. Instn. Civ. Engrs.*, **77**, 79-88.

Brayshaw, A.C. 1984. The characteristics and origin of cluster bedforms in coarse-grained alluvial channels. In: Koster, E.H. and Steel, R.J.S. (eds.), *Sedimentology of Gravels and Conglomerates*, Canadian Society of Petroleum Geologists, Memoir **10**, 77-85.

Brayshaw, A.C. 1985. Bed microtopography and entrainment thresholds in gravel-bed rivers. *Geological Society of America Bulletin*, 96, 218-223.

Brayshaw, A.C., Frostick, L.E. and Reid, I. 1983. The hydrodynamics of particle clusters and sediment entrainment in coarse alluvial channels. *Sedimentology*, 30, 137-143.

Bunte, K. 1990. Experiences and results from using a big-frame bed load sampler for coarse material bed load. In: Land, H. and Musy, A. (eds.), *Hydrology in Mountainous Regions I*, IAHS Publication, 193, 223-230.

Bunte, K. 1992. Particle number grain-size composition of bed load in a mountain stream. In: Billi, P., Hey, R.D., Thorne, C.R. and Tacconi, P. (eds.), *Dynamics of Gravel-Bed Rivers*, John Wiley & Sons, 55-72.

Carling, P.A. 1983. Threshold of coarse sediment transport in broad and narrow natural streams. *Earth Surface Processes and Landforms*, 8, 1-18.

Carling, P.A. 1988. The concept of dominant discharge applied to two gravel-bed streams in relation to channel stability thresholds. *Earth Surface Processes and Landforms*, 13, 355-367.

Church, M. and Hassan, M.A. 1992. Size and distance of travel of unconstrained clasts on a streambed. *Water Resources Research*, 28, 299-303.

Custer, S.G. 1992. A review of natural-gravel-transport-detection experiments at Squaw Creek, Montana, 1981-1991. In: *Channel Morphology and Flood Control: proceedings of the Corps of Engineers Workshop on Steep Streams*, 27-29 Oct. 1992, Seattle, Washington. U.S. Army Corps of Engineers Waterways Experiment Station miscellaneous paper HL-94-4, pp. 3-1 to 3-28.

Custer, S.G., Ergenzinger, P., Bugosh, N. and Anderson, B.C. 1987. Electromagnetic detection of pebble transport in streams: a method for measurement of sediment transport waves. In: Ethridge, F. and Flores, R. (eds.), *Recent Developments in Fluvial Sedimentology*, Society of Palaeontologists and Mineralogists Special Publication 39, 21-26.

De Jong, C. 1991. A re-appraisal of the significance of obstacle clasts in cluster bedform dispersal. *Earth Surface Processes and Landforms*, 16, 737-744.

De Jong, C. 1993. Temporal and spatial interactions between river bed roughness, geometry, bed load transport and flow hydraulics in mountain streams - examples from Squaw Creek, Montana (USA) and Lainbach/Schmiedlaine, Upper Bavaria (Germany). *Unpublished Ph.D. thesis*, Freie Universitat Berlin, Germany, 212 pp.

De Jong, C. and Ergenzinger, P. 1992. Unsteady flow, bed load transport and bed geometry responses in steep mountain torrents. In: Larsen, P. and Eisenhauer, N. (eds.), *Proceedings, 5th International Symposium on River Sedimentation and Sediment Management*, 1, 185-192, Karlsruhe, ISRS.

Dinehart, R.L. 1989. Dune migration in a steep, coarse-bedded stream. *Water Resources Research*, 25, 911-923.

Dinehart, R.L. 1992a. Evolution of coarse gravel bed forms: field measurements at flood stage. *Water Resources Research*, 28, 2667-2689.

Dinehart, R.L. 1992b. Gravel-bed deposition and erosion by bedform migration observed ultrasonically during storm flow, North Fork Toutle River, Washington. *Journal of Hydrology*, 136, 51-71.

Emmett, W.W. 1976. Bed load transport in two large gravel-bed rivers, Idaho and Washington. *Proceedings of the 3rd Federal Inter-agency Sedimentation Conference*, pp. 4.101-4.113.

Ergenzinger, P. and Custer, S.G. 1983. Determination of bed load transport using naturally magnetic tracers. First experiences at Squaw Creek, Gallatin County, Montana. *Water Resources Research*, 19, 187-193.

Ergenzinger, P., De Jong, C. and Christaller, G. 1994. Interrelationships between bed load transfer and river-bed adjustment in mountain rivers: an example from Squaw Creek, Montana. In: Kirkby, M.J. (ed.), *Process Models and Theoretical Geomorphology*, John Wiley & Sons, 141-158.

Ferguson, R.I. 1994. Critical discharge for entrainment of poorly sorted gravel. *Earth Surface Processes and Landforms*, 19, 179-186.

Ferguson, R.I., Prestegaard, K.L. and Ashworth, P.J. 1989. Influence of sand on gravel transport in a braided gravel bed river. *Water Resources Research*, 25, 635-643.

Francis, J.R.D. 1973. Experiments on the motion of solitary grains along the bed of a water-stream. *Proc. R. Soc. Lond.*, A332, 443-471.

Gilbert, G.K. and Murphy, E.D. 1914. Transportation of debris by running water. *U.S. Geological Survey Professional Paper*, 86, 263 pp.

Gomez, B. 1983. Temporal variations in bed load transport rates: the effect of progressive bed armouring. *Earth Surface Processes and Landforms*, 8, 41-54.

Gomez, B. and Emmett, W.W. 1991. Comments on sampling bed load in small streams. In: *Fifth Federal interagency sedimentation conference proceedings*, Washington, D.C., Federal Energy Regulatory Commission, pp. 2-65 to 2-72.

Gomez, B., Naff, R.L. and Hubble, D.W. 1989. Temporal variations in bed-load transport rates associated with the migration of bed-forms. *Earth Surface Processes and Landforms*, 14, 135-156.

Grant, G.E. 1987. Assessing effects of peak flow increases on stream channels: a rational approach. In: *Proceedings, California Watershed Management Conference*, West Sacramento, CA. pp. 142-149.

Hammond, F.D.C., Heathershaw, A.D. and Langhorne, D.N. 1984. A comparison between Shields' threshold criterion and the movement of loosely packed gravel in a tidal channel. *Sedimentology*, 31, 51-62.

Harrelson, C.C., Rawlins, C.L. and Potyondy, J.P. 1994. Stream channel reference sites: an illustrated guide to field technique. *U.S.D.A. Forest Service Gen. Tech. Rep.* RM-245.

Helley, E.J. and Smith, W. 1971. Development and calibration of a pressure-difference bed load sampler. *U.S. Geological Survey Open-file Report*, Menlo Park, California.

Hey, R.D. 1979. Flow resistance in gravel-bed rivers. *ASCE Journal of Hydraulics Division*, 105, 365-379.

Hubbell, D.W. 1987. Bed load sampling and analysis. In: Thorne, C.R., Bathurst, J.C. and Hey, R.D. (eds.), *Sediment Transport in Gravel-Bed Rivers*, John Wiley & Sons, 89-118.

Iseya, F. and Ikeda, H. 1987. Pulsations in bed load transport rates induced by a longitudinal sediment sorting: a flume study using sand and gravel mixtures. *Geografiska Annaler*, 69A, 15-27.

Jackson, W.L. and Beschta, R.L. 1982. A model of two-phase bedload transport in an Oregon Coast Range Stream. *Earth Surface Processes and Landforms*, 7, 517-527.

Komar, P.D. 1987. Selective grain entrainment by a current from a bed of mixed sizes: a reanalysis. *Journal of Sedimentary Petrology*, 57, 203-211.

Komar, P.D. 1989. Flow-competence evaluations of the hydraulic parameters of floods: an assessment of the technique. In: Beven, K. and Carling, P. (eds), *Floods: Hydrological, Sedimentological and Geomorphological Implications*, John Wiley & Sons, 107-134.

Komar, P.D. and Carling, P.A. 1991. Grain sorting in gravel-bed streams and the choice of particle sizes for flow-competence evaluations. *Sedimentology*, 38, 489-502.

Komar, P.D. and Li, Z. 1986. Pivoting analysis of the selective entrainment of sediments by shape and size with application to gravel threshold. *Sedimentology*, 33, 425-436.

Komar, P.D. and Shih, S. 1992. Equal mobility versus changing bed load grain sizes in gravel-bed streams. In: Billi, P., Hey, R.D., Thorne, C.R. and Tacconi, P. (eds.), *Dynamics of Gravel-Bed Rivers*, John Wiley & Sons, 73-108.

Kondolf, G.M. 1997. Application of the pebble count: notes on purpose, method, and variants. *Journal of the American Water Resources Association*, 33, 79-87.

Kuhnle, R.A. and Southard, J.B. 1988. Bed load transport fluctuations in a gravel bed laboratory channel. *Water Resources Research*, 24, 247-260.

Langbein, W.B. and Leopold, L.B. 1968. River channel bars and dunes - theory of kinematic waves. *U.S. Geological Survey Professional Paper*, 422-L, 20 pp.

Laronne, J.B. and Carson, M.A. 1976. Interrelationships between bed morphology and bed-material transport for a small, gravel-bed channel. *Sedimentology*, 23, 67-85.

Leopold, L.B. 1970. An improved method for size distribution of stream bed gravel. *Water Resources Research*, 6, 1357-1366.

Leopold, L.B. 1992. Sediment size that determines channel morphology. In: Billi, P., Hey, R.D., Thorne, C.R. and Tacconi, P. (eds.), *Dynamics of Gravel-Bed Rivers*, John Wiley & Sons, 297-311.

Leopold, L.B. and Emmett, W.W. 1976. Bed load measurements, East Fork River, Wyoming. *Proceedings of the National Academy of Sciences*, U.S.A., 73, 1000-1004.

Leopold, L.B. and Emmett, W.W. 1977. 1976: Bed load measurements, East Fork River, Wyoming. *Proceedings of the National Academy of Sciences*, U.S.A., 74, 2644-2648.

Lisle, T.E. and Madej, M.A. 1992. Spatial variation in armouring in a channel with high sediment supply. In: Billi, P., Hey, R.D., Thorne, C.R. and Tacconi, P. (eds.), *Dynamics of Gravel-Bed Rivers*, John Wiley & Sons, 277-293.

Marcus, W.A., Ladd, S.C., Stoughton, J.A. and Stock, J.W. 1995. Pebble counts and the role of user-dependent bias in documenting sediment size distributions. *Water Resources Research*, **31**, 2625-2631.

Milhous, R.T. 1973. Sediment transport in a gravel-bottomed stream. *Unpublished Ph.D. thesis*, Oregon State University, Corvallis, 232 pp.

Naden, P. 1987. An erosion criterion for gravel-bed rivers. *Earth Surface Processes and Landforms*, **12**, 83-93.

Parker, G. and Klingeman, P.C. 1982. On why gravel-bed streams are paved. *Water Resources Research*, **18**, 1409-1423.

Parker, G., Dhamotharan, S. and Stefan, H. 1982a. Model experiments on mobile, paved gravel bed streams. *Water Resources Research*, **18**, 1395-1408.

Parker, G., Klingeman, P.C. and McLean, D.G. 1982b. Bed load and size distribution in gravel-bed streams. *ASCE Journal of Hydraulics Division*, **108**, 544-571.

Petit, F. 1987. The relationship between shear stress and the shaping of the bed of a pebble-loaded river, La Rulles - Ardenne. *Catena*, **14**, 453-468.

Petit, F. 1994. Dimensionless critical shear stress evaluations from flume experiments using different gravel beds. *Earth Surface Processes and Landforms*, **19**, 565-576.

Pitlick, J. 1992. Flow resistance under conditions of intense gravel transport. *Water Resources Research*, **28**, 891-903.

Powell, D.M. and Ashworth, P.J. 1995. Spatial pattern of flow competence and bed load transport in a divided gravel bed river. *Water Resources Research*, **31**, 741-752.

Prestegaard, K.L. 1983. Variables influencing water-surface slopes in gravel-bed streams at bankfull stage. *Geological Society of America Bulletin*, **94**, 673-678.

Rantz, S.E. and others 1982. Measurement and computation of streamflow. *U.S. Geological Survey Water-Supply Paper*, **2175**, v. 1 and 2, pp. 631.

Reid, I., Brayshaw, A.C. and Frostick, L.E. 1984. An electromagnetic device for automatic detection of bed load motion and its field applications. *Sedimentology*, **31**, 269-276.

Reid, I. and Frostick, L.E. 1984. Particle interaction and its effect on the thresholds of initial and final bed load motion in coarse alluvial channels. In: Koster, E.H. and Steel, R.J.S. (eds.), *Sedimentology of Gravels and Conglomerates*, Canadian Society of Petroleum Geologists, Memoir 10, 61-68.

Reid, I., Frostick, L.E. and Layman, J.T. 1985. The incidence and nature of bed load transport during flood flows in coarse-grained alluvial channels. *Earth Surface Processes and Landforms*, 10, 33-44.

Reid, I., Frostick, L.E. and Brayshaw, A.C. 1992. Microform roughness elements and the selective entrainment and entrapment of particles in gravel-bed rivers. In: Billi, P., Hey, R.D., Thorne, C.R. and Tacconi, P. (eds.), *Dynamics of Gravel-Bed Rivers*, John Wiley & Sons, 253-276.

Reid, I., Laronne, J.B. and Powell, D.M. 1995. The Nahal Yatir bed load database: sediment dynamics in a gravel-bed ephemeral stream. *Earth Surface Processes and Landforms*, 20, 845-857.

Ross, C.P. 1959. Geology of Glacier National Park and the Flathead Region, Northwestern Montana. *U.S. Geological Survey Professional Paper*, 296, pp. 125.

Schoklitsch, A. 1962. *Handbuch des Wasserbaues*, 3rd edn., Springer, Vienna.

Sear, D.A. 1996. Sediment transport processes in pool-riffle sequences. *Earth Surface Processes and Landforms*, 21, 241-262.

Shields, A. 1936. Application of similarity principles and turbulence research to bed-load movement. *Mitteilungen der preussischen Nersuchsanstalt fur Wassen Brau end Schiffbuar*. In: Ott, W.P. and Unchelen, J.C. (translators), California Institute of Technology, Pasadena, Report 167.

Whitaker, A.C. and Potts, D.F. 1996. Validation of two threshold models for bed load initiation in an upland gravel-bed stream. *Proceedings AWRA Annual Symposium; Watershed Restoration - Physical, Biological and Chemical Considerations*, July 1996, Syracuse, NY.

White, W.R. and Day, T.J. 1982. Transport of graded gravel bed material. In: Hey, R.D., Bathurst, J.C. and Thorne, C.R. (eds.), *Gravel-Bed Rivers*, John Wiley & Sons, 181-223.

Whiting, P.J., Dietrich, W.E., Leopold, L.B., Drake, T.G. and Shreve, R.L. 1988. Bed load sheets in heterogeneous sediment. *Geology*, 16, 105-108.

Wiberg, P.L. and Smith, J.D. 1987. Calculation of the critical shear stress for motion of uniform and heterogeneous sediments. *Water Resources Research*, **23**, 471-489.

Wilcock, P.R. 1992. Flow competence: a criticism of a classic concept. *Earth Surface Processes and Landforms*, **17**, 289-298.

Wilcock, P.R. 1996. Estimating local bed shear stress from velocity observations. *Water Resources Research*, **32**, 3361-3366.

Wilcock, P.R. and Southard, J.B. 1988. Experimental study of incipient motion in mixed-size sediment. *Water Resources Research*, **24**, 1137-1151.

Wohl, E.E., Anthony, D.J., Madsen, S.W. and Thompson, D.M. 1996. A comparison of surface sampling methods for coarse fluvial sediments. *Water Resources Research*, **32**, 3219-3226.

Wolman, M.G. 1954. A method of sampling coarse river-bed material. *American Geophysical Union Transactions*, **35**, 951-956.

APPENDICES

135

APPENDIX - A

Cross-sectional velocity measurements taken with Price AA current meter at 0.6 flow depth to estimate discharge during May and June floods, 1995.

Cross Section Velocities - May 1995
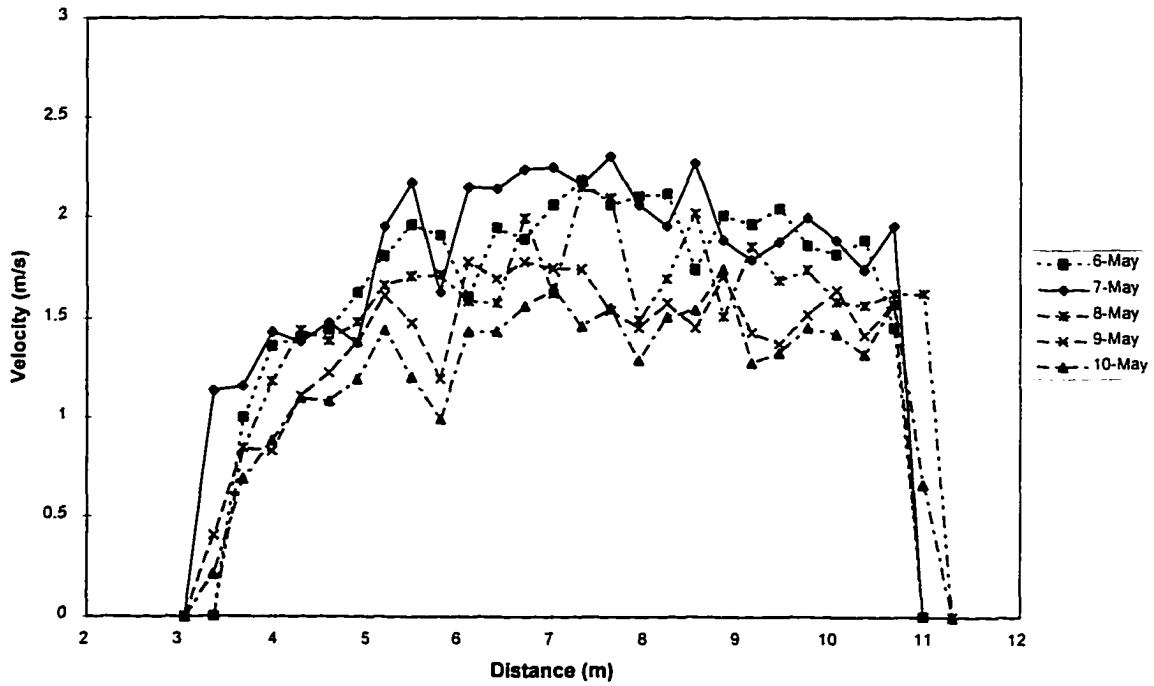
Cross Section Velocities - June 1995
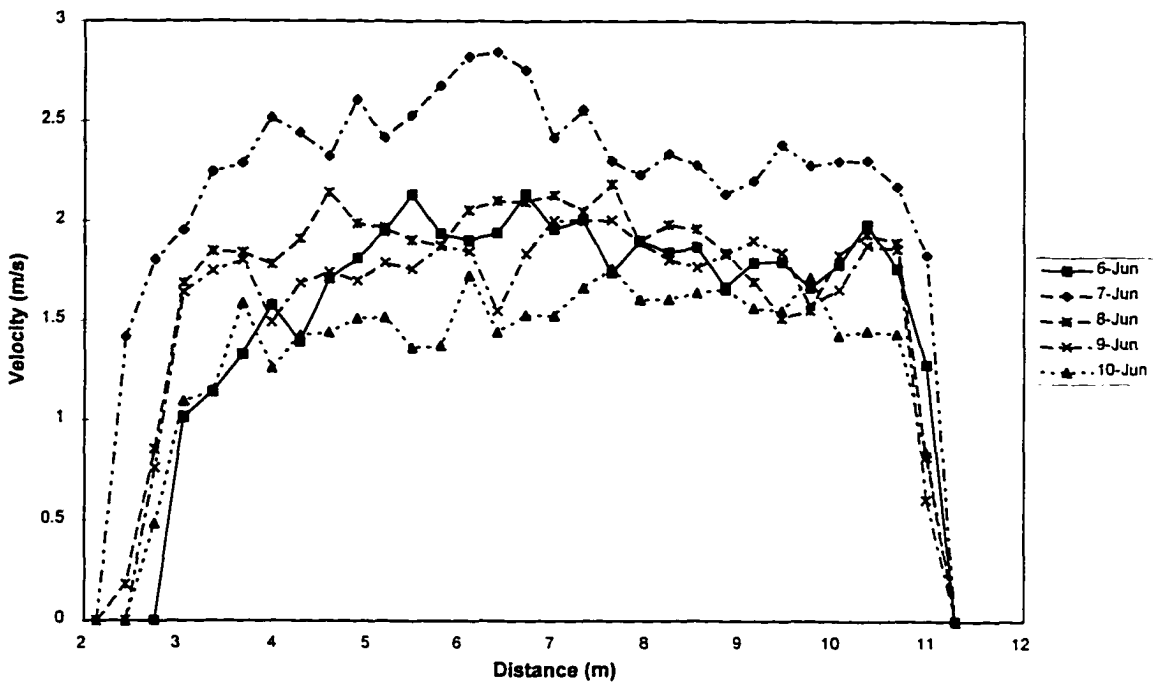
APPENDIX - B1

Mass/unit width/unit time: Coarse bed load transport rates and fractional transport rates for each of the 120 individual bed load samples obtained in the May and June floods, 1995.

Sample #	Sample time (min.)	Fractional bed load transport rates >38 mm (kg/m/min.)						Total bed load >38 mm (kg/m/min.)	Mean channel shear stress (N/m²)
		<51	<64	<76	<90	<128	<180		
					May 6-10, 1995				
1	1	-	-	-	-	4.42	0.00	12.16	57.2
2	2	-	-	-	-	1.02	0.00	2.84	56.9
3	2	-	-	-	-	0.28	0.00	3.30	56.4
4	2	-	-	-	-	2.44	0.79	16.70	56.1
5	2	-	-	-	-	0.85	0.00	15.74	55.9
6	2	-	-	-	-	3.91	1.70	19.72	55.6
7	2	-	-	-	-	0.00	0.00	9.94	55.3
8	4	-	-	-	-	3.46	1.42	34.63	55.3
9	2	8.05	7.14	6.12	1.81	1.81	0.00	24.94	55.3
10	2	11.11	6.80	6.01	3.67	3.40	0.00	31.00	55.3
11	2	0.52	0.16	0.34	0.00	0.00	0.00	1.02	55.0
12	10	5.22	2.53	0.98	0.36	1.00	0.00	10.09	55.0
13	0.5	9.25	3.63	1.81	0.00	9.61	0.00	24.31	55.0
14	4	1.34	0.60	0.10	0.00	0.00	0.00	2.04	55.0
15	4	1.00	0.14	0.16	0.00	0.00	0.00	1.29	55.0
16	4	2.10	1.34	0.26	0.00	0.00	0.91	4.60	55.0
17	4	1.81	0.75	0.51	0.00	0.00	0.00	3.07	53.7
18	4	3.54	0.85	0.15	0.00	0.00	0.00	4.54	53.7
19	4	1.63	0.57	0.00	0.00	0.00	0.00	2.20	54.5
20	2.3	5.84	1.77	1.34	0.00	1.60	0.00	10.55	54.0
21	2	7.62	3.92	2.27	0.57	1.25	2.31	17.94	54.0
22	2	6.53	3.11	1.25	0.00	0.00	0.00	10.88	53.4
23	2	13.22	7.85	1.02	0.41	2.11	0.00	24.60	53.4
24	2	3.58	1.59	0.68	0.50	0.00	0.00	6.35	54.8
25	2	4.69	3.63	0.79	0.84	1.20	0.00	11.16	54.8
26	2	10.43	4.08	2.27	0.00	0.86	0.00	17.64	54.8
27	2	5.67	3.17	1.81	0.00	0.63	0.00	11.29	55.0
28	2	1.77	0.91	0.59	0.00	0.00	0.00	3.27	52.3
29	2	1.81	0.86	0.48	0.00	0.00	0.00	3.15	52.3
30	4	7.24	2.83	1.47	0.23	0.51	0.00	12.29	52.3
31	2	7.03	4.08	1.97	0.36	0.00	0.00	13.45	52.1
32	2	1.61	0.84	0.00	0.00	0.00	0.00	2.45	52.3
33	2	3.13	1.41	0.00	0.00	0.00	0.00	4.54	52.3
34	2	7.03	2.00	0.50	0.45	0.00	0.00	9.98	51.8
35	2	5.26	1.97	0.66	0.91	1.27	0.00	10.07	51.0
36	2	2.20	1.77	0.25	0.98	0.00	0.00	5.19	51.5
37	2	0.93	0.45	0.00	0.00	0.00	0.00	1.38	51.0
38	2	6.35	2.15	0.95	1.02	0.00	0.00	10.48	51.5
39	2	2.20	1.27	0.00	0.00	0.00	0.00	3.47	51.8
40	2	1.07	0.23	0.00	0.00	0.00	0.00	1.29	47.5
41	4	0.16	0.08	0.00	0.00	0.00	0.00	0.24	47.2
42	6	2.66	0.73	0.44	0.00	0.15	0.00	3.98	48.0

Sample #	Sample time (min.)	Fractional bed load transport rates >38 mm (kg/m/min.)						Total bed load >38 mm (kg/m/min.)	Mean channel shear stress (N/m²)
		<51	<64	<76	<90	<128	<180		
43	6	4.05	1.40	0.36	0.00	0.33	0.00	6.14	47.5
44	4	0.14	0.00	0.00	0.00	0.00	0.00	0.14	47.2
45	6	1.36	0.73	0.00	0.00	0.00	0.00	2.09	46.9
46	6	0.14	0.00	0.00	0.00	0.00	0.00	0.14	46.4
47	10	0.60	0.10	0.05	0.00	0.00	0.00	0.75	46.1
48	10	1.10	0.46	0.00	0.00	0.00	0.00	1.56	46.4
49	30	1.77	0.63	0.09	0.06	0.05	0.00	2.59	45.8
50	10	0.23	0.09	0.14	0.00	0.00	0.00	0.45	45.0
51	20	0.28	0.06	0.02	0.00	0.00	0.00	0.36	45.3
52	20	0.21	0.04	0.02	0.05	0.00	0.00	0.33	45.3
53	30	0.13	0.03	0.00	0.03	0.00	0.00	0.19	45.0
54	60	0.05	0.00	0.01	0.00	0.00	0.00	0.07	45.3
June 6-11, 1995									
55	2	0.52	0.29	1.13	0.00	0.00	0.00	1.95	56.7
56	2	7.62	3.45	2.95	0.68	0.00	0.00	14.69	57.2
57	2	1.36	1.36	0.23	0.00	0.86	0.00	3.81	57.5
58	2	3.58	2.06	0.00	1.13	2.49	0.00	9.27	57.5
59	2	0.41	0.50	0.00	0.00	0.00	0.00	0.91	57.2
60	2	1.11	1.25	0.00	0.00	0.00	0.00	2.36	57.7
61	2	0.36	0.73	0.00	0.00	0.73	0.00	1.81	57.5
62	2	7.94	4.31	2.72	0.95	0.00	0.00	15.92	58.0
63	2	5.78	2.72	2.18	0.77	0.45	0.00	11.90	57.7
64	2	1.41	1.27	0.39	0.45	0.41	0.00	3.92	57.7
65	2	2.68	2.47	1.68	0.91	0.45	0.00	8.19	58.0
66	2	7.39	3.51	0.57	0.52	0.00	0.00	12.00	58.0
67	2	6.94	4.54	2.00	0.39	1.38	0.00	15.24	58.3
68	2	1.38	0.63	0.00	0.00	0.73	0.00	2.74	58.0
69	2	3.17	3.85	2.49	0.00	0.00	0.00	9.52	59.1
70	2	1.50	0.68	0.20	1.07	0.00	0.00	3.45	63.2
71	2	0.50	1.13	0.23	0.45	0.63	0.00	2.95	62.9
72	2	2.95	2.49	1.61	0.86	0.77	0.00	8.68	63.7
73	2	2.54	1.79	2.63	0.00	1.47	0.00	8.44	64.0
74	2	0.54	0.18	0.00	0.00	0.00	0.00	0.73	64.2
75	2	1.52	1.81	0.91	0.00	2.04	0.00	6.28	64.0
76	2	3.38	2.31	1.66	0.45	2.43	0.00	10.23	64.5
77	2	8.68	6.12	3.22	0.50	5.56	0.00	24.08	65.1
78	2	0.84	0.45	1.07	1.00	1.63	0.00	4.99	66.1
79	2	8.68	7.03	3.08	0.43	2.68	1.72	23.63	66.4
80	2	4.17	3.83	1.36	1.75	0.98	0.00	12.09	66.7
81	2	15.22	8.00	6.98	1.47	8.10	2.56	42.34	67.2
82	0.5	3.99	4.72	3.27	2.63	3.54	0.00	18.15	-
83	1	11.25	7.48	4.17	0.00	1.13	0.00	24.04	63.6
84	1	1.86	1.18	2.59	0.00	0.00	0.00	5.62	62.1
85	1	6.80	7.48	2.04	3.17	2.27	0.00	21.77	64.4
86	1	9.52	9.07	2.86	0.00	4.40	0.00	25.85	62.1
87	1	8.34	3.54	0.59	0.00	2.86	0.00	15.33	62.4
88	1	10.52	9.80	4.67	1.22	3.85	0.00	30.07	61.8
89	1	18.19	14.97	8.53	2.31	6.89	0.00	50.88	63.6

Sample #	Sample time (min.)	Fractional bed load transport rates >38 mm (kg/m/min.)						Total bed load >38 mm (kg/m/min.)	Mean channel shear stress (N/m²)
		<51	<64	<76	<90	<128	<180		
90	1	10.66	4.44	3.76	0.91	1.81	0.00	21.59	63.0
91	1	1.50	0.50	0.00	0.82	0.00	0.00	2.81	61.8
92	1	3.49	1.95	0.00	0.00	0.00	0.00	5.44	63.0
93	2	8.14	4.31	2.00	1.36	0.43	0.00	16.24	62.1
94	1	5.90	2.59	1.13	0.95	1.00	1.72	13.29	63.6
95	2	10.63	4.94	3.65	1.20	2.72	0.00	23.15	60.6
96	2	5.51	4.15	1.11	0.00	0.00	0.00	10.77	53.2
97	2	8.48	4.10	1.79	0.00	0.00	0.00	14.38	53.8
98	2	9.46	5.90	0.84	0.91	2.24	0.00	19.34	51.1
99	2	9.25	5.22	2.99	0.43	0.61	0.00	18.50	52.6
100	2	3.17	1.47	0.00	0.00	0.57	0.00	5.22	51.7
101	2	0.45	0.45	0.00	0.00	0.00	0.00	0.91	53.2
102	4	0.70	0.31	0.14	0.00	0.23	0.00	1.37	51.7
103	4	1.16	0.46	0.46	0.27	0.00	0.00	2.36	51.7
104	10	0.09	0.10	0.00	0.00	0.00	0.00	0.19	51.7
105	10	2.54	1.12	0.44	0.38	0.19	0.00	4.68	52.3
106	10	0.77	0.36	0.34	0.00	0.00	0.00	1.47	47.3
107	10	4.23	2.64	0.76	0.34	0.17	0.00	8.14	47.3
108	4	1.55	0.71	0.34	0.00	0.00	0.00	2.61	47.9
109	4	1.45	0.40	0.16	0.54	0.00	0.00	2.55	48.8
110	4	0.84	0.15	0.18	0.00	0.00	0.00	1.17	49.4
111	4	1.45	0.91	0.22	0.00	0.00	0.00	2.57	49.1
112	4	1.21	0.22	0.00	0.00	0.00	0.00	1.43	48.5
113	4	4.46	2.21	0.60	0.34	0.44	0.00	8.05	49.1
114	4	8.34	3.49	1.98	0.25	0.33	0.00	14.40	48.8
115	4	0.50	0.24	0.00	0.39	0.00	0.00	1.12	49.7
116	4	2.21	2.19	0.31	0.27	0.00	0.00	4.98	48.8
117	4	3.23	2.01	0.73	0.00	0.42	0.00	6.38	48.8
118	4	1.36	0.76	0.96	0.71	0.45	0.00	4.25	49.7
119	4	1.08	0.66	0.60	0.00	0.48	0.00	2.81	49.1
120	4	3.49	0.79	0.85	0.00	0.00	0.00	5.14	49.4

APPENDIX - B2

Particle numbers/unit width/unit time: Coarse bed load transport rates and fractional transport rates for each of the 120 individual bed load samples obtained in the May and June floods, 1995.

Sample #	Sample time (min.)	Fractional bed load transport rates >38 mm (particle #'s/m/min.)						Total bed load >38 mm (#/m/min.)	Mean channel shear stress (N/m²)
		<51	<64	<76	<90	<128	<180		
May 6-10, 1995									
1	1	-	-	-	-	-	-	-	57.2
2	2	-	-	-	-	-	-	-	56.9
3	2	-	-	-	-	-	-	-	56.4
4	2	-	-	-	-	-	-	-	56.1
5	2	-	-	-	-	-	-	-	55.9
6	2	-	-	-	-	-	-	-	55.6
7	2	-	-	-	-	-	-	-	55.3
8	4	-	-	-	-	-	-	-	55.3
9	2	64.5	22.0	11.0	1.0	1.0	0.0	99.5	55.3
10	2	83.0	22.5	9.5	3.5	3.0	0.0	121.5	55.3
11	2	3.5	0.5	0.5	0.0	0.0	0.0	4.5	55.0
12	10	39.9	9.1	1.8	0.3	0.8	0.0	51.9	55.0
13	0.5	62.0	12.0	2.0	0.0	4.0	0.0	80.0	55.0
14	4	10.5	2.0	0.3	0.0	0.0	0.0	12.8	55.0
15	4	7.8	0.5	0.3	0.0	0.0	0.0	8.5	55.0
16	4	15.8	4.3	0.5	0.0	0.0	0.3	20.8	55.0
17	4	14.0	2.3	1.0	0.0	0.0	0.0	17.3	53.7
18	4	26.3	2.8	0.3	0.0	0.0	0.0	29.3	53.7
19	4	11.8	2.0	0.0	0.0	0.0	0.0	13.8	54.5
20	2.3	43.8	6.9	1.7	0.0	0.9	0.0	53.2	54.0
21	2	58.0	14.0	4.0	0.5	1.0	0.5	78.0	54.0
22	2	49.5	10.5	3.0	0.0	0.0	0.0	63.0	53.4
23	2	101.0	24.5	2.0	0.5	1.5	0.0	129.5	53.4
24	2	26.0	5.5	1.0	0.5	0.0	0.0	33.0	54.8
25	2	32.0	12.0	1.0	1.0	1.0	0.0	47.0	54.8
26	2	75.5	14.0	4.0	0.0	1.0	0.0	94.5	54.8
27	2	44.5	11.0	3.0	0.0	0.5	0.0	59.0	55.0
28	2	13.0	3.0	0.5	0.0	0.0	0.0	16.5	52.3
29	2	11.5	2.5	1.0	0.0	0.0	0.0	15.0	52.3
30	4	55.8	9.8	2.5	0.3	0.5	0.0	68.8	52.3
31	2	51.5	14.5	3.0	0.5	0.0	0.0	69.5	52.1
32	2	11.5	2.5	0.0	0.0	0.0	0.0	14.0	52.3
33	2	24.0	4.5	0.0	0.0	0.0	0.0	28.5	52.3
34	2	52.0	7.5	1.0	0.5	0.0	0.0	61.0	51.8
35	2	40.0	6.5	1.0	0.5	0.5	0.0	48.5	51.0
36	2	17.0	6.0	0.5	1.0	0.0	0.0	24.5	51.5
37	2	6.5	1.5	0.0	0.0	0.0	0.0	8.0	51.0
38	2	47.0	7.0	2.0	1.0	0.0	0.0	57.0	51.5
39	2	16.5	4.5	0.0	0.0	0.0	0.0	21.0	51.8
40	2	6.5	0.5	0.0	0.0	0.0	0.0	7.0	47.5
41	4	1.0	0.3	0.0	0.0	0.0	0.0	1.3	47.2
42	6	21.2	2.7	0.5	0.0	0.2	0.0	24.5	48.0

Sample #	Sample time (min.)	Fractional bed load transport rates >38 mm (particle #'s/m/min.)						Total bed load >38 mm (#/m/min.)	Mean channel shear stress (N/m^2)
		<51	<64	<76	<90	<128	<180		
43	6	32.5	4.7	0.7	0.0	0.2	0.0	38.0	47.5
44	4	1.0	0.0	0.0	0.0	0.0	0.0	1.0	47.2
45	6	10.8	2.7	0.0	0.0	0.0	0.0	13.5	46.9
46	6	1.2	0.0	0.0	0.0	0.0	0.0	1.2	46.4
47	10	4.2	0.3	0.1	0.0	0.0	0.0	4.6	46.1
48	10	7.5	1.3	0.0	0.0	0.0	0.0	8.8	46.4
49	30	13.8	2.2	0.2	0.1	0.0	0.0	16.3	45.8
50	10	1.8	0.2	0.2	0.0	0.0	0.0	2.2	45.0
51	20	2.0	0.2	0.1	0.0	0.0	0.0	2.3	45.3
52	20	1.5	0.1	0.1	0.1	0.0	0.0	1.7	45.3
53	30	0.9	0.1	0.0	0.0	0.0	0.0	1.0	45.0
54	60	0.4	0.0	0.0	0.0	0.0	0.0	0.4	45.3
				June 6-11, 1995					
55	2	3.0	1.0	1.5	0.0	0.0	0.0	5.5	56.7
56	2	55.5	12.5	6.0	1.0	0.0	0.0	75.0	57.2
57	2	9.5	4.0	0.5	0.0	0.5	0.0	14.5	57.5
58	2	27.0	6.5	0.0	1.0	2.5	0.0	37.0	57.5
59	2	3.0	2.0	0.0	0.0	0.0	0.0	5.0	57.2
60	2	8.0	3.5	0.0	0.0	0.0	0.0	11.5	57.7
61	2	2.5	2.0	0.0	0.0	0.5	0.0	5.0	57.5
62	2	58.0	15.5	5.0	0.5	0.0	0.0	79.0	58.0
63	2	41.0	9.0	3.5	1.0	0.5	0.0	55.0	57.7
64	2	10.5	4.0	0.5	0.5	0.5	0.0	16.0	57.7
65	2	19.5	8.5	3.0	1.0	0.5	0.0	32.5	58.0
66	2	54.0	12.0	1.0	0.5	0.0	0.0	67.5	58.0
67	2	50.5	15.5	3.0	0.5	1.0	0.0	70.5	58.3
68	2	9.5	2.0	0.0	0.0	0.5	0.0	12.0	58.0
69	2	24.0	12.5	3.5	0.0	0.0	0.0	40.0	59.1
70	2	12.0	1.5	0.5	1.0	0.0	0.0	15.0	63.2
71	2	4.0	3.5	0.5	0.5	0.5	0.0	9.0	62.9
72	2	21.5	7.5	3.0	1.0	0.5	0.0	33.5	63.7
73	2	17.5	4.5	4.0	0.0	1.0	0.0	27.0	64.0
74	2	4.0	0.5	0.0	0.0	0.0	0.0	4.5	64.2
75	2	9.0	6.0	1.5	0.0	1.0	0.0	17.5	64.0
76	2	23.5	7.5	3.0	0.5	1.0	0.0	35.5	64.5
77	2	61.5	20.0	6.0	0.5	3.5	0.0	91.5	65.1
78	2	6.0	1.5	2.0	1.0	1.0	0.0	11.5	66.1
79	2	66.5	23.5	5.5	0.5	2.5	0.5	99.0	66.4
80	2	30.0	12.5	2.0	2.0	1.0	0.0	47.5	66.7
81	2	109.5	27.5	11.5	1.5	5.5	0.5	156.0	67.2
82	0.5	28.0	14.0	6.0	2.0	2.0	0.0	52.0	-
83	1	87.0	23.0	8.0	0.0	1.0	0.0	119.0	63.6
84	1	14.0	5.0	5.0	0.0	0.0	0.0	24.0	62.1
85	1	54.0	23.0	4.0	3.0	1.0	0.0	85.0	64.4
86	1	68.0	27.0	5.0	0.0	3.0	0.0	103.0	62.1
87	1	55.0	12.0	1.0	0.0	3.0	0.0	71.0	62.4
88	1	83.0	32.0	9.0	1.0	3.0	0.0	128.0	61.8
89	1	137.0	46.0	15.0	2.0	5.0	0.0	205.0	63.6

Sample #	Sample time (min.)	Fractional bed load transport rates >38 mm (particle #'s/m/min.)						Total bed load >38 mm (#/m/min.)	Mean channel shear stress (N/m^2)
		<51	<64	<76	<90	<128	<180		
90	1	80.0	15.0	6.0	1.0	1.0	0.0	103.0	63.0
91	1	13.0	2.0	0.0	1.0	0.0	0.0	16.0	61.8
92	1	23.0	6.0	0.0	0.0	0.0	0.0	29.0	63.0
93	2	60.5	13.0	3.5	1.5	0.5	0.0	79.0	62.1
94	1	44.0	8.0	2.0	1.0	1.0	1.0	57.0	63.6
95	2	79.0	17.5	6.5	1.0	1.5	0.0	105.5	60.6
96	2	43.5	14.0	2.0	0.0	0.0	0.0	59.5	53.2
97	2	66.0	12.5	2.5	0.0	0.0	0.0	81.0	53.8
98	2	73.5	20.5	1.5	1.0	1.0	0.0	97.5	51.1
99	2	69.0	17.0	5.0	0.5	0.5	0.0	92.0	52.6
100	2	23.5	4.5	0.0	0.0	0.5	0.0	28.5	51.7
101	2	3.5	1.0	0.0	0.0	0.0	0.0	4.5	53.2
102	4	5.5	1.0	0.3	0.0	0.3	0.0	7.0	51.7
103	4	8.5	1.5	0.8	0.3	0.0	0.0	11.0	51.7
104	10	0.6	0.3	0.0	0.0	0.0	0.0	0.9	51.7
105	10	18.8	3.9	0.7	0.4	0.1	0.0	23.9	52.3
106	10	5.9	1.1	0.5	0.0	0.0	0.0	7.5	47.3
107	10	32.9	8.9	1.4	0.4	0.1	0.0	43.7	47.3
108	4	11.8	2.8	0.8	0.0	0.0	0.0	15.3	47.9
109	4	11.5	1.3	0.3	0.5	0.0	0.0	13.5	48.8
110	4	6.0	0.5	0.3	0.0	0.0	0.0	6.8	49.4
111	4	11.3	2.8	0.3	0.0	0.0	0.0	14.3	49.1
112	4	9.8	0.8	0.0	0.0	0.0	0.0	10.5	48.5
113	4	34.3	7.8	1.0	0.3	0.3	0.0	43.5	49.1
114	4	68.3	11.5	3.0	0.3	0.3	0.0	83.3	48.8
115	4	3.5	1.0	0.0	0.5	0.0	0.0	5.0	49.7
116	4	17.5	7.3	0.5	0.3	0.0	0.0	25.5	48.8
117	4	23.8	7.0	1.3	0.0	0.5	0.0	32.5	48.8
118	4	9.3	2.5	1.8	0.5	0.3	0.0	14.3	49.7
119	4	8.0	2.3	1.0	0.0	0.3	0.0	11.5	49.1
120	4	26.8	2.8	1.5	0.0	0.0	0.0	31.0	49.4

APPENDIX - B3

Flow hydraulics for each of the 120 individual bed load samples obtained in the May and June floods, 1995. Flow depth, velocity, unit discharge, and shear stress are mean cross sectional values.

Sample #	Flow width (m)	Flow depth (m)	Flow velocity (m/s)	Discharge (m³/s)	Unit discharge (m²/s)	Shear stress (N/m²)
			May 6-10, 1995			
1	7.62	0.58	1.75	7.78	1.02	57.2
2	7.62	0.58	1.74	7.70	1.01	56.9
3	7.62	0.58	1.72	7.54	0.99	56.4
4	7.62	0.57	1.71	7.46	0.98	56.1
5	7.62	0.57	1.70	7.38	0.97	55.9
6	7.62	0.57	1.69	7.30	0.96	55.6
7	7.62	0.56	1.68	7.22	0.95	55.3
8	7.93	0.56	1.62	7.22	0.91	55.3
9	7.93	0.56	1.62	7.22	0.91	55.3
10	7.93	0.56	1.62	7.22	0.91	55.3
11	7.93	0.56	1.61	7.15	0.90	55.0
12	7.93	0.56	1.61	7.15	0.90	55.0
13	7.93	0.56	1.61	7.15	0.90	55.0
14	7.93	0.56	1.61	7.15	0.90	55.0
15	7.93	0.56	1.61	7.15	0.90	55.0
16	7.93	0.56	1.61	7.15	0.90	55.0
17	7.93	0.55	1.56	6.77	0.85	53.7
18	7.93	0.55	1.56	6.77	0.85	53.7
19	7.93	0.56	1.59	6.99	0.88	54.5
20	7.93	0.55	1.57	6.84	0.86	54.0
21	7.93	0.55	1.57	6.84	0.86	54.0
22	7.93	0.54	1.55	6.69	0.84	53.4
23	7.93	0.54	1.55	6.69	0.84	53.4
24	7.93	0.56	1.60	7.07	0.89	54.8
25	7.93	0.56	1.60	7.07	0.89	54.8
26	7.93	0.56	1.60	7.07	0.89	54.8
27	7.93	0.56	1.61	7.15	0.90	55.0
28	7.93	0.53	1.51	6.40	0.81	52.3
29	7.93	0.53	1.51	6.40	0.81	52.3
30	7.93	0.53	1.51	6.40	0.81	52.3
31	7.93	0.53	1.50	6.32	0.80	52.1
32	7.93	0.53	1.51	6.40	0.81	52.3
33	7.93	0.53	1.51	6.40	0.81	52.3
34	7.93	0.53	1.49	6.25	0.79	51.8
35	7.93	0.52	1.46	6.04	0.76	51.0
36	7.93	0.53	1.48	6.18	0.78	51.5
37	7.93	0.52	1.46	6.04	0.76	51.0
38	7.93	0.53	1.48	6.18	0.78	51.5
39	7.93	0.53	1.49	6.25	0.79	51.8
40	7.93	0.48	1.34	5.16	0.65	47.5
41	7.93	0.48	1.34	5.09	0.64	47.2
42	7.93	0.49	1.36	5.29	0.67	48.0
43	7.93	0.48	1.34	5.16	0.65	47.5

Sample #	Flow width (m)	Flow depth (m)	Flow velocity (m/s)	Discharge (m³/s)	Unit discharge (m²/s)	Shear stress (N/m²)
44	7.93	0.48	1.34	5.09	0.64	47.2
45	7.93	0.48	1.33	5.03	0.63	46.9
46	7.93	0.47	1.31	4.90	0.62	46.4
47	7.93	0.47	1.30	4.84	0.61	46.1
48	7.93	0.47	1.31	4.90	0.62	46.4
49	7.93	0.47	1.29	4.78	0.60	45.8
50	7.93	0.46	1.26	4.59	0.58	45.0
51	7.93	0.46	1.27	4.66	0.59	45.3
52	7.93	0.46	1.27	4.66	0.59	45.3
53	7.93	0.46	1.26	4.59	0.58	45.0
54	7.93	0.46	1.27	4.66	0.59	45.3
June 6-11, 1995						
55	8.54	0.58	1.54	7.62	0.89	56.7
56	8.54	0.58	1.56	7.78	0.91	57.2
57	8.54	0.59	1.57	7.86	0.92	57.5
58	8.54	0.59	1.57	7.86	0.92	57.5
59	8.54	0.58	1.56	7.78	0.91	57.2
60	8.54	0.59	1.58	7.94	0.93	57.7
61	8.54	0.59	1.57	7.86	0.92	57.5
62	8.54	0.59	1.59	8.03	0.94	58.0
63	8.54	0.59	1.58	7.94	0.93	57.7
64	8.54	0.59	1.58	7.94	0.93	57.7
65	8.54	0.59	1.59	8.03	0.94	58.0
66	8.54	0.59	1.59	8.03	0.94	58.0
67	8.54	0.59	1.60	8.11	0.95	58.3
68	8.54	0.59	1.59	8.03	0.94	58.0
69	8.54	0.60	1.62	8.36	0.98	59.1
70	8.54	0.64	1.76	9.68	1.13	63.2
71	8.54	0.64	1.75	9.59	1.12	62.9
72	8.54	0.65	1.78	9.86	1.15	63.7
73	8.54	0.65	1.79	9.96	1.17	64.0
74	8.54	0.66	1.80	10.05	1.18	64.2
75	8.54	0.65	1.79	9.96	1.17	64.0
76	8.54	0.66	1.81	10.14	1.19	64.5
77	8.54	0.66	1.82	10.33	1.21	65.1
78	8.54	0.67	1.86	10.71	1.25	66.1
79	8.54	0.68	1.87	10.81	1.27	66.4
80	8.54	0.68	1.88	10.91	1.28	66.7
81	8.54	0.69	1.90	11.10	1.30	67.2
82	9.15	-	-	15.45	1.69	-
83	9.15	0.65	1.76	10.42	1.14	63.6
84	9.15	0.63	1.72	9.99	1.09	62.1
85	9.15	0.66	1.78	10.69	1.17	64.4
86	9.15	0.63	1.72	9.99	1.09	62.1
87	9.15	0.64	1.73	10.08	1.10	62.4
88	9.15	0.63	1.72	9.90	1.08	61.8
89	9.15	0.65	1.76	10.42	1.14	63.6
90	9.15	0.64	1.74	10.25	1.12	63.0
91	9.15	0.63	1.72	9.90	1.08	61.8

Sample #	Flow width (m)	Flow depth (m)	Flow velocity (m/s)	Discharge (m³/s)	Unit discharge (m²/s)	Shear stress (N/m²)
92	9.15	0.64	1.74	10.25	1.12	63.0
93	9.15	0.63	1.72	9.99	1.09	62.1
94	9.15	0.65	1.76	10.42	1.14	63.6
95	9.15	0.62	1.69	9.56	1.04	60.6
96	8.96	0.54	1.55	7.53	0.84	53.2
97	8.96	0.55	1.56	7.68	0.86	53.8
98	8.96	0.52	1.50	6.99	0.78	51.1
99	8.96	0.54	1.53	7.37	0.82	52.6
100	8.96	0.53	1.51	7.14	0.80	51.7
101	8.96	0.54	1.55	7.53	0.84	53.2
102	8.96	0.53	1.51	7.14	0.80	51.7
103	8.96	0.53	1.51	7.14	0.80	51.7
104	8.96	0.53	1.51	7.14	0.80	51.7
105	8.96	0.53	1.53	7.29	0.81	52.3
106	8.78	0.48	1.42	6.03	0.69	47.3
107	8.78	0.48	1.42	6.03	0.69	47.3
108	8.78	0.49	1.44	6.18	0.70	47.9
109	8.78	0.50	1.46	6.40	0.73	48.8
110	8.78	0.50	1.48	6.54	0.75	49.4
111	8.78	0.50	1.47	6.47	0.74	49.1
112	8.78	0.49	1.46	6.32	0.72	48.5
113	8.78	0.50	1.47	6.47	0.74	49.1
114	8.78	0.50	1.46	6.40	0.73	48.8
115	8.78	0.51	1.49	6.62	0.75	49.7
116	8.78	0.50	1.46	6.40	0.73	48.8
117	8.78	0.50	1.46	6.40	0.73	48.8
118	8.78	0.51	1.49	6.62	0.75	49.7
119	8.78	0.50	1.47	6.47	0.74	49.1
120	8.78	0.50	1.48	6.54	0.75	49.4

APPENDIX - B4

The three largest particle sizes together with sample mass and flow condition for each of the 120 individual bed load samples obtained in the May and June floods, 1995. Unit discharge and shear stress are mean cross sectional values.

Sample #	Sample mass >38 mm (kg)	Largest bed load particle sizes (mm)				Unit discharge (m²/s)	Shear stress (N/m²)
		Largest	2nd largest	3rd largest	Mean of 3		
			May 6-10, 1995				
1	10.6	120	-	-	-	1.02	57.2
2	4.9	100	-	-	-	1.01	56.9
3	5.7	90	-	-	-	0.99	56.4
4	28.6	135	-	-	-	0.98	56.1
5	25.8	104	-	-	-	0.97	55.9
6	34.7	134	-	-	-	0.96	55.6
7	17.0	90	-	-	-	0.95	55.3
8	115.7	155	130	-	143	0.91	55.3
9	49.9	120	116	95	110	0.91	55.3
10	62.0	105	103	98	102	0.91	55.3
11	2.0	70	60	-	65	0.90	55.0
12	100.9	125	110	110	115	0.90	55.0
13	12.2	110	100	74	95	0.90	55.0
14	8.2	75	74	64	71	0.90	55.0
15	5.2	74	60	54	63	0.90	55.0
16	18.4	131	80	67	93	0.90	55.0
17	12.3	89	80	75	81	0.85	53.7
18	18.1	78	68	68	71	0.85	53.7
19	8.8	70	65	65	67	0.88	54.5
20	24.6	117	98	85	100	0.86	54.0
21	35.9	175	100	95	123	0.86	54.0
22	21.8	76	72	69	72	0.84	53.4
23	49.2	124	100	100	108	0.84	53.4
24	12.7	80	73	66	73	0.89	54.8
25	22.3	106	95	80	94	0.89	54.8
26	35.3	105	93	90	96	0.89	54.8
27	22.6	98	87	87	91	0.90	55.0
28	6.5	76	76	71	74	0.81	52.3
29	6.3	75	75	58	69	0.81	52.3
30	49.2	109	93	86	96	0.81	52.3
31	26.9	85	83	80	83	0.80	52.1
32	4.9	68	64	62	65	0.81	52.3
33	9.1	88	74	70	77	0.81	52.3
34	20.0	85	80	70	78	0.79	51.8
35	20.1	123	87	85	98	0.76	51.0
36	10.4	86	84	75	82	0.78	51.5
37	2.8	64	62	58	61	0.76	51.0
38	21.0	89	88	79	85	0.78	51.5
39	6.9	70	70	61	67	0.79	51.8
40	2.6	59	58	55	57	0.65	47.5
41	1.0	65	52	50	56	0.64	47.2
42	23.9	100	78	75	84	0.67	48.0

Sample #	Sample mass >38 mm (kg)	Largest bed load particle sizes (mm)				Unit discharge (m²/s)	Shear stress (N/m²)
		Largest	2nd largest	3rd largest	Mean of 3		
43	36.8	90	82	81	84	0.65	47.5
44	0.5	54	50	49	51	0.64	47.2
45	12.6	78	72	70	73	0.63	46.9
46	0.9	58	57	52	56	0.62	46.4
47	7.5	70	65	61	65	0.61	46.1
48	15.6	75	74	65	71	0.62	46.4
49	77.7	94	88	74	85	0.60	45.8
50	4.5	88	80	76	81	0.58	45.0
51	7.3	75	70	66	70	0.59	45.3
52	6.5	82	80	64	75	0.59	45.3
53	5.7	85	70	58	71	0.58	45.0
54	4.0	82	-	-	82	0.59	45.3
		June 6-11, 1995					
55	3.9	103	80	75	86	0.89	56.7
56	29.4	103	99	81	94	0.91	57.2
57	7.6	100	75	70	82	0.92	57.5
58	18.5	120	110	106	112	0.92	57.5
59	1.8	71	60	60	64	0.91	57.2
60	4.7	74	73	64	70	0.93	57.7
61	3.6	108	72	63	81	0.92	57.5
62	31.8	94	88	77	86	0.94	58.0
63	23.8	105	85	82	91	0.93	57.7
64	7.8	115	88	76	93	0.93	57.7
65	16.4	96	88	85	90	0.94	58.0
66	24.0	87	79	75	80	0.94	58.0
67	30.5	103	95	83	94	0.95	58.3
68	5.5	93	-	-	93	0.94	58.0
69	19.0	91	76	72	80	0.98	59.1
70	6.9	89	87	86	87	1.13	63.2
71	5.9	105	89	77	90	1.12	62.9
72	17.4	113	87	82	94	1.15	63.7
73	16.9	100	93	75	89	1.17	64.0
74	1.5	64	-	-	64	1.18	64.2
75	12.6	122	103	67	97	1.17	64.0
76	20.5	120	104	87	104	1.19	64.5
77	48.2	124	120	105	116	1.21	65.1
78	10.0	102	96	89	96	1.25	66.1
79	47.3	146	113	105	121	1.27	66.4
80	24.2	96	91	89	92	1.28	66.7
81	84.7	144	124	120	129	1.30	67.2
82	9.1	110	85	83	93	1.69	-
83	24.0	98	95	81	91	1.14	63.6
84	5.6	95	90	75	87	1.09	62.1
85	21.8	114	88	77	93	1.17	64.4
86	25.9	107	100	92	100	1.09	62.1
87	15.3	94	94	90	93	1.10	62.4
88	30.1	96	94	91	94	1.08	61.8
89	50.9	127	112	98	112	1.14	63.6
90	21.6	105	86	86	92	1.12	63.0

Sample #	Sample mass >38 mm (kg)	Largest bed load particle sizes (mm)				Unit discharge (m²/s)	Shear stress (N/m²)
		Largest	2nd largest	3rd largest	Mean of 3		
91	2.8	84	59	59	67	1.08	61.8
92	5.4	67	65	61	64	1.12	63.0
93	32.5	95	85	81	87	1.09	62.1
94	13.3	144	107	84	112	1.14	63.6
95	46.3	110	92	92	98	1.04	60.6
96	21.5	85	71	68	75	0.84	53.2
97	28.8	84	74	74	77	0.86	53.8
98	38.7	121	98	84	101	0.78	51.1
99	37.0	98	89	88	92	0.82	52.6
100	10.4	97	75	68	80	0.80	51.7
101	1.8	62	56	46	55	0.84	53.2
102	5.5	109	65	63	79	0.80	51.7
103	9.4	80	78	69	76	0.80	51.7
104	1.9	66	59	58	61	0.80	51.7
105	46.8	92	87	83	87	0.81	52.3
106	14.7	76	75	74	75	0.69	47.3
107	81.4	95	89	87	90	0.69	47.3
108	10.4	94	69	64	76	0.70	47.9
109	10.2	84	81	76	80	0.73	48.8
110	4.7	75	63	53	64	0.75	49.4
111	10.3	80	65	65	70	0.74	49.1
112	5.7	65	56	56	59	0.72	48.5
113	32.2	95	83	80	86	0.74	49.1
114	57.6	98	90	87	92	0.73	48.8
115	4.5	89	85	69	81	0.75	49.7
116	19.9	87	67	67	74	0.73	48.8
117	25.5	97	95	81	91	0.73	48.8
118	17.0	94	87	86	89	0.75	49.7
119	11.2	100	89	73	87	0.74	49.1
120	20.5	81	73	70	75	0.75	49.4